

Mixing among the neutral Higgs bosons and rare B decays in the CP violating MSSM

Tai-Fu Feng^{a,b,c,d}, Xue-Qian Li^{c,e}, Jukka Maalampi^b

^a *Center for Theoretical Physics, Seoul National University, Seoul, 151-742, Korea*

^b *Department of Physics, 40014 University of Jyväskylä, Finland*

^c *CCAST (World Laboratory), P. O. Box 8730, Beijing 100080, China*

^d *Department of Physics, Dalian University of Technology, Dalian 116024, China and*

^e *Department of Physics, Nankai University, Tianjin 300071, China*

(Dated: December 28, 2018)

Abstract

Considering corrections from two-loop Feynman diagrams which involve gluino at large $\tan\beta$, we analyze the effects of possible CP phases on the rare B decays: $\bar{B}_s \rightarrow l^+l^-$ and $\bar{B} \rightarrow Kl^+l^-$ in the CP violating minimal supersymmetric extension of the standard model. It is shown that the results of exact two loop calculations obviously differ from that including one-loop contributions plus threshold radiative corrections. The numerical analysis indicates that the possibly large CP phases strongly affect the theoretical estimation of the branching ratios, and this results coincide with the conclusion of some other works appearing in recent literature.

PACS numbers: 11.30.Er, 12.60.Jv, 13.20.He, 99.35.+d

Keywords: two-loop, rare B decays, supersymmetry

I. INTRODUCTION

The rare B decays serve as a good probe for the new physics beyond the standard model (SM) since they do not seriously suffer from the uncertainties caused by the long distance effects. The forthcoming experiments of the B factories will make more precise measurements on the rare processes and it is believed that those measurements should set even stricter constraints on the parameter space of new physics. Among those plausible new physics scenarios beyond the SM, the simplest and most favorable extension is the Minimal Supersymmetric Model (MSSM) [1]. In the MSSM, there are five physical scalars (Higgs) compared to the SM where there is only one. The contribution of those neutral Higgs bosons to the rare B processes have been extensively discussed in literature. The main conclusion of the analysis is that the branching ratios of the processes such as $\bar{B}_s \rightarrow l^+ l^-$, $\bar{B}_s \rightarrow K l^+ l^-$ *etc.* are enhanced for larger values of $\tan \beta$, which is the ratio of the two vacuum expectation values (VEVs) of the neutral Higgs fields, even within the minimal flavor violating (MFV)¹ supersymmetry scenario.

In addition to the SM CP phase which exists in the CKM matrix, there are three more possible sources for the CP violation phases in the MSSM Lagrangian. The first one is the μ parameter in the superpotential which is complex and the second source is the corresponding soft breaking parameters, namely, the complex masses of the $SU(3) \times SU(2) \times U(1)$ gauginos in the soft breaking terms induce three CP phases. As the third one, there are several CP phases emerging from the scalar soft mass matrices $\mathbf{m}_{Q,U,D,L,R}^2$ and the soft trilinear coupling matrices $\mathbf{A}_{U,D,E}$. Generally, only the off-diagonal elements of the soft mass matrices can be complex due to the hermiticity of these matrices. By contrast, the trilinear coupling matrices $\mathbf{A}_{U,D,E}$ can have complex diagonal elements[2]. Actually, the CP phases must be constrained by the present experimental results. The most rigorous constraints on those CP phases come from the experimental bounds of the electron and neutron electric dipole moments (EDMs), which are $d_e < 4.3 \times 10^{-27} e \cdot cm$ [3] and $d_n < 6.5 \times 10^{-26} e \cdot cm$ [4], respectively. The bound of the EDM of H_g^{199} : $d_{H_g^{199}} < 9. \times 10^{-28} e \cdot cm$ [5] is also measured with high accuracy. In order to make the theoretical prediction consistent with the experimental data, three approaches are adopted in literature. One possibility is to make the CP phases sufficiently small, i.e.

¹ That is, the Cabibbo-Kobayashi-Maskawa (CKM) matrix is assumed to be the only source of flavor mixing.

smaller than 10^{-2} [6]. Alternatively one can also assume a mass suppression by making the supersymmetry spectra heavy enough, i.e. in a range of several TeV[7], or invoke a cancellation among different contributions to the fermion EDMs [8].

In the second scenario, a series of works[9, 10, 11, 12] analyzes the mixing among the neutral Higgs bosons in the CP violating MSSM. Considering the constraints from the experimental upper bounds of the electron and neutron electric dipole moments (EDMs), the soft trilinear coupling for the third generation scalar quarks can have large CP phases. Due to the large Yukawa couplings for the third generation quarks, the radiative corrections can lead to a large mixing among the would-be CP-even and CP-odd neutral Higgs bosons. This mixing causes drastic changes for the couplings between the neutral Higgs and quarks, the neutral Higgs and gauge bosons, and the self couplings among the Higgs fields, thus the consequence is that the lower bound of the mass of the lightest neutral Higgs is relaxed to 60 GeV.

Presently, the calculations of the effective hamiltonian for the transition $b \rightarrow sl^+l^-$ are presented by the authors of Ref.[13, 14, 15, 16, 17, 18] within the MSSM and THDM models. However, those works are all focusing on the CP-conserving processes. As pointed out in Ref.[19], the CP violation phases which induce mixing among the neutral Higgs bosons affect the effective Hamiltonian of $b \rightarrow sl^+l^-$ significantly, especially for larger $\tan\beta$ values. However, their analysis [19] only included the leading terms in $\tan^3\beta$ which originate from the counter diagrams.

In this work, we analyze the rare B -decays: $B \rightarrow X_s\gamma$, $\bar{B}_s^0 \rightarrow l^+l^-$ and $\bar{B} \rightarrow Kl^+l^-$ ($l = \mu, \tau$) in the CP violating MSSM. In order to reduce the number of free parameters, we assume no additional sources of flavor violation other than the CKM matrix elements. In our calculation, we consider all possible contributions from the one-loop box, γ -, Z - and Higgs-penguin diagrams, as well as the threshold radiative corrections to the effective Hamiltonian for $b \rightarrow sl^+l^-$ at first. The threshold radiative corrections indicate a sum of the SUSY QCD and SUSY electroweak corrections to the effective vertex $H_u^* D^c Q$ at larger $\tan\beta$ values[20, 21, 22, 23]. Although threshold radiative corrections approximate the exact two-loop results adequately when the supersymmetry energy scale is sufficiently high, the authors of Ref. [24, 25] pointed out that the difference between threshold radiative approximation and exact two loop calculation is obvious in some regions of the parameter space of the MSSM. As a comparison and complement to the results of threshold radiative corrections

which were already derived and evaluated in literature, we present calculations of the exact two-loop corrections from gluino at large $\tan\beta$ here. Those two-loop results, which include the gluino corrections to the penguin vertices $\bar{s}bZ$, $\bar{s}bH$, and the gluino corrections to the four fermion interaction $\bar{s}b\bar{l}l$, are explicitly presented in this work. The gluino corrections to the penguin vertex $\bar{s}b\gamma$ can be found in our previous analysis[25].

In the second section, we will present the modified couplings involving the neutral Higgs bosons in the CP violating MSSM. The effective Lagrangian for rare B decay modes is given in the third section. We also show the newly derived theoretical formulations of those decay branching ratios *etc.* in this section. Section **IV** is devoted to the numerical analysis and discussion, our conclusion is made in the last section. Some tedious formulae are collected in the appendices.

II. MIXING AMONG NEUTRAL HIGGS BOSONS AND RELEVANT COUPLINGS

In this section, we present the modified Yukawa couplings of the neutral Higgs to the squarks and sleptons where the effects induced by the CP violation phases are taken into account. The most general form of the superpotential which has the gauge invariance and retains all the conservation laws of the SM is written as

$$\mathcal{W} = \mu_H \epsilon_{ij} \hat{H}_i^1 \hat{H}_j^2 + \epsilon_{ij} h_{IJ}^l \hat{H}_i^1 \hat{L}_j^I \hat{R}^J + \epsilon_{ij} h_{IJ}^d \hat{H}_i^1 \hat{Q}_j^I \hat{D}^J + \epsilon_{ij} h_{IJ}^u \hat{H}_i^2 \hat{Q}_j^I \hat{U}^J, \quad (1)$$

where \hat{H}^1 , \hat{H}^2 are the Higgs superfields; \hat{Q}^I and \hat{L}^I are quark and lepton superfields in doublets of the weak SU(2), where I=1, 2, 3 are the indices of generations; the rest superfields \hat{U}^I , \hat{D}^I and \hat{R}^I are the scalar quark superfields of u- and d-types and charged leptons in singlets of the weak SU(2) respectively. Indices i, j are contracted for SU(2), and h^l , $h^{u,d}$ are the Yukawa couplings. To explicitly break supersymmetry, the soft-supersymmetry breaking terms are introduced as

$$\begin{aligned} \mathcal{L}_{soft} = & -m_{H^1}^2 H_i^{1*} H_i^1 - m_{H^2}^2 H_i^{2*} H_i^2 - m_{L^I}^2 \tilde{L}_i^{I*} \tilde{L}_i^I - m_{R^I}^2 \tilde{R}^{I*} \tilde{R}^I - m_{Q^I}^2 \tilde{Q}_i^{I*} \tilde{Q}_i^I - m_{U^I}^2 \tilde{U}^{I*} \tilde{U}^I \\ & - m_{D^I}^2 \tilde{D}^{I*} \tilde{D}^I + (m_1 \lambda_B \lambda_1 + m_2 \lambda_A^i \lambda_A^i + m_3 \lambda_G^a \lambda_G^a + h.c.) + [\mu B \epsilon_{ij} H_i^1 H_j^2 + \epsilon_{ij} A_I^l H_i^1 \tilde{L}_j^I \tilde{R}^I \\ & + \epsilon_{ij} A_I^d H_i^1 \tilde{Q}_j^I \tilde{D}^I + \epsilon_{ij} A_I^u H_i^2 \tilde{Q}_j^I \tilde{U}^I + h.c.], \end{aligned} \quad (2)$$

where $m_{H^1}^2$, $m_{H^2}^2$, $m_{L^I}^2$, $m_{R^I}^2$, $m_{Q^I}^2$, $m_{U^I}^2$ and $m_{D^I}^2$ are the squared masses of the superparticles, m_3 , m_2 , m_1 denote the masses of λ_G^a ($a = 1, 2, \dots, 8$), λ_A^i ($i = 1, 2, 3$) and λ_B ,

which are the $SU(3) \times SU(2) \times U(1)$ gauginos. B is a free parameter in unit of mass. With the soft-supersymmetry breaking terms in Eq.(2), we can study the phenomenology in the framework of the MSSM.

By the effective potential which accounts for the two-loop Yukawa and QCD corrections via the renormalization group equation (RGE), the squared mass matrix of the neutral Higgs bosons is written as:

$$\hat{\mathbf{m}}_{H^0}^2 = \begin{pmatrix} \begin{pmatrix} m_a^2 s_\beta^2 - \frac{8m_w^2 s_w^2}{e^2} \left[\lambda_1 c_\beta^2 \right] \\ + \mathbf{Re}(\lambda_5) s_\beta^2 + \mathbf{Re}(\lambda_6) s_\beta c_\beta \end{pmatrix} & \begin{pmatrix} -m_a^2 s_\beta c_\beta - \frac{8m_w^2 s_w^2}{e^2} \left[\left(\lambda_3 + \lambda_4 \right) s_\beta c_\beta \right] \\ + \mathbf{Re}(\lambda_6) c_\beta^2 + \mathbf{Re}(\lambda_7) s_\beta^2 \end{pmatrix} & \begin{pmatrix} \mathbf{Im}(\lambda_5) s_\beta \\ + \mathbf{Im}(\lambda_6) c_\beta \end{pmatrix} \\ \begin{pmatrix} -m_a^2 s_\beta c_\beta - \frac{8m_w^2 s_w^2}{e^2} \left[\left(\lambda_3 + \lambda_4 \right) s_\beta c_\beta \right] \\ + \mathbf{Re}(\lambda_6) c_\beta^2 + \mathbf{Re}(\lambda_7) s_\beta^2 \end{pmatrix} & \begin{pmatrix} m_a^2 c_\beta^2 - \frac{8m_w^2 s_w^2}{e^2} \left[\lambda_2 s_\beta^2 \right] \\ + \mathbf{Re}(\lambda_5) c_\beta^2 + \mathbf{Re}(\lambda_7) s_\beta c_\beta \end{pmatrix} & \begin{pmatrix} \mathbf{Im}(\lambda_5) s_\beta \\ + \mathbf{Im}(\lambda_6) c_\beta \end{pmatrix} \\ \mathbf{Im}(\lambda_5) s_\beta + \mathbf{Im}(\lambda_6) c_\beta & \mathbf{Im}(\lambda_5) c_\beta + \mathbf{Im}(\lambda_7) s_\beta & m_a^2 \end{pmatrix} \quad (3)$$

with the squared mass m_a^2 being

$$m_a^2 = m_{H^\pm}^2 - \frac{4m_w^2 s_w^2}{e^2} \left(\frac{1}{2} \lambda_4 - \mathbf{Re}(\lambda_5) \right), \quad (4)$$

where the parameters m_{H^\pm} represent the masses of the physical charged Higgs-bosons. The concrete expressions of the parameters λ_i ($i = 1, 2, \dots, 7$) can be found in Ref. [10]. Since the squared mass matrix of neutral Higgs $m_{H^0}^2$ is symmetric, we can find an orthogonal matrix \mathcal{Z}_H to diagonalize it:

$$\mathcal{Z}_H^T \hat{\mathbf{m}}_{H^0}^2 \mathcal{Z}_H = \text{diag}(m_{H_1^0}^2, m_{H_2^0}^2, m_{H_3^0}^2). \quad (5)$$

Correspondingly, the modified interactions related to our calculation are listed below:

$$\begin{aligned} \mathcal{L}_{H_k^0 \tilde{\chi}_\beta^+ \chi_\alpha^+} &= \frac{e}{\sqrt{2} s_w} H_k^0 \tilde{\chi}_\beta^+ \left\{ \left(\kappa_{H^k}^1 \right)_{\beta\alpha} \omega_- + \left(\kappa_{H^k}^2 \right)_{\beta\alpha} \omega_+ \right\} \chi_\alpha^+, \\ \mathcal{L}_{H_k^0 \tilde{t}_\beta^* \tilde{t}_\alpha} &= \frac{e m_w}{s_w c_w^2} \left(\zeta_{tH}^k \right)_{ji} H_k^0 \tilde{t}_i \tilde{t}_j^*, \\ \mathcal{L}_{H_k^0 \tilde{D}_\beta^* \tilde{D}_\alpha} &= \frac{e m_w}{s_w c_w^2} \left(\zeta_{sH}^k \right)_{ji} H_k^0 \tilde{s}_i \tilde{s}_j^*, \\ \mathcal{L}_{H_i^0 H^\pm W^\mp} &= \frac{e}{2 s_w} \left\{ \left[s_\beta \mathcal{Z}_H^{2i} + c_\beta \mathcal{Z}_H^{3i} + i \mathcal{Z}_H^{1i} \right] W_\mu^+ \left(H_i^0 (i \partial^\mu H^-) - (i \partial^\mu H_i^0) H^- \right) \right. \\ &\quad \left. - \left[s_\beta \mathcal{Z}_H^{2i} + c_\beta \mathcal{Z}_H^{3i} - i \mathcal{Z}_H^{1i} \right] W_\mu^- \left(H_i^0 (i \partial^\mu H^+) - (i \partial^\mu H_i^0) H^+ \right) \right\}, \end{aligned}$$

$$\begin{aligned}
\mathcal{L}_{H_i^0 G^\pm W^\mp} &= \frac{e}{2s_w} \left\{ \left[-c_\beta \mathcal{Z}_H^{2i} + s_\beta \mathcal{Z}_H^{3i} \right] W_\mu^+ \left(H_i^0 (i\partial^\mu G^-) - (i\partial^\mu H_i^0) G^- \right) \right. \\
&\quad \left. - \left[-c_\beta \mathcal{Z}_H^{2i} + s_\beta \mathcal{Z}_H^{3i} \right] W_\mu^- \left(H_i^0 (i\partial^\mu G^+) - (i\partial^\mu H_i^0) G^+ \right) \right\}, \\
\mathcal{L}_{H_i^0 W^\pm W^\mp} &= \frac{em_w}{s_w} \left(c_\beta \mathcal{Z}_H^{2i} + s_\beta \mathcal{Z}_H^{3i} \right) H_i^0 W_\mu^+ W^{-\mu}.
\end{aligned} \tag{6}$$

The couplings $\kappa_{H^\rho}^{1,2}$, $\zeta_{(t,s)H}^\rho$ are presented in appendix C. Since the SUSY-QCD modifies the Yukawa coupling $\bar{t}bH^+$ remarkably[22] for larger $\tan\beta$ values, we should consider the SUSY-QCD effects on the effective lagrangian which only includes one loop contributions. Re-summing the dominant supersymmetric corrections for larger $\tan\beta$ to all orders, as well as the leading and next-to-leading logarithms of the standard QCD corrections, one can write the interaction as[20, 21]

$$\begin{aligned}
\mathcal{L}_{H\bar{q}q} &= \frac{em_b(Q)}{2m_w s_w s_\beta c_\beta} \left\{ V_{tb}^* \chi_{FC} \left[c_\beta \mathcal{Z}_H^{3k} - s_\beta \mathcal{Z}_H^{2k} - i\mathcal{Z}_H^{1k} \right] \left[V_{td} \bar{b}\omega_- d + V_{ts} \bar{b}\omega_- s \right] H_k^0 \right. \\
&\quad \left. - s_\beta \chi_B \left[\mathcal{Z}_H^{2k} + \Delta \mathcal{Z}_H^{3k} + i(s_\beta - c_\beta \Delta) \mathcal{Z}_H^{1k} \right] \bar{b}\omega_- b H_k^0 + h.c. \right\} \\
&+ \frac{e}{\sqrt{2}s_w} \left\{ V_{tb}^* \left[\frac{m_t(Q)}{m_w \tan\beta} \bar{b}\omega_+ t + \xi_H^b \frac{m_b(Q)}{m_w} \tan\beta \bar{b}\omega_- t \right] H^- + V_{tb}^* \left[\frac{m_t(Q)}{m_w} \bar{b}\omega_+ t \right. \right. \\
&\quad \left. \left. - \xi_G^b \frac{m_b(Q)}{m_w} \bar{b}\omega_- t \right] G^- + \sum \xi_{CKM}^{ib*} V_{ib}^* \left[\frac{m_{u_i}(Q)}{m_w \tan\beta} \bar{b}\omega_+ u_i + \frac{m_b(Q)}{m_w} \tan\beta \bar{b}\omega_- u_i \right] H^- \right. \\
&\quad \left. + \sum \xi_{CKM}^{ib*} V_{ib}^* \left[\frac{m_{u_i}(Q)}{m_w} \bar{b}\omega_+ u_i - \frac{m_b(Q)}{m_w} \bar{b}\omega_- u_i \right] G^- + \sum \xi_{CKM}^{ti*} V_{ti}^* \left[\frac{m_t(Q)}{m_w \tan\beta} \bar{d}_i \omega_+ t \right. \right. \\
&\quad \left. \left. + \frac{m_{d_i}(Q)}{m_w} \tan\beta \bar{d}_i \omega_- t \right] H^- + \sum \xi_{CKM}^{ti*} V_{ti}^* \left[\frac{m_t(Q)}{m_w} \bar{d}_i \omega_+ t - \frac{m_{d_i}(Q)}{m_w} \bar{d}_i \omega_- t \right] G^- + h.c. \right\} \tag{7}
\end{aligned}$$

where Q is the characteristic energy scale of the process. The $\tan\beta$ -enhancing radiative corrections are

$$\begin{aligned}
\chi_B &= \frac{1}{1 + \tan\beta\Delta}, \\
\chi_{FC} &= -\chi_B \frac{em_t(Q) \tan\beta\Delta^{EW}}{\sqrt{2}m_w s_w s_\beta [1 + \tan\beta\Delta^S]}, \\
\xi_H^b &= \chi_B \left(1 + \Delta^S - h_t \cot\beta\Delta^{EW} \right), \\
\xi_G^b &= \chi_B (1 + \Delta), \\
\xi_{CKM}^{ub} &= \xi_{CKM}^{cb} = \xi_{CKM}^{td} = \xi_{CKM}^{ts} = \frac{1 + \tan\beta\Delta}{1 + \tan\beta\Delta^S}, \\
\xi_{CKM}^{tb} &= \xi_{CKM}^{ud} = \xi_{CKM}^{cs} = 1, \\
\Delta &= \Delta^S + h_t \Delta^{EW}, \\
\Delta^S &= \frac{2\alpha_s}{3\pi} m_{\tilde{g}}^* \mu_H^* I(m_{\tilde{b}_L}, m_{\tilde{b}_R}, |m_{\tilde{g}}|),
\end{aligned}$$

$$\Delta^{EW} = \frac{1}{64\pi^2} \mu_H^* A_t I(m_{\tilde{t}_L}, m_{\tilde{t}_R}, |\mu_H|) , \quad (8)$$

with the vertex function[23]

$$I(a, b, c) = \frac{1}{(a^2 - b^2)(b^2 - c^2)(a^2 - c^2)} \left[a^2 b^2 \ln\left(\frac{a^2}{b^2}\right) + b^2 c^2 \ln\left(\frac{b^2}{c^2}\right) + c^2 a^2 \ln\left(\frac{c^2}{a^2}\right) \right] . \quad (9)$$

While deriving Eq. (7) and Eq. (8), we consider the fact that $m_t \gg (m_c, m_u)$; $m_b \gg (m_s, m_d)$ and $|V_{tb}| \gg (|V_{ts}|, |V_{td}|, |V_{ub}|, |V_{cb}|)$. Computations without these approximations were given in Ref.[21]. The running quark masses are evaluated by

$$\begin{aligned} m_t(Q) &= U_6(Q, m_t) \cdot m_t(m_t) , \\ m_b(Q) &= U_6(Q, m_t) \cdot U_5(m_t, m_b) \cdot m_b(m_b) , \end{aligned} \quad (10)$$

where we have assume that there are no other colored particles with masses between Q and m_t . The evolution factor U_f reads

$$\begin{aligned} U_f(Q_2, Q_1) &= \left(\frac{\alpha_s(Q_2)}{\alpha_s(Q_1)} \right)^{d_f} \left[1 + \frac{\alpha_s(Q_1) - \alpha_s(Q_2)}{4\pi} J_f \right] , \\ d_f &= \frac{12}{33 - 2f} , \\ J_f &= -\frac{8982 - 504f + 40f^2}{3(33 - f)^2} , \end{aligned} \quad (11)$$

where, f is the number of active quark flavors. With those preparations given above, we can discuss the rare B decays in the CP violating MSSM.

III. THE EFFECTIVE HAMILTON AND DECAY WIDTH FOR RARE B DECAYS

A. The effective Hamiltonian

The processes which we are interested in, are $\bar{B}_s \rightarrow l^+ l^-$ and $\bar{B} \rightarrow K l^+ l^-$, both of them originate from the transition $b \rightarrow s$. Integrating out the heavy degrees of freedom in the full theory, an effective Hamiltonian is obtained [26]:

$$H_{eff} = -\frac{4G_F}{\sqrt{2}} V_{ts}^* V_{tb} \left\{ \sum_{i=1}^{10} C_i(\mu) \mathcal{O}_i(\mu) + \sum_{i=9}^{10} C'_i \mathcal{O}'_i + C_S \mathcal{O}_S + C_P \mathcal{O}_P + C'_S \mathcal{O}'_S + C'_P \mathcal{O}'_P \right\} \quad (12)$$

with $C_2(m_w) = (\xi_{\text{CKM}}^{ts})^* \xi_{\text{CKM}}^{tb}$, V_{ij} represent the physical CKM entries, and ξ_{CKM}^{ti} is the $\tan\beta$ -enhanced radiative corrections to the effective CKM entries. The operators in the effective Hamiltonian are:

$$\begin{aligned}
\mathcal{O}_1 &= (\bar{s}_\alpha \gamma_\mu \omega_- c_\beta) (\bar{c}_\beta \gamma^\mu \omega_- b_\alpha) , \\
\mathcal{O}_2 &= (\bar{s}_\alpha \gamma_\mu \omega_- c_\alpha) (\bar{c}_\beta \gamma^\mu \omega_- b_\beta) , \\
\mathcal{O}_3 &= (\bar{s}_\alpha \gamma_\mu \omega_- c_\alpha) \sum_{q=u,d,s,c,b} (\bar{q}_\beta \gamma^\mu \omega_- q_\beta) , \\
\mathcal{O}_4 &= (\bar{s}_\alpha \gamma_\mu \omega_- c_\beta) \sum_{q=u,d,s,c,b} (\bar{q}_\beta \gamma^\mu \omega_- q_\alpha) , \\
\mathcal{O}_5 &= (\bar{s}_\alpha \gamma_\mu \omega_- c_\alpha) \sum_{q=u,d,s,c,b} (\bar{q}_\beta \gamma^\mu \omega_+ q_\beta) , \\
\mathcal{O}_6 &= (\bar{s}_\alpha \gamma_\mu \omega_- c_\beta) \sum_{q=u,d,s,c,b} (\bar{q}_\beta \gamma^\mu \omega_+ q_\alpha) , \\
\mathcal{O}_7 &= \frac{em_b}{(4\pi)^2} \bar{s}_\alpha F \cdot \sigma \omega_+ b_\alpha , \\
\mathcal{O}_8 &= \frac{em_b}{(4\pi)^2} \bar{s}_\alpha T_{\alpha\beta}^a G^a \cdot \sigma \omega_+ b_\beta , \\
\mathcal{O}_9 &= \frac{e^2}{(4\pi)^2} (\bar{s}_\alpha \gamma_\mu \omega_- b_\alpha) (\bar{l} \gamma^\mu l) , \\
\mathcal{O}_{10} &= \frac{e^2}{(4\pi)^2} (\bar{s}_\alpha \gamma_\mu \omega_- b_\alpha) (\bar{l} \gamma^\mu \gamma_5 l) , \\
\mathcal{O}'_9 &= \frac{e^2}{(4\pi)^2} (\bar{s}_\alpha \gamma_\mu \omega_+ b_\alpha) (\bar{l} \gamma^\mu l) , \\
\mathcal{O}'_{10} &= \frac{e^2}{(4\pi)^2} (\bar{s}_\alpha \gamma_\mu \omega_+ b_\alpha) (\bar{l} \gamma^\mu \gamma_5 l) , \\
\mathcal{O}_s &= \frac{e^2}{(4\pi)^2} (\bar{s}_\alpha \omega_+ b_\alpha) (\bar{l} l) , \\
\mathcal{O}_P &= \frac{e^2}{(4\pi)^2} (\bar{s}_\alpha \omega_+ b_\alpha) (\bar{l} \gamma_5 l) , \\
\mathcal{O}'_s &= \frac{e^2}{(4\pi)^2} (\bar{s}_\alpha \omega_- b_\alpha) (\bar{l} l) , \\
\mathcal{O}'_P &= \frac{e^2}{(4\pi)^2} (\bar{s}_\alpha \omega_- b_\alpha) (\bar{l} \gamma_5 l) .
\end{aligned} \tag{13}$$

In our calculations, we adopt the Feynman rules in the 't Hooft-Feynman gauge with $\xi = 1$. Within the framework of the MFV CP violating MSSM, the one loop Feynman diagrams that contribute to the effective Hamiltonian (Eq.12) can be found in the literature. For example, the one-loop γ -, Z - penguin diagrams are presented in Ref.[27] and the

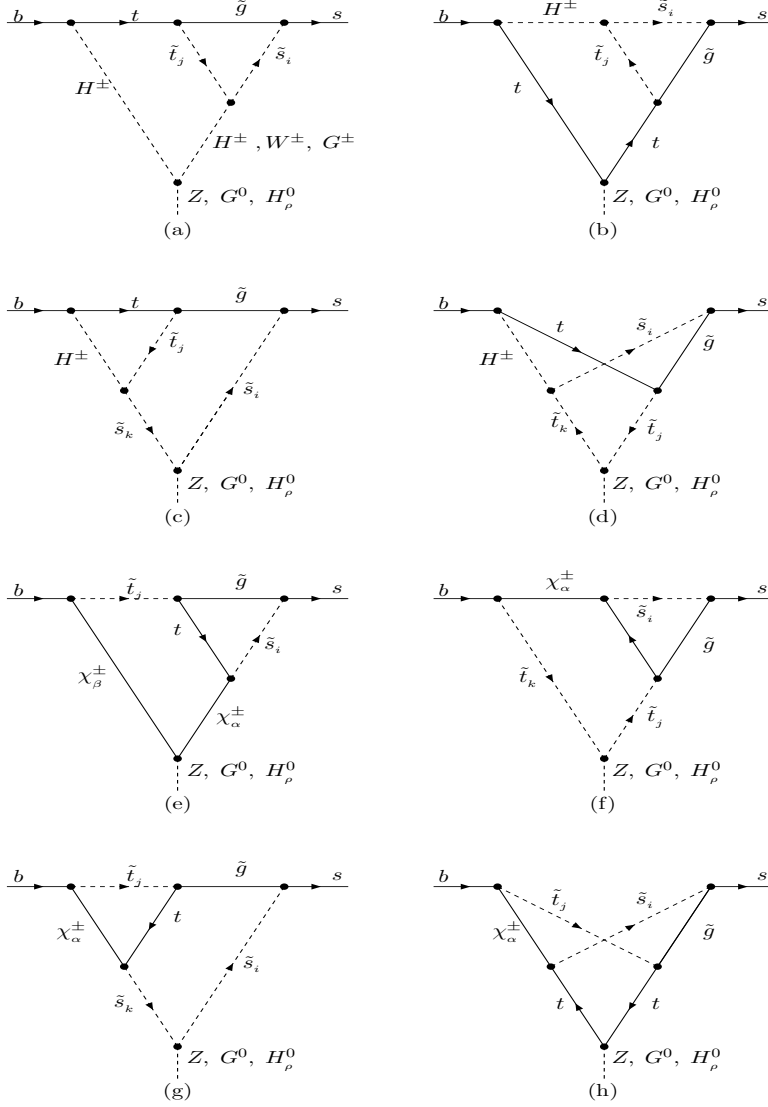


FIG. 1: The corrections of two-loop diagrams involving gluino (later we abbreviate them as "the two loop gluino corrections") to the penguin vertices $\bar{s}bZ$, $\bar{s}bH$ at large $\tan\beta$.

Higgs penguin and box diagrams are given in Ref.[28]. At the electro-weak scale, the one loop Wilson coefficients in Eq.12 are divided into several pieces:

$$\begin{aligned}
C_i(\mu_W) &= C_i^\gamma(\mu_W) + C_i^Z(\mu_W) + C_i^{box}(\mu_W), \quad (i = 9, 10) \\
C'_i(\mu_W) &= C_i^{\prime\gamma}(\mu_W) + C_i^{\prime Z}(\mu_W) + C_i^{\prime box}(\mu_W), \quad (i = 9, 10) \\
C_i(\mu_W) &= C_i^{H_i^0}(\mu_W) + C_i^{count}(\mu_W) + C_i^{box}(\mu_W) + C_i^{resum}(\mu_W), \quad (i = S, P) \\
C'_i(\mu_W) &= C_i^{\prime H_i^0}(\mu_W) + C_i^{\prime count}(\mu_W) + C_i^{\prime box}(\mu_W), \quad (i = S, P).
\end{aligned} \tag{14}$$

Here, we collect the Wilson coefficients corresponding to the one loop γ -, Z -, H_k^0 - penguin and box contributions in the appendix A. In order to include the threshold radiative corrections of gluinos, we have replaced the tree-level vertices by the corresponding interactions which are presented in Eq. (7). Similarly, we can obtain the contributions which originate from a resummation of high order threshold effects on the Wilson coefficients of the operators involving down-type quarks:

$$\begin{aligned} C_S^{\text{resum}}(\mu_W) &= \frac{\sqrt{x_b x_l}}{2s_\beta c_\beta^2 x_{H_k^0}} \chi_{FC}^* \mathcal{Z}_H^{2k} (c_\beta \mathcal{Z}_H^{3k} - s_\beta \mathcal{Z}_H^{2k} + i \mathcal{Z}_H^{1k}) \\ C_P^{\text{resum}}(\mu_W) &= -i \frac{\sqrt{x_b x_l}}{2c_\beta^2 x_{H_k^0}} \chi_{FC}^* \mathcal{Z}_H^{1k} (c_\beta \mathcal{Z}_H^{3k} - s_\beta \mathcal{Z}_H^{2k} + i \mathcal{Z}_H^{1k}), \end{aligned} \quad (15)$$

with $c_\beta = \cos \beta$, $s_\beta = \sin \beta$, and $x_i = \frac{m_i^2}{m_W^2}$.

As we mentioned in the introduction, there are obvious differences between the results from exact two-loop calculations and that from threshold radiative approximation which is derived in terms of the heavy mass expanding method. In the large $\tan \beta$ scenario, corrections from the two-loop Feynman diagrams including gluino to the penguin vertices $\bar{s}bZ$, $\bar{s}bH$ are drawn in Fig.1. Correspondingly, the corrections to the Wilson coefficients from the two-loop penguin diagrams are written as

$$\begin{aligned} \delta(C_9)_{2P} &= \frac{\alpha_s}{8\pi s_w^2} \frac{m_b t_\beta}{m_w} (1 - 4s_w^2) \mathcal{P}_Z, \\ \delta(C_{10})_{2P} &= -\frac{\alpha_s}{8\pi s_w^2} \frac{m_b t_\beta}{m_w} \mathcal{P}_Z, \\ \delta(C_S)_{2P} &= \frac{\alpha_s}{4\pi s_w^2} \frac{m_b m_{lI} t_\beta^2}{m_w^2} \sum_{\rho=1}^3 (\mathcal{Z}_H)_{2\rho} \frac{1}{s_\beta x_{H^\rho}} \mathcal{P}_{H^\rho}, \\ \delta(C_P)_{2P} &= \frac{\alpha_s}{4\pi s_w^2 c_w^2} \frac{m_b m_{lI} t_\beta}{m_w^2} \mathcal{P}_G - i \frac{\alpha_s}{4\pi s_w^2} \frac{m_b m_{lI} t_\beta^2}{m_w^2} \sum_{\rho=1}^3 (\mathcal{Z}_H)_{1\rho} \frac{1}{x_{H^\rho}} \mathcal{P}_{H^\rho}, \end{aligned} \quad (16)$$

with $\mathcal{P}_{Z,G} = \sum_{i=1}^8 \mathcal{P}_{Z,G}^{(i)}$, $\mathcal{P}_{H^\rho} = \sum_{i=1}^{10} \mathcal{P}_{H^\rho}^{(i)}$. We list the expression of those nonzero form factors $\mathcal{P}_{Z,G}^{(i)}$, $\mathcal{P}_{H^\rho}^{(i)}$ in the appendix B in order to shorten the length of text.

We should also include the two loop gluino correction to the four fermion interactions $\bar{s}b\bar{l}l$ for completeness. The Feynman diagrams are plotted in Fig.2. Correspondingly, the corrections to the Wilson coefficients from those two loop box diagrams are formulated as

$$\delta(C_9)_{2B} = -\frac{2\alpha_s}{3\pi s_w^2} t_\beta \mathcal{B}_V,$$

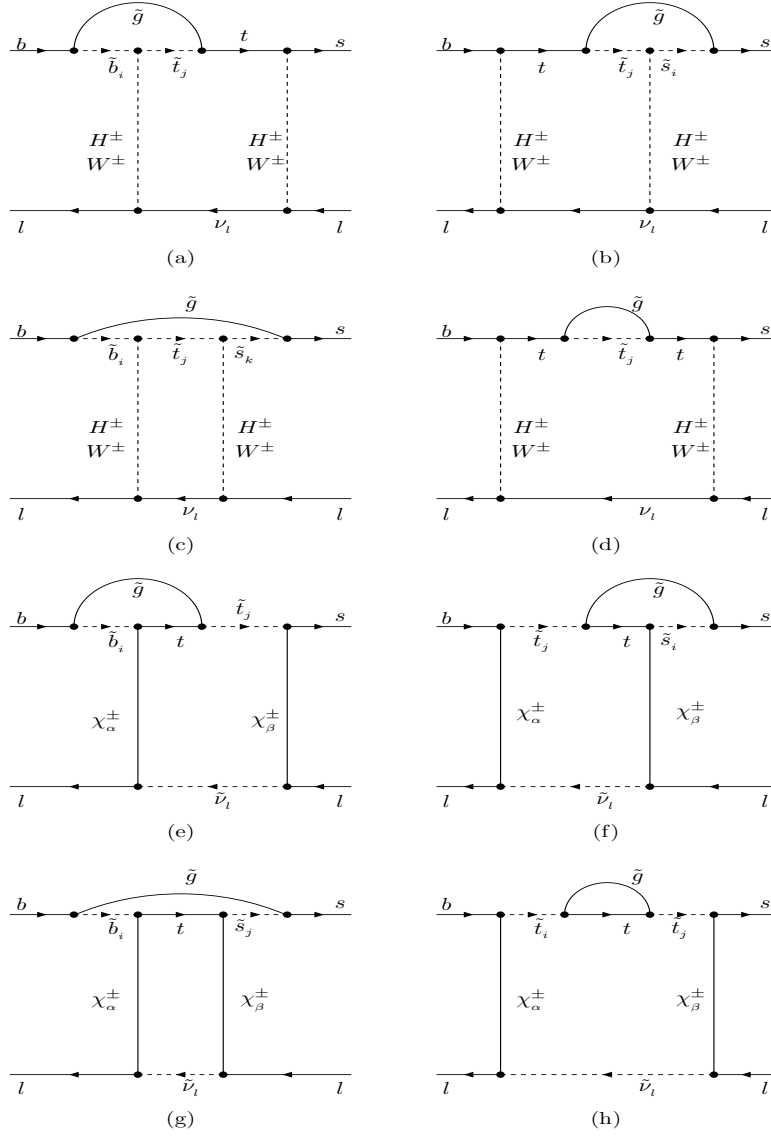


FIG. 2: The two loop gluino corrections to the four fermion interactions $\bar{s}b\bar{l}l$ at large $\tan\beta$.

$$\begin{aligned}
\delta(C_{10})_{2B} &= -\frac{2\alpha_s}{3\pi s_w^2} t_\beta \mathcal{B}_A, \\
\delta(C'_9)_{2B} &= -\frac{2\alpha_s}{3\pi s_w^2} t_\beta \mathcal{B}'_V, \\
\delta(C'_{10})_{2B} &= -\frac{2\alpha_s}{3\pi s_w^2} t_\beta \mathcal{B}'_A, \\
\delta(C_S)_{2B} &= -\frac{2\alpha_s}{3\pi s_w^2} t_\beta \mathcal{B}_S, \\
\delta(C_P)_{2B} &= -\frac{2\alpha_s}{3\pi s_w^2} t_\beta \mathcal{B}_P,
\end{aligned}$$

$$\begin{aligned}
\delta(C'_S)_{2B} &= -\frac{2\alpha_s}{3\pi s_w^2} t_\beta \mathcal{B}'_S, \\
\delta(C'_P)_{2B} &= -\frac{2\alpha_s}{3\pi s_w^2} t_\beta \mathcal{B}'_P,
\end{aligned} \tag{17}$$

with

$$\begin{aligned}
\mathcal{B}'_{V,A} &= \mathcal{B}'_{V,A}^{(1)} + \mathcal{B}'_{V,A}^{(2)}, \\
\mathcal{B}_{S,P} &= \sum_{i=1}^9 \mathcal{B}_{S,P}^{(i)}, \\
\mathcal{B}'_{S,P} &= \sum_{i=1}^6 \mathcal{B}'_{S,P}^{(i)}.
\end{aligned} \tag{18}$$

The concrete expressions of those nonzero form factors $\mathcal{B}'_{V,A}^{(i)}$, $\mathcal{B}_{S,P}^{(i)}$, $\mathcal{B}'_{S,P}^{(i)}$ can be found in the appendix C. In Eq. 16 and Eq. 17, we adopt the \overline{MS} scheme to remove the UV-divergences which are caused by the divergent sub-diagrams [29].

When the effective Lagrangian is applied to the hadronic processes whose characteristic energy scale is about m_b , we should evolve those Wilson coefficients from the weak scale down to the hadronic scale. The running depends on the anomalous dimension matrix of the concerned operators[30]. The Wilson coefficients obtained at the weak scale are regarded as the initial conditions for the renormalization group equations (RGEs). Up to the leading order (LO), the Wilson coefficients at hadronic scale are given as[31, 32, 33]

$$\begin{aligned}
C_7(m_b) &= \eta^{-\frac{16}{23}} \left[C_7(m_w) + \frac{8}{3} \left(C_8(m_w) - \frac{2021}{468} C_2(m_w) \right) (\eta^{\frac{2}{23}} - 1) \right. \\
&\quad \left. + \frac{389}{540} C_2(m_w) (\eta^{\frac{10}{23}} - 1) + \frac{107}{702} C_2(m_w) (\eta^{\frac{28}{23}} - 1) \right], \\
C'_7(m_b) &= \eta^{-\frac{16}{23}} \left[C'_7(m_w) + \frac{8}{3} C'_8(m_w) (\eta^{\frac{2}{23}} - 1) \right], \\
C_9(m_b) &= C_9(m_w) + \frac{4\pi}{\alpha_s(m_w)} \left[-\frac{4}{33} (1 - \eta^{\frac{11}{23}}) + \frac{8}{87} (1 - \eta^{-\frac{29}{23}}) \right] C_2(m_w), \\
C_{10}(m_b) &= C_{10}(m_w),
\end{aligned} \tag{19}$$

with $\eta = \frac{\alpha_s(m_b)}{\alpha_s(m_w)}$. The most stringent constraint on the supersymmetry parameter space comes from the rare decay of B -meson: $B \rightarrow X_s \gamma$ [34]. The theoretical prediction on the branching ratio of the inclusive process $B \rightarrow X_s \gamma$ is given as [33, 35]

$$\begin{aligned}
BR(B \rightarrow X_s \gamma) &= \frac{\Gamma(B \rightarrow X_s \gamma)}{\Gamma(B \rightarrow X_c e \bar{\nu}_e)} BR(B \rightarrow X_c e \bar{\nu}_e) \\
&= \frac{|V_{ts}^* V_{tb}|^2}{|V_{cb}|^2} \frac{6\alpha_{em} |C_7(m_b)|^2}{\pi \rho(\frac{m_c}{m_b}) \left(1 - \frac{2\alpha_s(m_b)}{3\pi} f(\frac{m_c}{m_b}) \right)} BR(B \rightarrow X_c e \bar{\nu}_e),
\end{aligned} \tag{20}$$

where α_{em} is the QED fine structure constant and the phase factor is

$$\rho\left(\frac{m_c}{m_b}\right) = 1 - 8\left(\frac{m_c}{m_b}\right)^2 + 8\left(\frac{m_c}{m_b}\right)^6 + \left(\frac{m_c}{m_b}\right)^8 - 24\left(\frac{m_c}{m_b}\right)^4 \ln \frac{m_c}{m_b},$$

and the one-loop QCD correction to the semileptonic decay gives $f(\frac{m_c}{m_b}) \simeq 2.4$ [36]. When we calculate the branching ratios of other rare processes, the branching ratio of $B \rightarrow X_s \gamma$ which is experimentally measured with relatively high accuracy, must be considered as a prior constraint.

In the SM, the CP asymmetry of $B \rightarrow X_s \gamma$ process

$$A_{CP}(B \rightarrow X_s \gamma) = \frac{\Gamma(\bar{B} \rightarrow X_{\bar{s}} \gamma) - \Gamma(B \rightarrow X_s \gamma)}{\Gamma(\bar{B} \rightarrow X_{\bar{s}} \gamma) + \Gamma(B \rightarrow X_s \gamma)} \quad (21)$$

is calculated to be rather small: $A_{CP} \sim 0.5\%$ [35]. By the recent experimental measurement [37] of the CP asymmetry, we have

$$-0.30 \leq A_{CP}(B \rightarrow X_s \gamma) \leq 0.14 \quad (22)$$

at 95% C.L. In other word, the studies of the direct CP asymmetry in $B \rightarrow X_s \gamma$ may uncover new sources of CP violation which lie outside the SM. Applying Eq. 20, the CP asymmetry can be written as

$$A_{CP}(B \rightarrow X_s \gamma) = \frac{\alpha_s(\mu_b)}{|C_7(\mu_b)|^2} \left\{ \left[\frac{40}{81} - \frac{8z}{9} (v(z) + b(z, \delta)) \left(1 + \frac{V_{us}^* V_{ub}}{V_{ts}^* V_{tb}} \right) \right] \mathbf{Im}[C_2(\mu_b) C_7^*(\mu_b)] \right. \\ \left. - \frac{4}{9} \mathbf{Im}[C_8(\mu_b) C_7^*(\mu_b)] + \frac{8z}{27} b(z, \delta) \mathbf{Im} \left[\left(1 + \frac{V_{us}^* V_{ub}}{V_{ts}^* V_{tb}} \right) C_2(\mu_b) C_8^*(\mu_b) \right] \right\} \quad (23)$$

where $z = (m_c/m_b)^2$, $v(z)$ and $b(z, \delta)$ can be found in [38].

B. The decay width for two rare B processes

1. $\bar{B}_s \rightarrow l^+ l^-$ ($l = \mu, \tau$)

The decay constant of the pseudoscalar meson \bar{B}_s is defined as [15]:

$$\langle 0 | \bar{s} \gamma_\mu \gamma_5 b | \bar{B}_s(P) \rangle = i p_\mu f_{B_s}. \quad (24)$$

With the equation of motion for quark fields, Eq. (24), one can write

$$\langle 0 | \bar{s} \gamma_5 b | \bar{B}_s(P) \rangle = i f_{B_s} \frac{m_{B_s}^2}{m_b + m_s}. \quad (25)$$

Correspondingly, we derive the branching ratio as

$$BR(\bar{B}_s \rightarrow l^+ l^-) = \frac{\alpha_{em}^2 G_F^2 |V_{ts}^* V_{tb}|^2}{16\pi^3} m_{B_s} \tau_{B_s} \sqrt{1 - 4m_l^2/m_{B_s}^2} \left\{ \left(1 - \frac{4m_l^2}{m_{B_s}^2}\right) |F_S|^2 + |F_P + 2m_l F_A|^2 \right\}, \quad (26)$$

with m_{B_s} and τ_{B_s} denote mass and life time of the meson B_s respectively, and

$$\begin{aligned} F_S &= -\frac{i}{2} m_{B_s}^2 f_{B_s} \left\{ \frac{C_S m_b - C'_S m_s}{m_b + m_s} \right\}, \\ F_P &= -\frac{i}{2} m_{B_s}^2 f_{B_s} \left\{ \frac{C_P m_b - C'_P m_s}{m_b + m_s} \right\}, \\ F_A &= -\frac{i}{2} f_{B_s} (C_{10} - C'_{10}). \end{aligned} \quad (27)$$

A point should be noted that there a CP asymmetry is observable in this process

$$\begin{aligned} A_{CP} &= \frac{\Gamma(B_s \rightarrow \bar{l}l) - \Gamma(\bar{B}_s \rightarrow \bar{l}l)}{\Gamma(B_s \rightarrow \bar{l}l) + \Gamma(\bar{B}_s \rightarrow \bar{l}l)} \\ &= \frac{2\text{Im}(\xi_{CP})X_s}{(1 + |\xi_{CP}|^2)(1 + X_s^2)}, \end{aligned} \quad (28)$$

and as indicated in the formula, it is induced by the mixing of B_s and \bar{B}_s [39]. Here,

$$\begin{aligned} X_s &= \Delta m_{B_s} / \Gamma_{B_s}, \\ \xi_{CP} &= \frac{V_{ts}^* V_{tb} (C_S \sqrt{1 - 4m_l^2/m_{B_s}^2} + C_P + 2m_l C_{10}/m_{B_s})}{V_{ts} V_{tb}^* (C_S^* \sqrt{1 - 4m_l^2/m_{B_s}^2} - C_P^* - 2m_l C_{10}^*/m_{B_s})}, \end{aligned} \quad (29)$$

and Δm_{B_s} is the mass difference in $\bar{B}_s - B_s$ mixing, Γ_{B_s} denotes decay width of the meson B_s .

2. $\bar{B} \rightarrow Kl^+ l^-$ ($l = \mu, \tau$)

According to Ref.[40], the nonzero hadronic matrix elements for the exclusive decay $\bar{B} \rightarrow Kl^+ l^-$ are written as

$$\begin{aligned} \langle K(k) | \bar{s} \gamma_\mu b | \bar{B}(p) \rangle &= f_+(q^2) (2p - q)_\mu + (f_0(q^2) - f_+(q^2)) \frac{m_B^2 - m_K^2}{q^2} q_\mu, \\ \langle K(k) | \bar{s} i \sigma_{\mu\nu} q^\nu b | \bar{B}(p) \rangle &= -\frac{f_T(q^2)}{m_B + m_K} (q^2 (2p - q)_\mu - (m_B^2 - m_K^2) q_\mu), \\ \langle K(k) | \bar{s} b | \bar{B}(p) \rangle &= \frac{m_B^2 - m_K^2}{m_b - m_s} f_0(q^2), \end{aligned} \quad (30)$$

where $q^\mu = (p - k)^\mu$ is the four-momentum transferred to the dilepton system. The resulting form factors are parameterized as

$$\begin{aligned} f_0(s) &= f_0(0) \exp \left[c_1^0 \frac{s}{m_B^2} + c_2^0 \left(\frac{s}{m_B^2} \right)^2 + c_3^0 \left(\frac{s}{m_B^2} \right)^3 \right], \\ f_+(s) &= f_+(0) \exp \left[c_1^+ \frac{s}{m_B^2} + c_2^+ \left(\frac{s}{m_B^2} \right)^2 + c_3^+ \left(\frac{s}{m_B^2} \right)^3 \right], \\ f_T(s) &= f_T(0) \exp \left[c_1^T \frac{s}{m_B^2} + c_2^T \left(\frac{s}{m_B^2} \right)^2 + c_3^T \left(\frac{s}{m_B^2} \right)^3 \right]. \end{aligned} \quad (31)$$

With the effective Lagrangian Eq. (12) and the hadronic matrix elements Eq. (30), we can write the transition matrix elements for $\bar{B} \rightarrow Kl^+l^-$ as following

$$\mathcal{M} = F_s \bar{l}l + F_P \bar{l}\gamma_5 l + F_V p^\mu \bar{l}\gamma_\mu l + F_A p^\mu \bar{l}\gamma_\mu \gamma_5 l, \quad (32)$$

where p_μ denotes the four-momentum of the initial B meson, and the form factors F_i are Lorentz-invariant. Following Ref. [28], we define θ as the angle between the three-momenta \mathbf{p}_l and \mathbf{p}_s in the center-of-mass frame of the dilepton. The energy-angular distribution of the decay products is

$$\begin{aligned} \frac{d\Gamma(\bar{B} \rightarrow Kl^+l^-)}{ds d\cos\theta} &= \frac{\alpha_{em}^2 G_F^2 |V_{ts}^* V_{tb}|^2}{2^9 \pi^5 m_B^3} \lambda^{\frac{1}{2}}(m_B^2, m_K^2, s) \beta_l \left\{ s \left[\beta_l^2 |F_s|^2 + |F_P|^2 \right] \right. \\ &\quad + \frac{1}{4} \lambda(m_B^2, m_K^2, s) \left[1 - \beta_l^2 \cos^2 \theta \right] \left[|F_V|^2 + |F_A|^2 \right] \\ &\quad + 4m_l^2 m_B^2 |F_A|^2 + 2m_l \left[\lambda^{\frac{1}{2}}(m_B^2, m_K^2, s) \beta_l \mathbf{Re}(F_s F_V^*) \cos \theta \right. \\ &\quad \left. \left. + (m_B^2 - m_K^2 + s) \mathbf{Re}(F_P F_A^*) \right] \right\}, \end{aligned} \quad (33)$$

with $s = (p_{l^+} + p_{l^-})^2$, $\beta_l = \sqrt{1 - \frac{4m_l^2}{s}}$ and $\lambda(a, b, c) = a^2 + b^2 + c^2 - 2(ab + bc + ca)$. The kinematic quantities s , $\cos\theta$ have natural bounds

$$4m_l^2 \leq s \leq (m_B - m_K)^2, \quad -1 \leq \cos\theta \leq 1. \quad (34)$$

A particularly interesting quantity is the forward-backward asymmetry

$$\begin{aligned} A_{FB}(s) &= \frac{\int_0^1 d\cos\theta \frac{d\Gamma}{ds d\cos\theta} - \int_{-1}^0 d\cos\theta \frac{d\Gamma}{ds d\cos\theta}}{\int_0^1 d\cos\theta \frac{d\Gamma}{ds d\cos\theta} + \int_{-1}^0 d\cos\theta \frac{d\Gamma}{ds d\cos\theta}} \\ &= \frac{\alpha_{em}^2 G_F^2 |V_{ts}^* V_{tb}|^2}{2^8 \pi^5 m_B^3} m_l \lambda(m_B^2, m_K^2, s) \beta_l^2 \mathbf{Re}(F_s F_V^*) / \frac{d\Gamma}{ds}, \end{aligned} \quad (35)$$

where the dilepton invariant mass spectrum $\frac{d\Gamma}{ds}$ is given as

$$\frac{d\Gamma(\bar{B} \rightarrow Kl^+l^-)}{ds} = \frac{\alpha_{em}^2 G_F^2 |V_{ts}^* V_{tb}|^2}{2^8 \pi^5 m_B^3} \lambda^{\frac{1}{2}}(m_B^2, m_K^2, s) \beta_l \left\{ s \left[\beta_l^2 |F_s|^2 + |F_P|^2 \right] \right.$$

$$\begin{aligned}
& + \frac{1}{6} \lambda(m_B^2, m_K^2, s) \left[1 + \frac{2m_l^2}{s} \right] [|F_V|^2 + |F_A|^2] \\
& + 4m_l^2 m_B^2 |F_A|^2 + 2m_l(m_B^2 - m_K^2 + s) \text{Re}(F_P F_A^*) \Big\} . \quad (36)
\end{aligned}$$

The form factors are formulated as

$$\begin{aligned}
F_S &= \frac{1}{2} (m_B^2 - m_K^2) f_0(s) \left\{ \frac{C_S m_b + C'_S m_s}{m_b - m_s} \right\} , \\
F_P &= -m_l C_{10} \left\{ f_+(s) - \frac{m_B^2 - m_K^2}{s} [f_0(s) - f_+(s)] \right\} \\
&+ \frac{1}{2} (m_B^2 - m_K^2) f_0(s) \left\{ \frac{C_S m_b + C'_S m_s}{m_b - m_s} \right\} , \\
F_A &= C_{10} f_+(s) , \\
F_V &= \left\{ C_9 f_+(s) + 2C_7 m_b \frac{f_T(s)}{m_B + m_K} \right\} . \quad (37)
\end{aligned}$$

Our main interest is in the average forward-backward asymmetry $\langle A_{FB} \rangle$, which can be achieved from Eq.35 by integrating out the numerator and denominator separately over the dilepton invariant mass-square s . Basing on the preparations made above, we can numerically analyze the effects of various CP phases on the rare B decays in next section.

IV. NUMERICAL RESULTS

In this section, we present our numerical results for the rates of the rare B decays in the MSSM. As mentioned above, the most stringent constraint on the parameter space of 'new physics' beyond the SM is the experimental bound on the branching ratio of $B \rightarrow X_s \gamma$:

$$2. \times 10^{-4} < BR(B \rightarrow X_s \gamma) < 4.5 \times 10^{-4}.$$

In our numerical analysis, we take this as a constraint for the parameter space of the CP violating MSSM. The inputs of the SM sector are [41] $\alpha_{EW} = 1./128.8$, $m_W = 80.23\text{GeV}$, $m_Z = 91.18\text{GeV}$, $\alpha_s(m_Z) = 0.117$, $m_t^{pole} = 173.8\text{GeV}$. The on-shell running masses of top and bottom quarks are related to the corresponding pole masses through [23]

$$\begin{aligned}
m_t(m_t^{pole}) &= \frac{m_t^{pole}}{1 + 5/(3\pi)\alpha_s(m_t^{pole})} , \\
m_b(m_b^{pole}) &= \frac{m_b^{pole}}{1 + 5/(3\pi)\alpha_s(m_b^{pole})} . \quad (38)
\end{aligned}$$

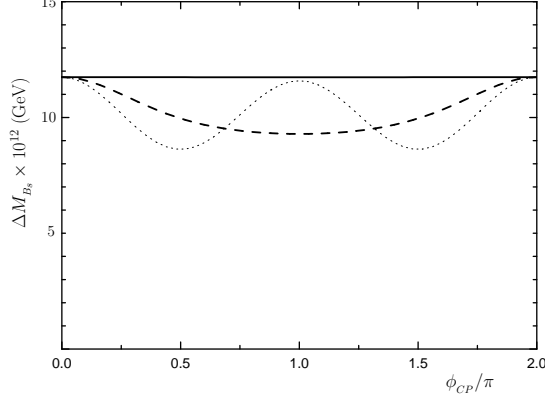


FIG. 3: Taking $\tan \beta = 20$, and $\mu_H = 300$ (GeV), ΔM_{B_s} varies with ϕ_{CP} where (a) solid line stands for $\phi_{CP} = \theta_2$ as well as $\theta_3 = \theta_t = 0$, (b) dash line stands for $\phi_{CP} = \theta_3$ as well as $\theta_2 = \theta_t = 0$, and (c) dot line stands for $\phi_{CP} = \theta_t$ as well as $\theta_2 = \theta_3 = 0$, respectively.

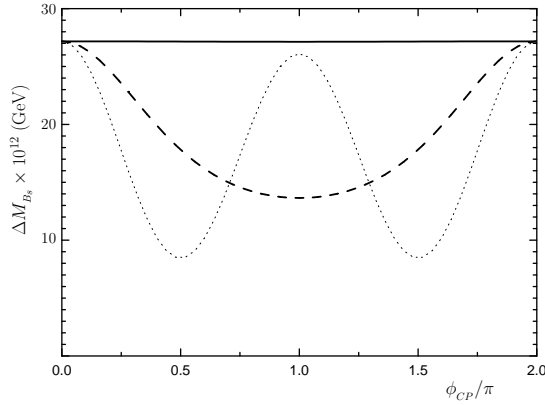


FIG. 4: Taking $\tan \beta = 50$, and $\mu_H = 100$ (GeV), ΔM_{B_s} varies with ϕ_{CP} where (a) solid line stands for $\phi_{CP} = \theta_2$ as well as $\theta_3 = \theta_t = 0$, (b) dash line stands for $\phi_{CP} = \theta_3$ as well as $\theta_2 = \theta_t = 0$, and (c) dot line stands for $\phi_{CP} = \theta_t$ as well as $\theta_2 = \theta_3 = 0$, respectively.

For the physical CKM matrix elements, we adopt the Wolfenstein parametrization and the corresponding parameters are set as $A = 0.85$, $\lambda = 0.22$, $\rho = 0.21$, $\eta = 0.34$ which stand for the central values permitted by present experiments [41]. In the hadronic sector, $m_{B_s} = 5.37\text{GeV}$, $m_B = 5.28\text{GeV}$, $m_K = 0.50\text{GeV}$, and $\tau_{B_s} = 1.46 \times 10^{-12}\text{s}$, $\tau_B = 1.54 \times 10^{-12}\text{s}$, and the decay constants are $f_B = f_{B_s} = 0.21\text{GeV}$.

Beside the constraint from the branching ratio of $BR(B \rightarrow X_s \gamma)$, other strong constraints on the new CP violating phases originate from the $\bar{B}_s - B_s$ mixing and resultant mass

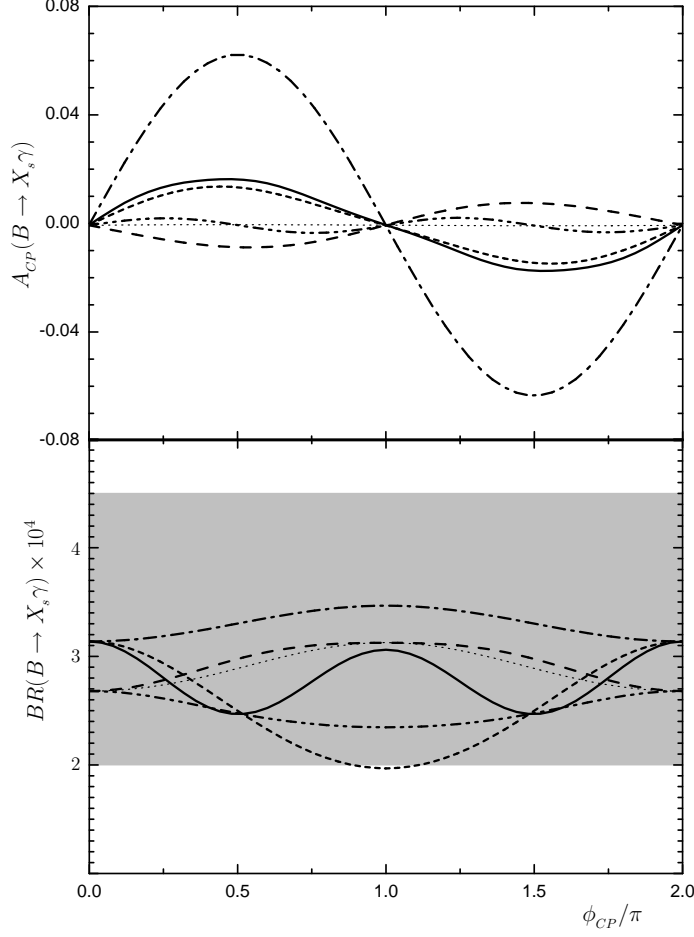


FIG. 5: $BR(B \rightarrow X_s \gamma)$ and $A_{CP}(B \rightarrow X_s \gamma)$ when $m_b^{pole} = 4.8\text{GeV}$, $\tan\beta = 20$, as well as $\mu_H = 300$ (GeV). In the figure, (a)solid line represents rigorous two loop analysis at $\phi_{CP} = \theta_2$ and $\theta_3 = \theta_t = 0$, (b)dash line represents one loop results plus threshold radiative corrections at $\phi_{CP} = \theta_2$ and $\theta_3 = \theta_t = 0$, (c)dash-dot line represents rigorous two loop analysis at $\phi_{CP} = \theta_3$ and $\theta_2 = \theta_t = 0$, (d)dotted line represents one loop results plus threshold radiative corrections at $\phi_{CP} = \theta_3$ and $\theta_2 = \theta_t = 0$, (e)short-dash line represents rigorous two loop analysis at $\phi_{CP} = \theta_t$ and $\theta_2 = \theta_3 = 0$, (f)dash-dot-dot line represents one loop results plus threshold radiative corrections at $\phi_{CP} = \theta_t$ and $\theta_2 = \theta_3 = 0$.

difference:

$$\Delta M_{B_s} > 9.48 \times 10^{-12} \text{ (GeV)}$$

as well as the mass difference in $\bar{B}_d - B_d$ mixing:

$$\Delta M_{B_d} = (3.304 \pm 0.046) \times 10^{-13} \text{ (GeV)}.$$

With $m_{H^\pm} = 300$ (GeV) and $\tan\beta \geq 10$, the theoretical estimation of the contributions to ΔM_{B_d} from the SM and two Higgs-doublet sectors fits the experimental bound very well. For the SUSY sector, the sfermion which contributes to ΔM_{B_s} , may belong to either the first generation or the third one. All the physical quantities which we are interested in, do not depend on the first generation parameters. Namely we are free to make our choice, no matter what parameters we set for the third generation of sfermions, we can assume that the new CP phases come from the first generation. Adding the SUSY contributions to that from SM and charged Higgs bosons, we still can make the total result satisfying the present experimental bound. Moreover, for the theoretical prediction on ΔM_{B_s} , we only consider the contributions of one-loop box diagrams and the threshold radiative corrections at large $\tan\beta$ [21]. Beside those parameters in the SM and two-Higgs-doublet sectors, the following supersymmetric parameters should be involved in our calculations μ_H , $m_{2,3}$, $m_{\tilde{Q}_{2,3}}$, $m_{\tilde{L}_{2,3}}$, $m_{\tilde{t}}$, $m_{\tilde{b}}$, $m_{\tilde{s}}$, as well as the trilinear Yukawa couplings A_t , A_b , A_s . So far, there are no model-independent constraints on the masses of supersymmetric particle within the framework of CP conservative MSSM. Based on the following assumptions

- $\tilde{\chi}_1^0$ ($\tilde{\gamma}$) is the lightest supersymmetric particle,
- except \tilde{t} and \tilde{b} , all scalar quarks are assumed to be degenerate in mass, i.e. $m_{\tilde{u}} = m_{\tilde{d}} = m_{\tilde{Q}}$,

with the Tevatron data, loose bounds on the Stop and Sbottom masses are found [42]

$$\begin{aligned} m_{\tilde{t}} &> 140 \text{ GeV or } < 64 \text{ GeV} , \\ m_{\tilde{b}} &> 210 \text{ GeV or } < 32 \text{ GeV} . \end{aligned} \tag{39}$$

When we take into account the effect of the supersymmetric CP phases, those bounds would be further relaxed. In spite of this fact, we still take the bounds in Eq. (39) seriously in our later numerical computations. Without losing too much generality, we fix the supersymmetric parameters as: $|m_2| = |m_3| = 300$ (GeV), $m_{\tilde{Q}_2} = m_{\tilde{L}_2} = 10$ (TeV), $m_{\tilde{s}} = 1$ (TeV), $A_s = 0$ (GeV), $m_{\tilde{Q}_3} = m_{\tilde{L}_3} = 400$ (GeV), $m_{\tilde{b}} = 500$ (GeV), and $m_{\tilde{t}} = |A_t| = |A_b| = 200$ (GeV) unless otherwise noted. Now, our numerical results should be affected by the following CP violating phases: $\theta_\mu = \arg(\mu_H)$, $\theta_2 = \arg(m_2)$, $\theta_3 = \arg(m_3)$, $\theta_t = \arg(A_t)$, $\theta_b = \arg(A_b)$. In order to reduce degrees of freedom further, we set $\theta_\mu = \theta_b = 0$. One of the reasons why we take this assumption on the parameter space is that the loop calculation for diagrams

inducing the lepton and neutron's EDMs restricts the argument to be $\theta_\mu \leq \pi/(5 \tan \beta)$ when those scalar fermions of the first generation are heavy enough. Additionally, we find that our numerical results depend on the argument θ_b rather moderately. Moreover, for the model we employ here, the mass of the lightest Higgs boson sets a strong constraint on the parameter space of the new physics. As indicated in the literature [9, 10, 11, 12, 21], the CP violation would cause changes to the neutral-Higgs-quark coupling, neutral Higgs-gauge-boson coupling and self-coupling of Higgs boson. The present experimental lower bound for the mass of the lightest Higgs boson is relaxed to 60 GeV. In our numerical analysis we take this constraint for the parameter space into account. Now, we present our numerical results item by item. Since the present experimental result of ΔM_{B_s} constrains the 'new' CP phases in our calculation strongly, we discuss the mass difference in $\bar{B}_s - B_s$ mixing firstly.

Taking $\tan \beta = 20$, $\mu_H = 300$ (GeV), we plot ΔM_{B_s} versus the CP phases ϕ_{CP} in Fig.3, where the solid line stands for $\phi_{CP} = \theta_2$ and $\theta_3 = \theta_t = 0$, the dash line stands for $\phi_{CP} = \theta_3$ as well as $\theta_2 = \theta_t = 0$, and the dot line stands for $\phi_{CP} = \theta_t$ and $\theta_2 = \theta_3 = 0$, respectively. Fig.4 is similar to Fig.3 except there $\tan \beta = 50$, $\mu_H = 100$ (GeV). Under our assumptions on the supersymmetric parameter space, the theoretical prediction on ΔM_{B_s} respects the experimental bound.

For inclusive decay $B \rightarrow X_s \gamma$, the present experimental observation on the branching ratio sets a constraint for the parameter space. Furthermore, the CP asymmetry in this process is highly sensitive to new CP violating phases because the SM contribution is only $\sim 0.5\%$. Taking $\tan \beta = 20$, $\mu_H = 300$ (GeV), we plot $BR(B \rightarrow X_s \gamma)$ and $A_{CP}(B \rightarrow X_s \gamma)$ versus the CP phases ϕ_{CP} in Fig.5, where the solid and dash lines represent $\phi_{CP} = \theta_2$ and $\theta_3 = \theta_t = 0$, the dash-dot and dot lines represent $\phi_{CP} = \theta_3$ and $\theta_2 = \theta_t = 0$, and the short-dash and dash-dot-dot lines represent $\phi_{CP} = \theta_t$ and $\theta_2 = \theta_3 = 0$, respectively. From this figure, it is easy to note that there are very obvious differences between the exact two loop analysis (solid line for $\phi_{CP} = \theta_2$, dash-dot line for $\phi_{CP} = \theta_3$, and short-dash line for $\phi_{CP} = \theta_t$, respectively) and the theoretical results which include one-loop contributions and threshold radiative corrections (dash line for $\phi_{CP} = \theta_2$, dot line for $\phi_{CP} = \theta_3$, and dash-dot-dot line for $\phi_{CP} = \theta_t$, respectively). Taking $\phi_{CP} = \theta_3$ as an example, the CP asymmetry from rigorous two loop analysis can reach 6%, and that from threshold radiative corrections is smaller than 1%, i.e. they are rather apart from each other, whereas the theoretical predictions made in the two scenarios on the branching ratios do not conflict with the present experimental

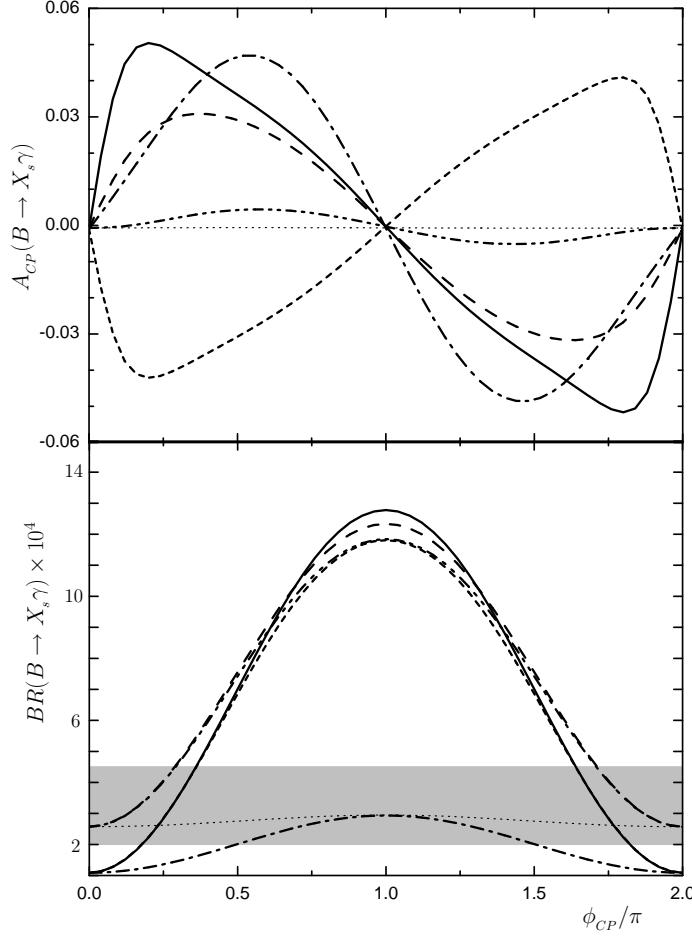


FIG. 6: $BR(B \rightarrow X_s \gamma)$ and $A_{CP}(B \rightarrow X_s \gamma)$ when $m_b^{pole} = 4.8\text{GeV}$, $\tan\beta = 50$, as well as $\mu_H = 100$ (GeV). In this figure, (a)solid line represents rigorous two loop analysis at $\phi_{CP} = \theta_2$ and $\theta_3 = \theta_t = 0$, (b)dash line represents one loop results plus threshold radiative corrections at $\phi_{CP} = \theta_2$ and $\theta_3 = \theta_t = 0$, (c)dash-dot line represents rigorous two loop analysis at $\phi_{CP} = \theta_3$ and $\theta_2 = \theta_t = 0$, (d)dotted line represents one loop results plus threshold radiative corrections at $\phi_{CP} = \theta_3$ and $\theta_2 = \theta_t = 0$, (e)short-dash line represents rigorous two loop analysis at $\phi_{CP} = \theta_t$ and $\theta_2 = \theta_3 = 0$, (f)dash-dot-dot line represents one loop results plus threshold radiative corrections at $\phi_{CP} = \theta_t$ and $\theta_2 = \theta_3 = 0$.

bound.

CP violation is induced by both Standard Model (SM) sector and SUSY sector. In the SM, the CP violating parameter $\eta = 0.34$ (in the Wolfenstein parametrization, and corresponds to the central value permitted by the present data) which indeed induces non-zero CP violation in concerned processes. Therefore, even the SUSY phase takes special values as

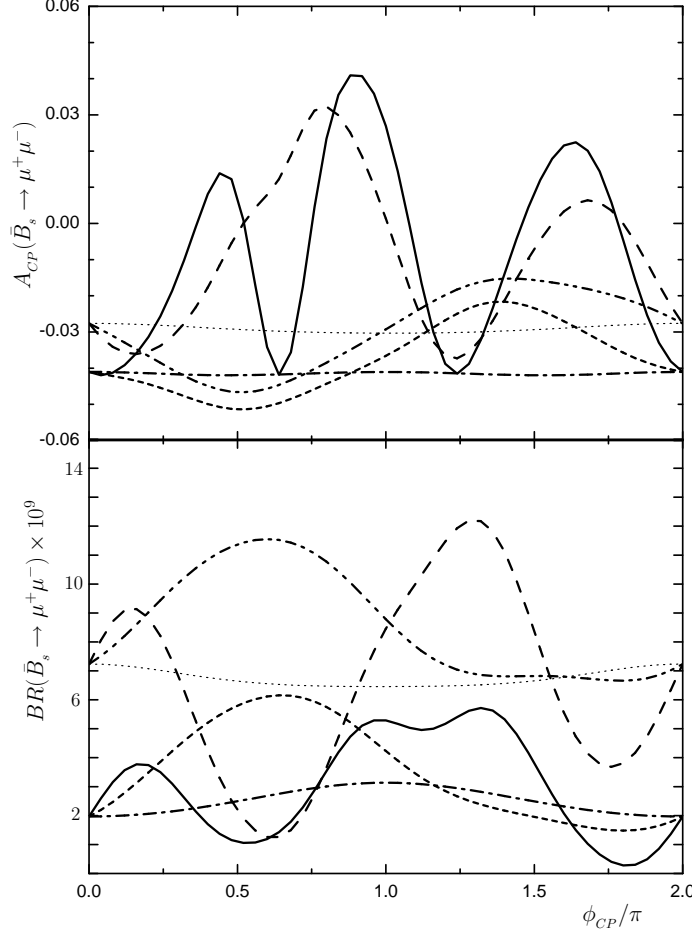


FIG. 7: $BR(\bar{B}_s \rightarrow \mu^+ \mu^-)$ and $A_{CP}(\bar{B}_s \rightarrow \mu^+ \mu^-)$ when $m_b^{pole} = 4.8\text{GeV}$, $\tan\beta = 20$ as well as $\mu_H = 300$ (GeV). In the figure (a)solid line stands for rigorous two loop analysis at $\phi_{CP} = \theta_2$ and $\theta_3 = \theta_t = 0$, (b)dash line stands for one loop results plus threshold radiative corrections at $\phi_{CP} = \theta_2$ and $\theta_3 = \theta_t = 0$, (c)dash-dot line stands for rigorous two loop analysis at $\phi_{CP} = \theta_3$ and $\theta_2 = \theta_t = 0$, (d)dotted line stands for one loop results plus threshold radiative corrections at $\phi_{CP} = \theta_3$ and $\theta_2 = \theta_t = 0$, (e)short-dash line stands for rigorous two loop analysis at $\phi_{CP} = \theta_t$ and $\theta_2 = \theta_3 = 0$, (f)dash-dot-dot line stands for one loop results plus threshold radiative corrections at $\phi_{CP} = \theta_t$ and $\theta_2 = \theta_3 = 0$.

$\phi_{CP} = 0, \pi, 2\pi$, CP asymmetry may still exist. However, for the process $B \rightarrow X_s \gamma$, the CP violation induced by the SM η is much smaller than 1%, by contraries, for the rare decay $B_s \rightarrow l^+ l^-$, the η -induced CP asymmetry is greater than 1%, and the effect is expected to be observable even as the SUSY phase $\phi_{CP} = 0, \pi, 2\pi$ and does not contribute. In a word, the process $B \rightarrow X_s \gamma$ provides a window for detecting the new CP sources beside that

existing in the CKM matrix.

Similar to Fig.5 except for $\tan\beta = 50$, $\mu_H = 100$ (GeV), we plot $BR(B \rightarrow X_s \gamma)$ and $A_{CP}(B \rightarrow X_s \gamma)$ versus the CP phases ϕ_{CP} in Fig.6. With the setting for the parameter space, the branching ratio $BR(B \rightarrow X_s \gamma)$ varies drastically with the CP phases $\phi_{CP} = \theta_{2,t}$, but depends on the CP phase $\phi_{CP} = \theta_3$ very gently. At $\phi_{CP} = \theta_2 = \pi/4$, the CP asymmetry of rigorous two loop analysis can reach 5%, and that of threshold radiative corrections is about 3%, meanwhile the theoretical predictions on the branching ratios in both scenarios satisfy the present experimental bound. When $\phi_{CP} = \theta_{3,t}$, the CP asymmetry from the strict two loop analysis can reach 4%, and that from threshold radiative corrections is less than 1%.

Now, we present our numerical results on the rare decays $\bar{B}_s \rightarrow l^+ l^-$, ($l = \mu, \tau$). The present experimental upper bound on the branching ratio is $BR(\bar{B}_s \rightarrow \mu^+ \mu^-) \leq 1.5 \times 10^{-7}$ at 90% C.L. [43]. Taking $\tan\beta = 20$, $\mu_H = 300$ (GeV), we plot $BR(\bar{B}_s \rightarrow \mu^+ \mu^-)$ and $A_{CP}(\bar{B}_s \rightarrow \mu^+ \mu^-)$ versus the CP phases ϕ_{CP} in Fig.7, where the solid and dash lines stand for $\phi_{CP} = \theta_2$ and $\theta_3 = \theta_t = 0$, the dash-dot and dot lines stand for $\phi_{CP} = \theta_3$ and $\theta_2 = \theta_t = 0$, and the short-dash and dash-dot-dot lines stand for $\phi_{CP} = \theta_t$ and $\theta_2 = \theta_3 = 0$, respectively. From this figure, it is easy to find that there are evident differences between exact two loop analysis (solid line for $\phi_{CP} = \theta_2$, dash-dot line for $\phi_{CP} = \theta_3$, and short-dash line for $\phi_{CP} = \theta_t$, respectively) and the theoretical results which originate from one-loop calculations plus threshold radiative corrections (dash line for $\phi_{CP} = \theta_2$, dot line for $\phi_{CP} = \theta_3$, and dash-dot-dot line for $\phi_{CP} = \theta_t$, respectively). For $\phi_{CP} = \theta_2 \simeq 3\pi/2$, the theoretical prediction on the branching ratio $BR(\bar{B}_s \rightarrow \mu^+ \mu^-)$ from one loop results plus threshold radiative corrections (dash line) can reach 1.2×10^{-8} approximately, the exact two loop analysis (solid line) modifies the branching ratio to 5×10^{-9} , and the CP asymmetry $A_{CP}(\bar{B}_s \rightarrow \mu^+ \mu^-)$ is about 3%. However, it is very difficult to detect this CP asymmetry $A_{CP}(\bar{B}_s \rightarrow \mu^+ \mu^-)$ in near future experiments with such a small branching ratio. As indicated above, the SM CP-odd parameter $\eta = 0.34$ (in Wolfstein parametrization) induces a non-vanishing CP asymmetry when supersymmetric CP phases $\phi_{CP} = 0, \pi, 2\pi$.

For larger $\tan\beta$, the situation is drastically different. Taking $\tan\beta = 50$, $\mu_H = 100$ (GeV), we plot $BR(\bar{B}_s \rightarrow \mu^+ \mu^-)$ and $A_{CP}(\bar{B}_s \rightarrow \mu^+ \mu^-)$ versus the CP phases ϕ_{CP} in Fig.8. Clearly, there are obvious differences between the results of one loop contribution plus threshold radiative corrections and that of corresponding rigorous two loop calculations.

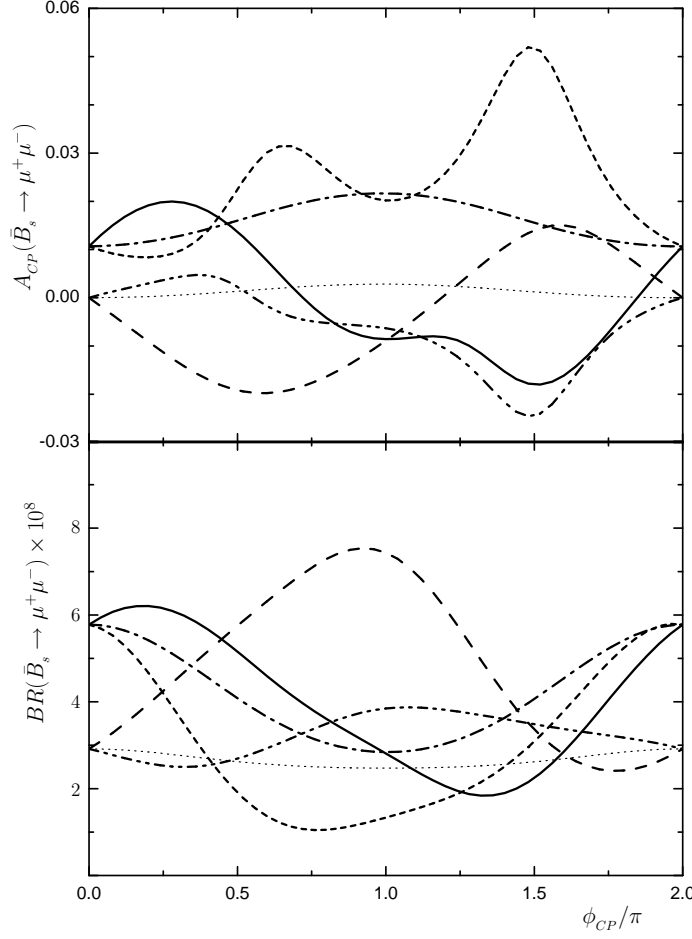


FIG. 8: $BR(\bar{B}_s \rightarrow \mu^+ \mu^-)$ and $A_{CP}(\bar{B}_s \rightarrow \mu^+ \mu^-)$ when $m_b^{pole} = 4.8\text{GeV}$, $\tan\beta = 50$ as well as $\mu_H = 100$ (GeV). In the figure, (a)solid line stands for rigorous two loop analysis at $\phi_{CP} = \theta_2$ and $\theta_3 = \theta_t = 0$, (b)dash line stands for one loop results plus threshold radiative corrections at $\phi_{CP} = \theta_2$ and $\theta_3 = \theta_t = 0$, (c)dash-dot line stands for rigorous two loop analysis at $\phi_{CP} = \theta_3$ and $\theta_2 = \theta_t = 0$, (d)dotted line stands for one loop results plus threshold radiative corrections at $\phi_{CP} = \theta_3$ and $\theta_2 = \theta_t = 0$, (e)short-dash line stands for rigorous two loop analysis at $\phi_{CP} = \theta_t$ and $\theta_2 = \theta_3 = 0$, (f)dash-dot-dot line stands for one loop results plus threshold radiative corrections at $\phi_{CP} = \theta_t$ and $\theta_2 = \theta_3 = 0$.

Additionally, the rigorous two loop prediction on the branching ratio $BR(\bar{B}_s \rightarrow \mu^+ \mu^-)$ surpasses 10^{-8} . Assuming the CP asymmetry to be induced by the CP phase $\phi_{CP} = \theta_t$, the two loop result for the CP asymmetry $A_{CP}(\bar{B}_s \rightarrow \mu^+ \mu^-)$ is about 5%, and the corresponding branching ratio is about 4×10^{-8} . Although it is very challenging, this CP asymmetry could be hopefully measured in forthcoming experiments.

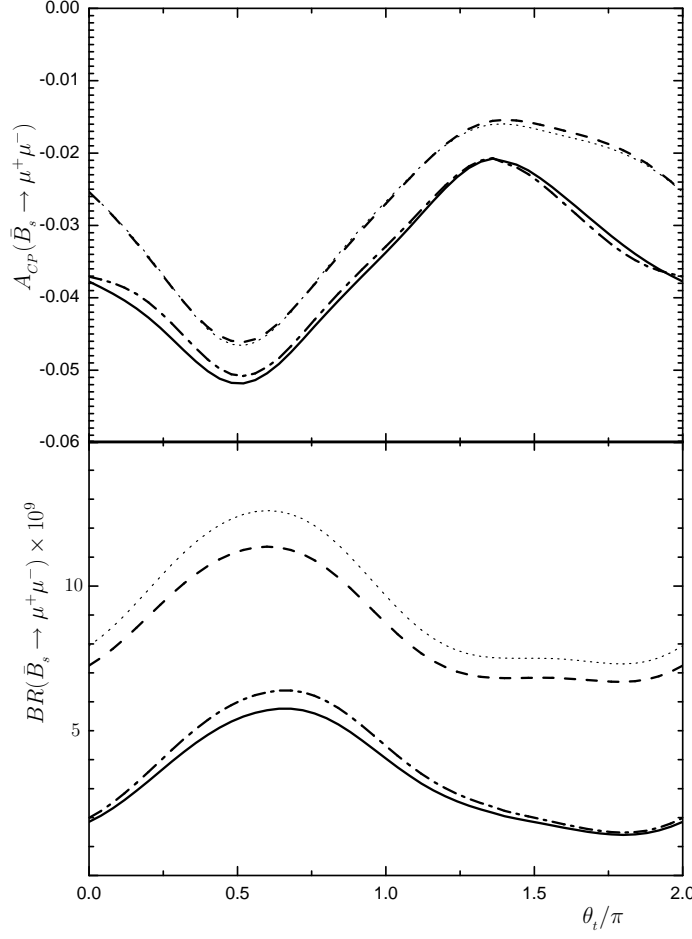


FIG. 9: Taking $\tan\beta = 20$, $\mu_H = 300$ (GeV), the branching ratio $BR(\bar{B}_s \rightarrow \mu^+\mu^-)$ and CP asymmetry $A_{CP}(\bar{B}_s \rightarrow \mu^+\mu^-)$ vary with the CP phase $\phi_{CP} = \theta_2$, where (a) solid line represents rigorous two-loop analysis with $m_b^{pole} = 4.6$ (GeV), (b) dash line represents one-loop result plus threshold radiative correction with $m_b^{pole} = 4.6$ (GeV), (c) dash-dot line represents rigorous two-loop analysis with $m_b^{pole} = 4.9$ (GeV), (d) dot line represents one-loop result plus threshold radiative correction with $m_b^{pole} = 4.9$ (GeV).

In Fig.7 and Fig.8, we choose the pole mass of b-quark as $m_b^{pole} = 4.8$ (GeV). Since the hadronic matrix elements depend on b-quark mass, we let m_b vary within a certain range which is allowed by the data and see how it affects the branching ratio $BR(\bar{B}_s \rightarrow \mu^+\mu^-)$ and the CP asymmetry $A_{CP}(\bar{B}_s \rightarrow \mu^+\mu^-)$. Taking $\tan\beta = 20$, $\mu_H = 300$ (GeV), we plot the branching ratio $BR(\bar{B}_s \rightarrow \mu^+\mu^-)$ and CP asymmetry $A_{CP}(\bar{B}_s \rightarrow \mu^+\mu^-)$ versus $\phi_{CP} = \theta_2$ in Fig.9. To investigate the impact of the b-quark mass on the measurable quantities, in the figure, we set it as $m_b^{pole} = 4.6$, and 4.9 (GeV), which correspond to the minimal

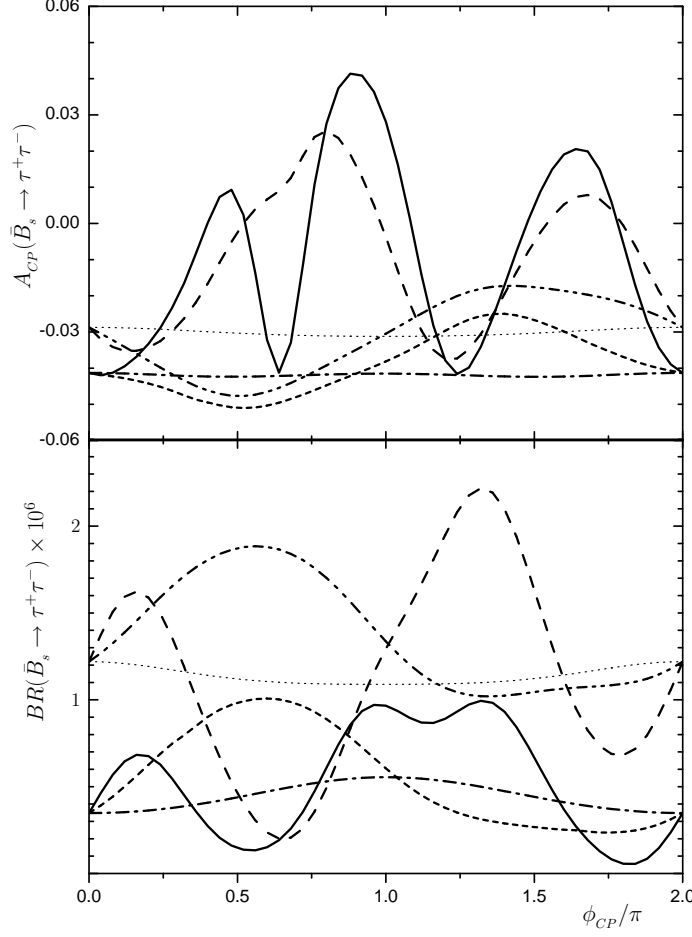


FIG. 10: $BR(\bar{B}_s \rightarrow \tau^+\tau^-)$ and $A_{CP}(\bar{B}_s \rightarrow \tau^+\tau^-)$ when $m_b^{pole} = 4.8\text{GeV}$, $\tan\beta = 20$ as well as $\mu_H = 300$ (GeV). In the figure, (a)solid line represents rigorous two loop analysis at $\phi_{CP} = \theta_2$ and $\theta_3 = \theta_t = 0$, (b)dash line represents one loop results plus threshold radiative corrections at $\phi_{CP} = \theta_2$ and $\theta_3 = \theta_t = 0$, (c)dash-dot line represents rigorous two loop analysis at $\phi_{CP} = \theta_3$ and $\theta_2 = \theta_t = 0$, (d)dotted line represents one loop results plus threshold radiative corrections at $\phi_{CP} = \theta_3$ and $\theta_2 = \theta_t = 0$, (e)short-dash line represents rigorous two loop analysis at $\phi_{CP} = \theta_t$ and $\theta_2 = \theta_3 = 0$, (f)dash-dot-dot line represents one loop results plus threshold radiative corrections at $\phi_{CP} = \theta_t$ and $\theta_2 = \theta_3 = 0$.

and maximal values permitted by the present experiments respectively. Particularly, the branching ratio $BR(\bar{B}_s \rightarrow \mu^+\mu^-)$ is relatively more sensitive to the b-quark mass. The present experimental errors approximately result in 5% theoretical uncertainty. As for the CP asymmetry $A_{CP}(\bar{B}_s \rightarrow \mu^+\mu^-)$, the corresponding theoretical uncertainty is only about 2%.

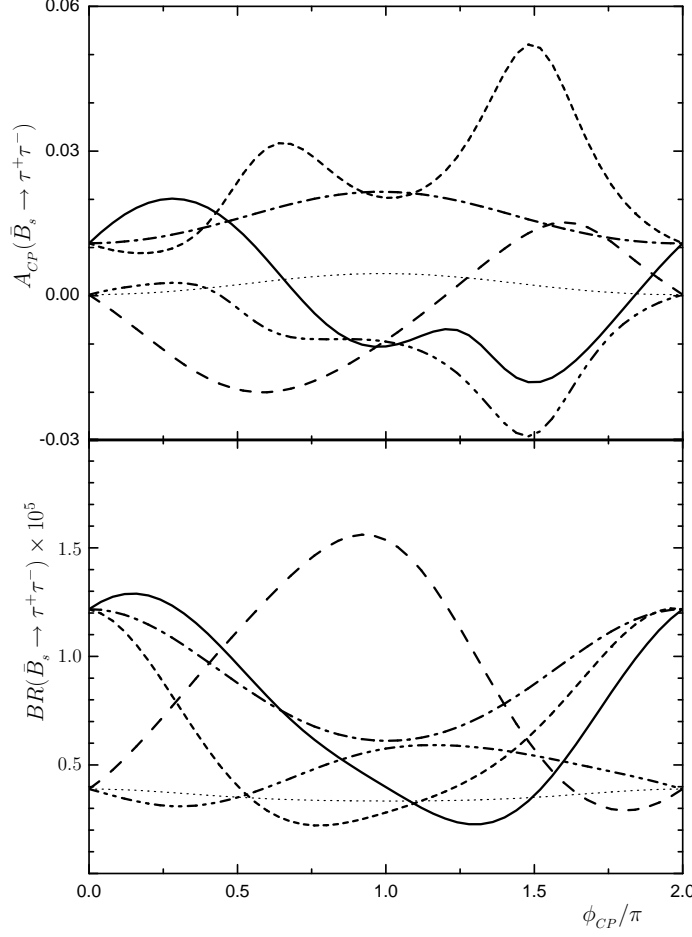


FIG. 11: $BR(\bar{B}_s \rightarrow \tau^+\tau^-)$ and $A_{CP}(\bar{B}_s \rightarrow \tau^+\tau^-)$ when $m_b^{pole} = 4.8\text{GeV}$, $\tan\beta = 50$ as well as $\mu_H = 100$ (GeV). In the figure, (a) solid line represents rigorous two loop analysis at $\phi_{CP} = \theta_2$ and $\theta_3 = \theta_t = 0$, (b) dash line represents one loop results plus threshold radiative corrections at $\phi_{CP} = \theta_2$ and $\theta_3 = \theta_t = 0$, (c) dash-dot line represents rigorous two loop analysis at $\phi_{CP} = \theta_3$ and $\theta_2 = \theta_t = 0$, (d) dot line represents one loop results plus threshold radiative corrections at $\phi_{CP} = \theta_3$ and $\theta_2 = \theta_t = 0$, (e) short-dash line represents rigorous two loop analysis at $\phi_{CP} = \theta_t$ and $\theta_2 = \theta_3 = 0$, (f) dash-dot-dot line represents one loop results plus threshold radiative corrections at $\phi_{CP} = \theta_t$ and $\theta_2 = \theta_3 = 0$.

Comparing with $BR(\bar{B}_s \rightarrow \mu^+\mu^-)$, the branching ratio $BR(\bar{B}_s \rightarrow \tau^+\tau^-)$ is enhanced strongly because τ mass is much heavier than μ mass. Taking $\tan\beta = 20$, $\mu_H = 300$ (GeV), we plot $BR(\bar{B}_s \rightarrow \tau^+\tau^-)$ and $A_{CP}(\bar{B}_s \rightarrow \tau^+\tau^-)$ versus the CP phases ϕ_{CP} in Fig.10. We find that the exact two loop predictions on the branching ratio $BR(\bar{B}_s \rightarrow \tau^+\tau^-)$ can reach $\sim 10^{-6}$ approximately, and the CP asymmetry $A_{CP}(\bar{B}_s \rightarrow \tau^+\tau^-)$ is about $\pm 3\%$ correspondingly.

When $\tan\beta = 50$, the branching ratio $BR(\bar{B}_s \rightarrow \tau^+\tau^-)$ is enhanced further. We plot $BR(\bar{B}_s \rightarrow \tau^+\tau^-)$ and $A_{CP}(\bar{B}_s \rightarrow \tau^+\tau^-)$ versus the CP phases $\phi_{CP} = \theta_{2,3,t}$ in Fig.11, with $\tan\beta = 50$, $\mu_H = 100$ (GeV). Assuming that the CP asymmetry is induced by the complex trilinear coupling A_t , the two loop theoretical prediction on the branching ratio $BR(\bar{B}_s \rightarrow \tau^+\tau^-)$ is about 8×10^{-6} , whereas $A_{CP}(\bar{B}_s \rightarrow \tau^+\tau^-) \simeq 5\%$ at $\theta_t = 3\pi/2$. Certainly, it is difficult to experimentally measure the rare decay $\bar{B}_s \rightarrow \tau^+\tau^-$. Similarly, the present experimental error for b-quark mass causes a theoretical uncertainties of $\sim 5\%$ for $BR(\bar{B}_s \rightarrow \tau^+\tau^-)$, and $\sim 2\%$ for $A_{CP}(\bar{B}_s \rightarrow \tau^+\tau^-)$ respectively.

We now discuss the branching ratio and forward-backward asymmetry in decays $\bar{B} \rightarrow Kl^+l^-$ ($l = \mu, \tau$). The form factors for $\bar{B} \rightarrow Kl^+l^-$ ($l = \mu, \tau$) decays are given in Table.I which correspond to the central values presented in [40].

$f_0(0)$	$f_+(0)$	$f_T(0)$	c_1^0	c_1^+	c_1^T	c_2^0	c_2^+	c_2^T	c_3^0	c_3^+	c_3^T
0.319	0.319	0.355	0.633	1.465	1.478	-0.095	0.372	0.373	0.591	0.782	0.700

TABLE I: The parameters for the parametrization Eq.31, they correspond to the central values presented in Ref.[40].

Taking $\tan\beta = 50$, $\mu_H = 100$ (GeV), we plot $BR(\bar{B} \rightarrow K\mu^+\mu^-)$ and $\langle A_{FB} \rangle (\bar{B} \rightarrow K\mu^+\mu^-)$ versus the various CP phases ϕ_{CP} in Fig.12, where the solid and dash lines stand for $\phi_{CP} = \theta_2$ and $\theta_3 = \theta_t = 0$, the dash-dot and dot lines stand for $\phi_{CP} = \theta_3$ and $\theta_2 = \theta_t = 0$, and the short-dash and dash-dot-dot lines stand for $\phi_{CP} = \theta_t$ and $\theta_2 = \theta_3 = 0$, respectively. This figure explicitly indicates that there are also obvious differences between the strict two loop results (solid line for $\phi_{CP} = \theta_2$, dash-dot line for $\phi_{CP} = \theta_3$, and short-dash line for $\phi_{CP} = \theta_t$, respectively) and the theoretical predictions which come from one-loop contributions plus threshold radiative corrections (dash line for $\phi_{CP} = \theta_2$, dot line for $\phi_{CP} = \theta_3$, and dash-dot-dot line for $\phi_{CP} = \theta_t$, respectively). It is noted that although the branching ratio $BR(\bar{B} \rightarrow K\mu^+\mu^-)$ can reach 3×10^{-7} , the average forward-backward asymmetry is too small to be detected in any forthcoming experiment.

Probably, the most interesting object to study is the rare decay $\bar{B} \rightarrow K\tau^+\tau^-$ because the average forward-backward asymmetry $\langle A_{FB} \rangle (\bar{B} \rightarrow K\tau^+\tau^-)$ is much larger than $\langle A_{FB} \rangle (\bar{B} \rightarrow K\mu^+\mu^-)$. Taking $\tan\beta = 20$, $\mu_H = 300$ (GeV), we plot $BR(\bar{B} \rightarrow K\tau^+\tau^-)$ and $\langle A_{FB} \rangle (\bar{B} \rightarrow K\tau^+\tau^-)$ versus the CP phases ϕ_{CP} in Fig.13. Certainly, there are

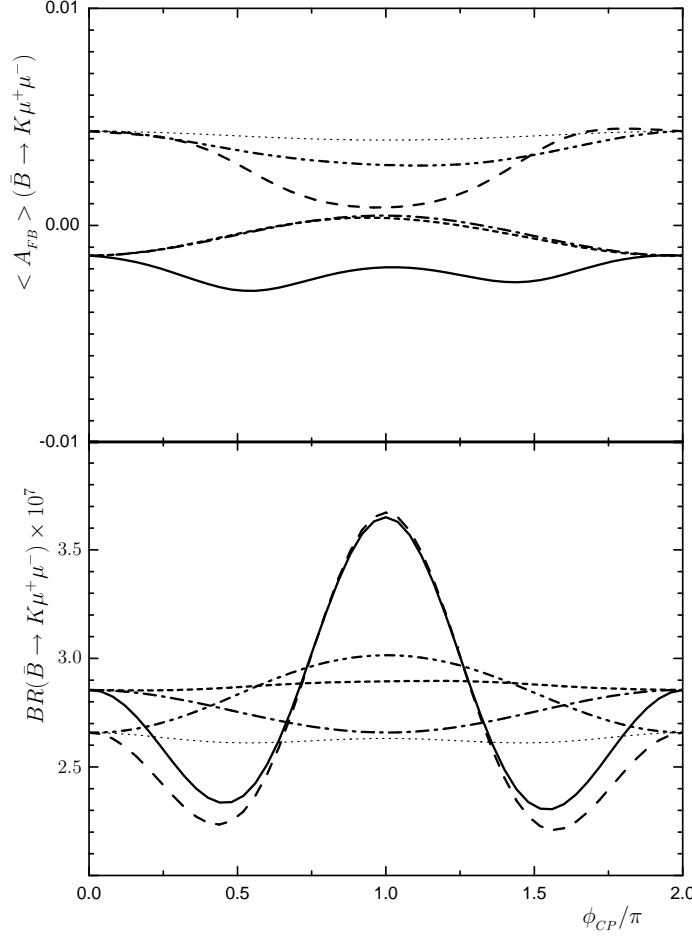


FIG. 12: $BR(\bar{B} \rightarrow K\mu^+\mu^-)$ and $A_{CP}(\bar{B} \rightarrow K\mu^+\mu^-)$ when $m_b^{pole} = 4.8\text{GeV}$, $\tan\beta = 50$ as well as $\mu_H = 100$ (GeV). In the figure, (a) solid line stands for rigorous two loop analysis at $\phi_{CP} = \theta_2$ and $\theta_3 = \theta_t = 0$, (b) dash line stands for one loop results plus threshold radiative corrections at $\phi_{CP} = \theta_2$ and $\theta_3 = \theta_t = 0$, (c) dash-dot line stands for rigorous two loop analysis at $\phi_{CP} = \theta_3$ and $\theta_2 = \theta_t = 0$, (d) dot line stands for one loop results plus threshold radiative corrections at $\phi_{CP} = \theta_3$ and $\theta_2 = \theta_t = 0$, (e) short-dash line stands for rigorous two loop analysis at $\phi_{CP} = \theta_t$ and $\theta_2 = \theta_3 = 0$, (f) dash-dot-dot line stands for one loop results plus threshold radiative corrections at $\phi_{CP} = \theta_t$ and $\theta_2 = \theta_3 = 0$.

evident differences between the theoretical prediction of the exact two loop calculations and that of one loop result plus threshold radiative corrections. When $\phi_{CP} = \theta_t = \pi/2$, if considering the one loop contributions plus threshold radiative corrections, one can have the branching ratio as $BR(\bar{B} \rightarrow K\tau^+\tau^-) \simeq 10^{-7}$, whereas the strict two-loop calculations modify it to 8×10^{-8} . The average forward-backward asymmetries $\langle A_{FB} \rangle(\bar{B} \rightarrow K\tau^+\tau^-)$

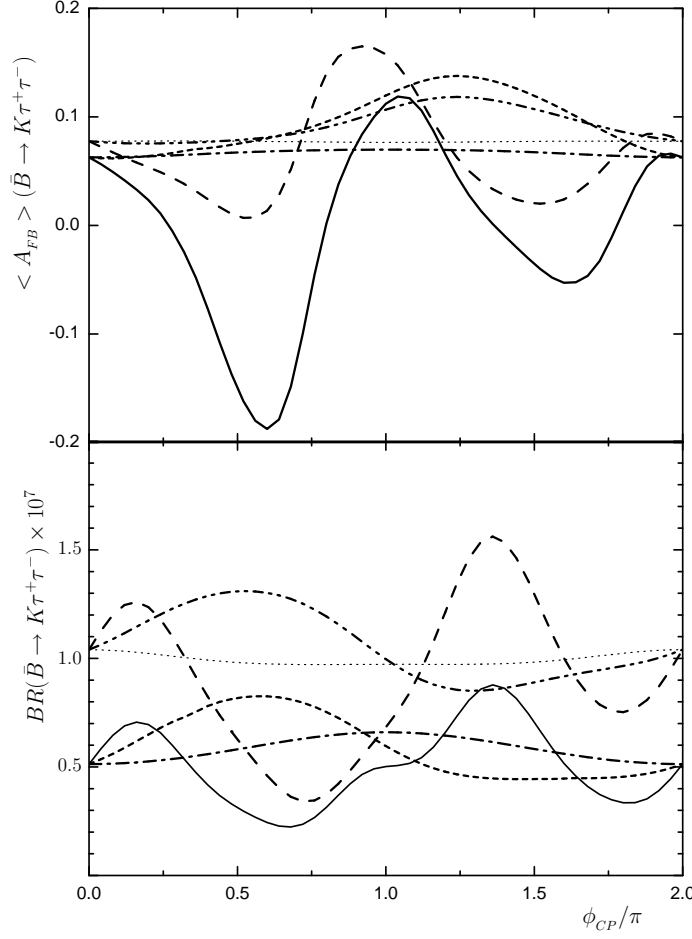


FIG. 13: $BR(\bar{B} \rightarrow K\tau^+\tau^-)$ and $A_{CP}(\bar{B} \rightarrow K\tau^+\tau^-)$ when $m_b^{pole} = 4.8\text{GeV}$, $\tan\beta = 20$ as well as $\mu_H = 300$ (GeV). In this figure, (a) solid line stands for rigorous two loop analysis at $\phi_{CP} = \theta_2$ and $\theta_3 = \theta_t = 0$, (b) dash line stands for one loop results plus threshold radiative corrections at $\phi_{CP} = \theta_2$ and $\theta_3 = \theta_t = 0$, (c) dash-dot line stands for rigorous two loop analysis at $\phi_{CP} = \theta_3$ and $\theta_2 = \theta_t = 0$, (d) dot line stands for one loop results plus threshold radiative corrections at $\phi_{CP} = \theta_3$ and $\theta_2 = \theta_t = 0$, (e) short-dash line stands for rigorous two loop analysis at $\phi_{CP} = \theta_t$ and $\theta_2 = \theta_3 = 0$, (f) dash-dot-dot line stands for one loop results plus threshold radiative corrections at $\phi_{CP} = \theta_t$ and $\theta_2 = \theta_3 = 0$.

are about 10% for both cases. For $\tan\beta = 50$, the branching ratio is enhanced further. When $\tan\beta = 50$, $\mu_H = 100$ (GeV) (Fig.14), the exact two loop calculations predict the branching ratio as $BR(\bar{B} \rightarrow K\tau^+\tau^-) \sim 5 \times 10^{-7}$, meanwhile the average forward-backward asymmetry $\langle A_{FB} \rangle(\bar{B} \rightarrow K\tau^+\tau^-) \sim 20\%$. If we can accumulate 10^{10} B mesons in experiments, one would be able to detect this asymmetry.

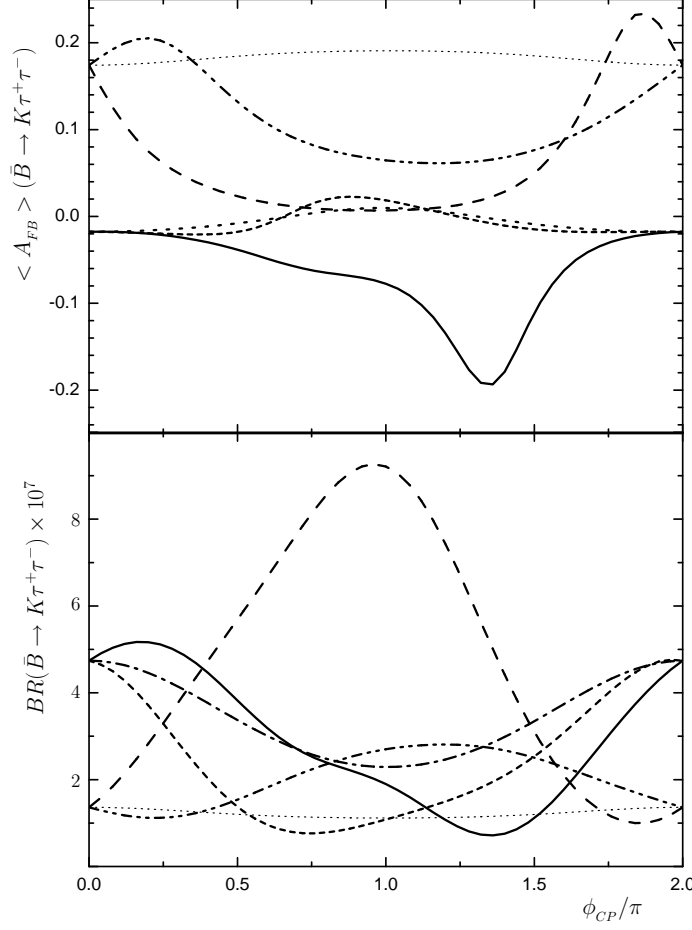


FIG. 14: $BR(\bar{B} \rightarrow K\tau^+\tau^-)$ and $A_{CP}(\bar{B} \rightarrow K\tau^+\tau^-)$ when $m_b^{pole} = 4.8\text{GeV}$, $\tan\beta = 50$ as well as $\mu_H = 100$ (GeV). In this figure, (a) solid line stands for rigorous two loop analysis at $\phi_{CP} = \theta_2$ and $\theta_3 = \theta_t = 0$, (b) dash line stands for one loop results plus threshold radiative corrections at $\phi_{CP} = \theta_2$ and $\theta_3 = \theta_t = 0$, (c) dash-dot line stands for rigorous two loop analysis at $\phi_{CP} = \theta_3$ and $\theta_2 = \theta_t = 0$, (d) dot line stands for one loop results plus threshold radiative corrections at $\phi_{CP} = \theta_3$ and $\theta_2 = \theta_t = 0$, (e) short-dash line stands for rigorous two loop analysis at $\phi_{CP} = \theta_t$ and $\theta_2 = \theta_3 = 0$, (f) dash-dot-dot line stands for one loop results plus threshold radiative corrections at $\phi_{CP} = \theta_t$ and $\theta_2 = \theta_3 = 0$.

In Fig.13 and Fig.14, we take the pole mass of b-quark as $m_b^{pole} = 4.8$ (GeV). The hadronic matrix elements depend on concrete values of b-quark mass. Taking $\tan\beta = 20$, $\mu_H = 300$ (GeV), we plot the branching ratio $BR(\bar{B} \rightarrow K\tau^+\tau^-)$ and the average forward-backward asymmetry $\langle A_{FB} \rangle(\bar{B} \rightarrow K\tau^+\tau^-)$ versus $\phi_{CP} = \theta_2$ in Fig.15. As for the b-quark mass, we set it as $m_b^{pole} = 4.6$ and 4.9 (GeV) respectively. Particularly, the

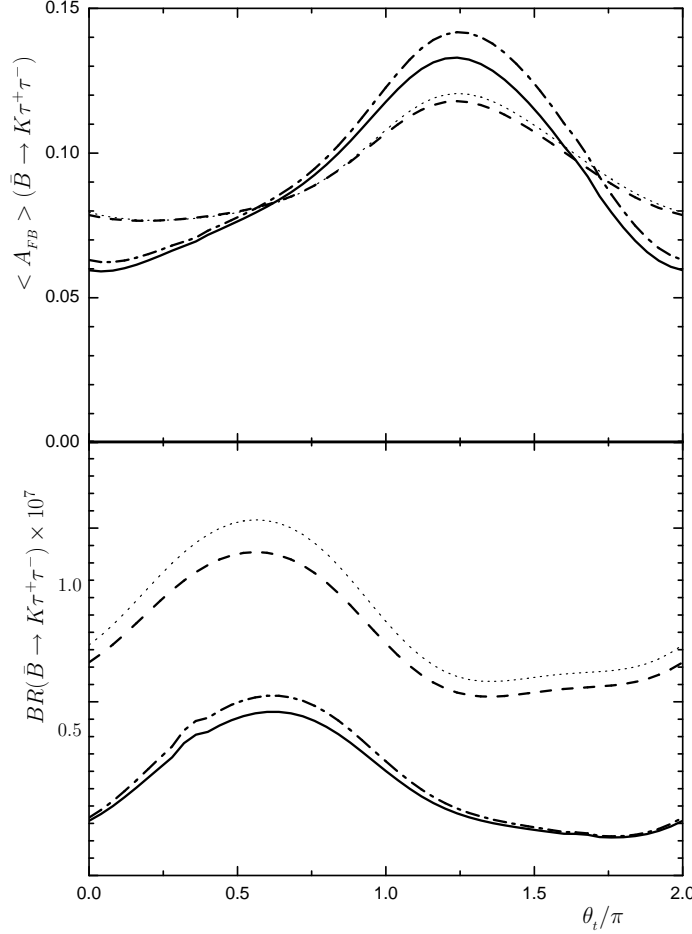


FIG. 15: Taking $\tan\beta = 20$ as well as $\mu_H = 300$ (GeV), the branching ratio $BR(\bar{B} \rightarrow K\tau^+\tau^-)$ and average forward-backward asymmetry $A_{FB}(\bar{B} \rightarrow K\tau^+\tau^-)$ vary with the CP phase $\phi_{CP} = \theta_2$, where (a)solid line represents rigorous two-loop analysis with $m_b^{pole} = 4.6$ (GeV); (b)dash line represents one-loop result plus threshold radiative correction with $m_b^{pole} = 4.6$ (GeV); (c)dash-dot line represents rigorous two-loop analysis with $m_b^{pole} = 4.9$ (GeV); (d)dot line represents one-loop result plus threshold radiative correction with $m_b^{pole} = 4.9$ (GeV).

experimental uncertainty for the b-quark mass leads to a theoretical uncertainty of $\sim 5\%$ for the branching ratio $BR(\bar{B} \rightarrow K\tau^+\tau^-)$, and $\sim 2\%$ for the average forward-backward asymmetry $\langle A_{FB} \rangle(\bar{B} \rightarrow K\tau^+\tau^-)$.

The present experimental upper bound of $BR(\bar{B}_s \rightarrow \mu^+\mu^-) < 1.5 \times 10^{-7}$ sets a stringent restriction on the supersymmetric parameter space. Along with the improvement of experimental precision and the accumulation of experimental data, this upper bound will be further modified. If so, we can expect that the new upper bound may lead to a concrete

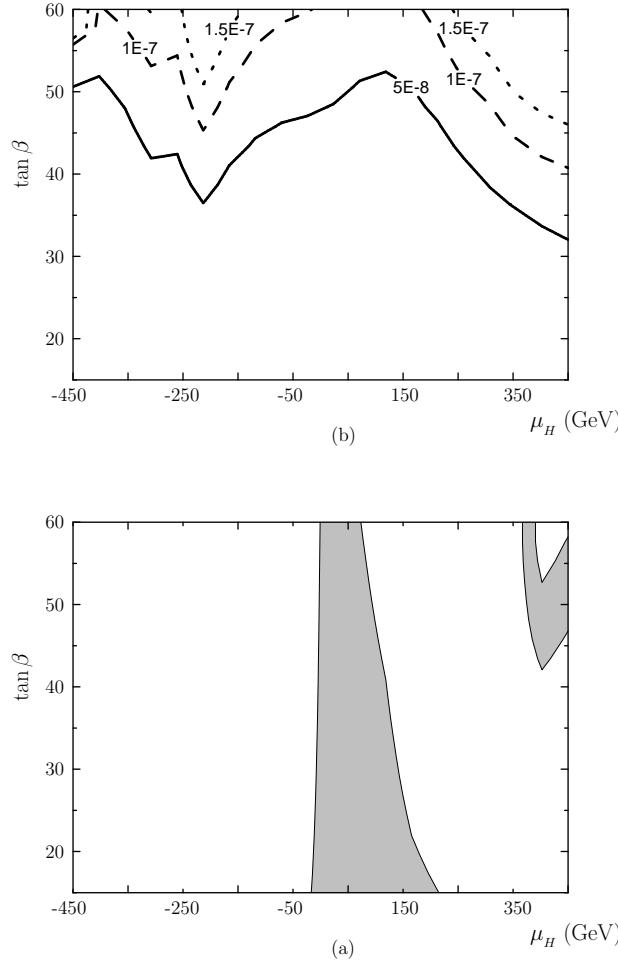


FIG. 16: Taking $m_b^{pole} = 4.8\text{GeV}$, $\theta_2 = \theta_3 = \theta_t = 0$, the correlation between μ_H and $\tan \beta$. In this figure, (a) the gray regions are permitted by the experimental bound on the branching ratio $BR(B \rightarrow X_s \gamma)$, (b) solid line represents $BR(\bar{B}_s \rightarrow \mu^+ \mu^-) = 5 \times 10^{-8}$, dash line represents $BR(\bar{B}_s \rightarrow \mu^+ \mu^-) = 10^{-7}$ and dot line represents $BR(\bar{B}_s \rightarrow \mu^+ \mu^-) = 1.5 \times 10^{-7}$.

constraint on the parameter space of our model. Using the exact two loop results, we plot the correlation of μ_H and $\tan \beta$ with the bound of the branching ratio $BR(B \rightarrow X_s \gamma)$ at $\theta_2 = \theta_3 = \theta_t = 0$ in Fig.16 (a). The gray region is permitted by the present experiments. Corresponding to the two loop results for the branching ratios of $BR(\bar{B}_s \rightarrow \mu^+ \mu^-)$, we plot the correlation between μ_H and $\tan \beta$ in Fig. 16 (b). Similar to Fig. 16 except for $\theta_t = \pi/2$, we plot the correlation of μ_H and $\tan \beta$ with the bound of the branching ratio $BR(B \rightarrow X_s \gamma)$ in Fig.17 (a). and possible new upper bound on the branching ratio $BR(\bar{B}_s \rightarrow \mu^+ \mu^-)$ (Fig. 17(b)). When $\theta_t = 0$, the rare decay $\bar{B}_s \rightarrow \mu^+ \mu^-$ will lead to a concrete constraint on the parameter space if the new experimental upper bound on the branching ratio $BR(\bar{B}_s \rightarrow \mu^+ \mu^-)$

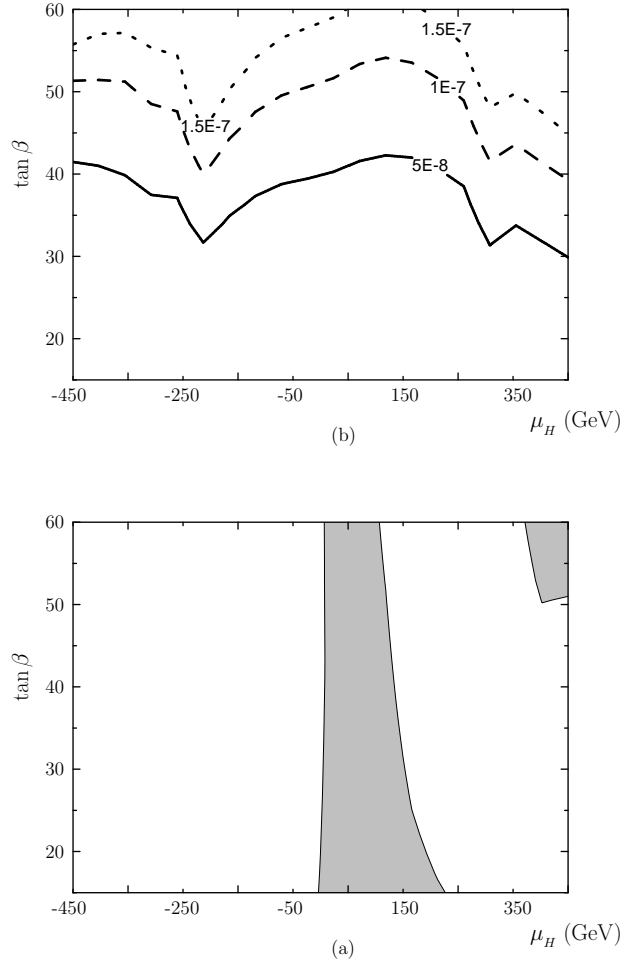


FIG. 17: Taking $m_b^{pole} = 4.8\text{GeV}$, $\theta_2 = \theta_3 = 0$, $\theta_t = \pi/2$, the correlation between μ_H and $\tan \beta$. In the figure, (a) the gray regions are permitted by the experimental bound on the branching ratio $BR(B \rightarrow X_s \gamma)$, (b) solid line represents $BR(\bar{B}_s \rightarrow \mu^+ \mu^-) = 5 \times 10^{-8}$, dash line represents $BR(\bar{B}_s \rightarrow \mu^+ \mu^-) = 10^{-7}$ and dot line represents $BR(\bar{B}_s \rightarrow \mu^+ \mu^-) = 1.5 \times 10^{-7}$.

reaches 10^{-7} . As for the case $\theta_t = \pi/2$, the branching ratio $BR(\bar{B}_s \rightarrow \mu^+ \mu^-)$ at 10^{-7} level will raise a stronger constraint on the model discussed here. Certainly, we plot Fig. 16 and Fig. 17 under the hypothesis that the scalar quarks of the third generation are relatively light. If we push the scalar quark masses of the third generation to $\geq 1\text{TeV}$, the situation would change drastically. Here we do not discuss such cases any further.

Now let us simply discuss the dependance of the branching ratios and CP asymmetries (or forward-back asymmetries) on squark masses in the rare processes $\bar{B}_s \rightarrow l^+ l^-$ and $\bar{B} \rightarrow Kl^+ l^-$. Taking $\tan \beta = 40$ and $\mu_H = -50$ (GeV), we plot the branching ratio $BR(\bar{B}_s \rightarrow \mu^+ \mu^-)$ as well as the CP asymmetry $A_{CP}(\bar{B}_s \rightarrow \mu^+ \mu^-)$ versus the mass of right handed

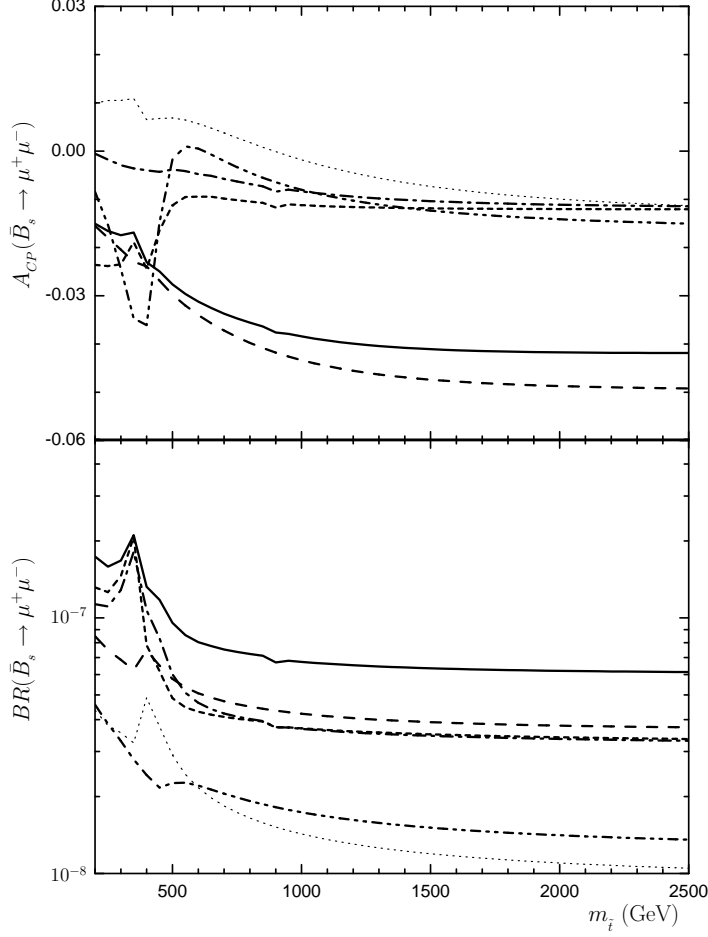


FIG. 18: Dependence of the branching ratio $BR(\bar{B}_s \rightarrow \mu^+\mu^-)$ and CP asymmetry $A_{CP}(\bar{B}_s \rightarrow \mu^+\mu^-)$ on the right handed scalar quark mass $m_{\tilde{t}}$, with $\tan\beta = 40$ and $\mu_H = -50$ (GeV). In this figure, (a)solid line stands for rigorous two loop analysis at $\theta_2 = \pi/2$ and $\theta_3 = \theta_t = 0$, (b)dash line stands for one loop results plus threshold radiative corrections at $\theta_2 = \pi/2$ and $\theta_3 = \theta_t = 0$, (c)dash-dot line stands for rigorous two loop analysis at $\theta_3 = \pi/2$ and $\theta_2 = \theta_t = 0$, (d)dotted line stands for one loop results plus threshold radiative corrections at $\theta_3 = \pi/2$ and $\theta_2 = \theta_t = 0$, (e)short-dash line stands for rigorous two loop analysis at $\theta_t = \pi/2$ and $\theta_2 = \theta_3 = 0$, (f)dash-dot-dot line stands for one loop results plus threshold radiative corrections at $\theta_t = -\pi/2$ and $\theta_2 = \theta_3 = 0$.

scalar top $m_{\tilde{t}}$ in Fig. 18. Owing to the interference between the contributions of left handed and right handed stop, there is a resonant peak at $m_{\tilde{t}} = 400$ GeV. When $m_{\tilde{t}} > 1.5$ TeV, the dependance of the branching ratio $BR(\bar{B}_s \rightarrow \mu^+\mu^-)$ and the CP asymmetry $A_{CP}(\bar{B}_s \rightarrow \mu^+\mu^-)$ on $m_{\tilde{t}}$ is very gentle. With the same choice of the parameter space,

we plot the branching ratio $BR(\bar{B} \rightarrow K\tau^+\tau^-)$ as well as the Forward-Back asymmetry $A_{FB}(\bar{B} \rightarrow K\tau^+\tau^-)$ versus the mass of right handed scalar top $m_{\tilde{t}}$ in Fig. 19. The resonance at $m_{\tilde{t}} = 400$ GeV also originates from the interference between the contributions of left handed and right handed stop. For the strict two-loop theoretical predictions on $BR(\bar{B} \rightarrow K\tau^+\tau^-)$, there is a small resonance around $m_{\tilde{t}} = 1$ TeV which is due to the interference between the contributions of right handed stop and that of right handed scalar s-quark. A similar discussion about the dependence of the branching ratio $BR(B \rightarrow X_s\gamma)$ and the CP asymmetry $A_{CP}(B \rightarrow X_s\gamma)$ on squark masses was given in our previous work [25], and here we omit repetitions. It is noted that at large $\tan\beta$ scenarios, the corrections from sbottom on the rare process $b \rightarrow sl^+l^-$ only originate from two-loop box diagrams. This is the reason why the dependence of those branching ratios, CP asymmetries, and Forward-Back asymmetries on the sbottom masses is very weak.

V. CONCLUSION

Considering the constraints from the branching ratio $BR(B \rightarrow X_s\gamma)$ and ΔM_{B_s} , we discuss the rare processes $B_s \rightarrow \mu^+\mu^-$, $\bar{B}_s \rightarrow \tau^+\tau^-$, $\bar{B} \rightarrow K\mu^+\mu^-$ and $\bar{B} \rightarrow K\tau^+\tau^-$ in the CP violating MSSM at large $\tan\beta$. We find that there are evident differences between the theoretical predictions of exact two loop calculations and that of one loop contributions plus threshold radiative corrections. Additionally, the branching ratio $BR(\bar{B}_s \rightarrow \mu^+\mu^-)$ of exact two loop calculations can exceed 10^{-8} , while the CP asymmetry can reach 3%. Although the two loop analysis predicts $BR(\bar{B} \rightarrow K\mu^+\mu^-) > 10^{-7}$, the average forward-backward asymmetry $\langle A_{FB} \rangle(\bar{B} \rightarrow K\mu^+\mu^-)$ is too small to be detected in future experiments. For the rare decay $\bar{B}_s \rightarrow \tau^+\tau^-$, one has $BR(\bar{B}_s \rightarrow \tau^+\tau^-) > 10^{-6}$, meanwhile $A_{CP}(\bar{B}_s \rightarrow \tau^+\tau^-) \sim 3\%$. Maybe, the most interesting object to study is the branching ratio $BR(\bar{B} \rightarrow K\tau^+\tau^-) > 10^{-7}$ along with a large average forward-backward asymmetry $\langle A_{FB} \rangle(\bar{B} \rightarrow K\tau^+\tau^-) \sim 20\%$. As a by-product, we also find that the CP asymmetry of inclusive decay $A_{CP}(B \rightarrow X_s\gamma)$ can reach 5%, which is much larger than the SM prediction also.

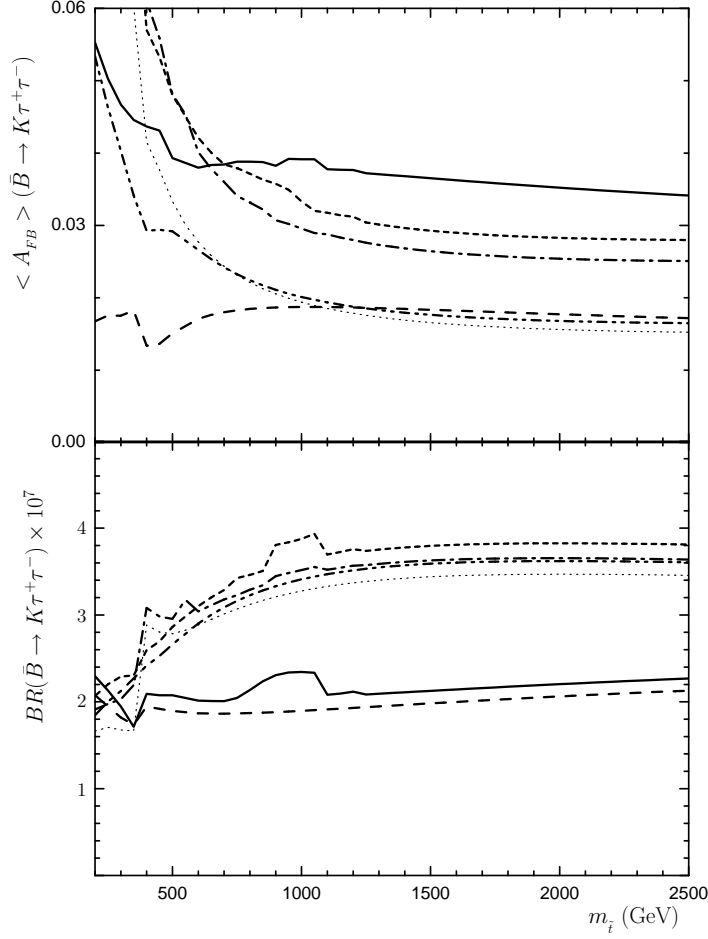


FIG. 19: Dependence of the branching ratio $BR(\bar{B} \rightarrow K\tau^+\tau^-)$ and average forward-backward asymmetry $A_{FB}(\bar{B} \rightarrow K\tau^+\tau^-)$ on the right handed scalar quark mass $m_{\tilde{t}}$, with $\tan\beta = 40$ and $\mu_H = -50$ (GeV). In this figure, (a) solid line stands for rigorous two loop analysis at $\theta_2 = \pi/2$ and $\theta_3 = \theta_t = 0$, (b) dash line stands for one loop results plus threshold radiative corrections at $\theta_2 = \pi/2$ and $\theta_3 = \theta_t = 0$, (c) dash-dot line stands for rigorous two loop analysis at $\theta_3 = \pi/2$ and $\theta_2 = \theta_t = 0$, (d) dot line stands for one loop results plus threshold radiative corrections at $\theta_3 = \pi/2$ and $\theta_2 = \theta_t = 0$, (e) short-dash line stands for rigorous two loop analysis at $\theta_t = \pi/2$ and $\theta_2 = \theta_3 = 0$, (f) dash-dot-dot line stands for one loop results plus threshold radiative corrections at $\theta_t = -\pi/2$ and $\theta_2 = \theta_3 = 0$.

Acknowledgments

The work has been supported by the Academy of Finland under the contracts no. 104915 and 107293, the ABRL Grant No. R14-2003-012-01001-0 of Korea, and also partly by the

National Natural Science Foundation of China(NNSFC).

APPENDIX A: THE ONE-LOOP WILSON COEFFICIENTS AT THE WEAK SCALE

The Wilson coefficients at the weak scale in Eq. (12) are given as

$$\begin{aligned}
C_7(\mu_w) = & \frac{\xi_{CKM}^{ts*} \xi_{CKM}^{tb}}{6} \left\{ x_t \left[\left(\frac{18x_t^2 - 11x_t - 1}{4(1-x_t)^3} + \frac{15x_t^2 - 16x_t + 4}{2(1-x_t)^4} \ln x_t \right) \right. \right. \\
& + \xi_G^b \left(\frac{5x_t - 3}{2(1-x_t)^2} - \frac{2-3x_t}{(1-x_t)^3} \ln x_t \right) \Big] \\
& + \frac{x_t}{\tan^2 \beta} \left[\frac{4x_t^2 + x_t x_H + 25x_H^2}{36(x_t - x_H)^3} - \frac{(3x_t^2 x_H + 2x_t x_H^2)(\ln x_t - \ln x_H)}{6(x_t - x_H)^4} \right] \\
& - \xi_H^b x_t \left[\frac{1}{(x_t - x_H)} + \frac{(x_H^2 + x_t x_H)(\ln x_t - \ln x_H)}{(x_t - x_H)^3} \right] \\
& - |\Gamma_{\tilde{t}_i \chi_\alpha}^L|^2 \left[\left(\frac{3}{2} x_{\chi_\alpha} \frac{\partial^2}{\partial^2 x_{\chi_\alpha}} + \frac{1}{6} x_{\chi_\alpha}^2 \frac{\partial^3}{\partial^3 x_{\chi_\alpha}} \right) \varrho_{1,1}(x_{\chi_\alpha}, x_{\tilde{t}_i}) \right. \\
& + \frac{\partial^2}{\partial^2 x_{\tilde{t}_i}} \varrho_{2,1}(x_{\tilde{t}_i}, x_{\chi_\alpha}) - \frac{1}{3} \frac{\partial^3}{\partial^3 x_{\tilde{t}_i}} \varrho_{3,1}(x_{\tilde{t}_i}, x_{\chi_\alpha}) \Big] \\
& - \frac{\sqrt{2x_{\chi_\alpha}}}{c_\beta} \Gamma_{\tilde{t}_i \chi_\alpha}^L \Gamma_{\tilde{t}_i \kappa_\alpha}^{R*} \left[\frac{3}{2} \frac{\partial^2}{\partial^2 x_{\chi_\alpha}} \varrho_{2,1}(x_{\chi_\alpha}, x_{\tilde{t}_i}) + \frac{\partial^2}{\partial^2 x_{\tilde{t}_i}} \varrho_{2,1}(x_{\tilde{t}_i}, x_{\chi_\alpha}) \right. \\
& \left. \left. - 2 \frac{\partial}{\partial x_{\tilde{t}_i}} \varrho_{1,1}(x_{\tilde{t}_i}, x_{\chi_\alpha}) \right] \right\}, \\
C_8(\mu_w) = & -\frac{\xi_{CKM}^{ts*} \xi_{CKM}^{tb}}{2} \left\{ x_t \left[\frac{(5x_t - 2) \ln x_t}{2(1-x_t)^4} - \frac{3x_t^2 - 13x_t + 4}{4(1-x_t)^3} \right] \right. \\
& + \xi_G^b x_t \left[\frac{\ln x_t}{(1-x_t)^3} + \frac{3-x_t}{2(1-x_t)^2} \right] \\
& + \xi_H^b x_t \left[\frac{x_H^2 (\ln x_t - \ln x_H)}{(x_H - x_t)^3} + \frac{3x_H - x_t}{2(x_H - x_t)^2} \right] \\
& - \frac{x_t}{\tan^2 \beta} \left[\frac{x_t x_H^2 (\ln x_t - \ln x_H)}{2(x_H - x_t)^4} + \frac{2x_H^2 + 5x_t x_H - x_t^2}{12(x_H - x_t)^3} \right] \\
& + \frac{|\Gamma_{\tilde{t}_i \chi_\alpha}^L|^2}{2} \left[\frac{\partial^2}{\partial^2 x_{\tilde{t}_i}} \varrho_{2,1}(x_{\tilde{t}_i}, x_{\chi_\alpha}) - \frac{1}{3} \frac{\partial^3}{\partial^3 x_{\tilde{t}_i}} \varrho_{3,1}(x_{\tilde{t}_i}, x_{\chi_\alpha}) \right] \\
& - \frac{\sqrt{2x_{\chi_\alpha}}}{2c_\beta} \Gamma_{\tilde{t}_i \chi_\alpha}^L \Gamma_{\tilde{t}_i \kappa_\alpha}^{R*} \left[\frac{\partial^2}{\partial^2 x_{\tilde{t}_i}} \varrho_{2,1}(x_{\tilde{t}_i}, x_{\chi_\alpha}) - 2 \frac{\partial}{\partial x_{\tilde{t}_i}} \varrho_{1,1}(x_{\tilde{t}_i}, x_{\chi_\alpha}) \right] \Big\},
\end{aligned}$$

$$\begin{aligned}
C_9^\gamma(\mu_W) = & \frac{\xi_{CKM}^{ts*} \xi_{CKM}^{tb}}{9} \left\{ \left[\frac{-19x_t^3 + 25x_t^2}{2(1-x_t)^3} + \frac{3x_t^4 - 30x_t^3 + 54x_t^2 - 32x_t + 8}{(1-x_t)^4} \ln x_t \right] \right. \\
& + \frac{x_t}{\tan^2 \beta} \left[-\frac{19x_t^2 + 109x_t x_H - 98x_H^2}{18(x_t - x_H)^3} + \frac{(3x_t^3 - 9x_t^2 x_H - 4x_H^3)(\ln x_t - \ln x_H)}{6(x_t - x_H)^4} \right] \\
& - |\Gamma_{\tilde{t}_i \chi_\alpha}^L|^2 \left[\left(3 \frac{\partial}{\partial x_{\chi_\alpha}} - \frac{15}{4} x_{\chi_\alpha} \frac{\partial^2}{\partial^2 x_{\chi_\alpha}} - \frac{7}{4} x_{\chi_\alpha}^2 \frac{\partial^3}{\partial^3 x_{\chi_\alpha}} \right) \varrho_{1,1}(x_{\chi_\alpha}, x_{\tilde{t}_i}) \right. \\
& \left. \left. - \frac{1}{6} \frac{\partial^3}{\partial x_{\tilde{t}_i}^3} \varrho_{3,1}(x_{\tilde{t}_i}, x_{\chi_\alpha}) \right] \right\},
\end{aligned}$$

$$\begin{aligned}
C_9^Z(\mu_W) = & -\frac{1-4s_W^2}{8s_W^2} \xi_{CKM}^{ts*} \xi_{CKM}^{tb} \left\{ \left[\frac{x_t(6-x_t)}{1-x_t} + \frac{(3x_t^2+2x_t)\ln x_t}{(1-x_t)^2} \right] \right. \\
& + \left[\frac{(3-2s_W^2)}{6\tan^2 \beta} x_t \frac{\partial}{\partial x_t} \varrho_{2,1}(x_t, x_H) + \frac{(3-4s_W^2)}{3\tan^2 \beta} x_t^2 \frac{\partial}{\partial x_t} \varrho_{1,1}(x_t, x_H) \right] \\
& + \left[\Gamma_{\tilde{t}_i \chi_\alpha}^L \Gamma_{\tilde{t}_i \chi_\beta}^{L*} \left(\xi_\chi^4 \right)_{\alpha\beta} T_1(x_{\tilde{t}_i}, x_{\chi_\alpha}, x_{\chi_\beta}) - \Gamma_{\tilde{t}_i \chi_\alpha}^L \Gamma_{\tilde{t}_j \chi_\alpha}^{L*} \left(\xi_t \right)_{ij} T_1(x_{\tilde{t}_i}, x_{\chi_\alpha}, x_{\chi_\beta}) \right. \\
& - 2\sqrt{x_{\chi_\alpha} x_{\chi_\beta}} \Gamma_{\tilde{t}_i \chi_\alpha}^L \Gamma_{\tilde{t}_i \chi_\beta}^{L*} \left(\xi_\chi^1 \right)_{\alpha\beta} T_0(x_{\tilde{t}_i}, x_{\chi_\alpha}, x_{\chi_\beta}) \\
& \left. + \frac{3-2s_W^2}{12} |\Gamma_{\tilde{t}_i \chi_\alpha}^L|^2 \frac{\partial}{\partial x_{\tilde{t}_i}} \varrho_{2,1}(x_{\tilde{t}_i}, x_{\chi_\alpha}) \right\},
\end{aligned}$$

$$C_{10}^Z(\mu_W) = \frac{1}{1-4s_W^2} C_9^Z(\mu_W),$$

$$\begin{aligned}
C_S^H(\mu_W) = & -\frac{\sqrt{x_t x_b}}{4s_W^2 s_\beta c_\beta} \xi_{CKM}^{ts*} \xi_{CKM}^{tb} \sum_{k=1}^3 \frac{\mathcal{Z}_H^{2k}}{x_{H_k^0}} \left\{ \xi_G^b s_\beta \left(c_\beta \mathcal{Z}_H^{2k} - s_\beta \mathcal{Z}_H^{3k} \right) E(x_t) \right. \\
& + \xi_H^b s_\beta \tan \beta \left(s_\beta \mathcal{Z}_H^{2k} + c_\beta \mathcal{Z}_H^{3k} + i \mathcal{Z}_H^{1k} \right) Q_+(x_t, x_H) + \xi_G^b x_t^2 \left[\left(\mathcal{Z}_H^{3k} \right. \right. \\
& + i 3 c_\beta \mathcal{Z}_H^{1k} \left. \right) R_1(x_t) + \left(c_\beta^2 (1+2s_\beta^2) \mathcal{Z}_H^{3k} \right) - s_\beta c_\beta (1-2s_\beta^2) \mathcal{Z}_H^{2k} + i c_\beta \mathcal{Z}_H^{1k} \left. \right) R_2(x_t) \left. \right] \\
& - \xi_H^b x_t \left[\left(\mathcal{Z}_H^{3k} + i c_\beta \mathcal{Z}_H^{1k} \right) \frac{\partial}{\partial x_t} \varrho_{2,1}(x_t, x_H) + \left(\mathcal{Z}_H^{3k} - i c_\beta \mathcal{Z}_H^{1k} \right) x_t \frac{\partial}{\partial x_t} \varrho_{1,1}(x_t, x_H) \right. \\
& - s_\beta \left(c_\beta (1+2s_\beta^2) \mathcal{Z}_H^{2k} + s_\beta (1+2c_\beta^2) \mathcal{Z}_H^{3k} \right) x_t \frac{\partial}{\partial x_H} \varrho_{1,1}(x_H, x_t) \left. \right] \\
& + \left[\frac{c_\beta^2 - s_\beta^2}{c_\beta} \left(s_\beta [s_\beta - (1+2\frac{s_W^2}{c_W^2}) c_\beta^2] \mathcal{Z}_H^{2k} + c_\beta [(1+2\frac{s_W^2}{c_W^2}) s_\beta^2 - c_\beta^2] \mathcal{Z}_H^{3k} \right) \right. \\
& + \frac{i}{c_\beta} \mathcal{Z}_H^{1k} \left. \right] x_t P_+(x_t, x_H) + 2 \tan \beta \left[\Gamma_{\tilde{t}_i \chi_\alpha}^L \Gamma_{\tilde{t}_i \chi_\beta}^{R*} \left(\kappa_{H^k}^1 \right)_{\alpha\beta} T_1(x_{\tilde{t}_i}, x_{\chi_\alpha}, x_{\chi_\beta}) \right. \\
& + \sqrt{x_{\chi_\alpha} x_{\chi_\beta}} \Gamma_{\tilde{t}_i \chi_\alpha}^L \Gamma_{\tilde{t}_i \chi_\beta}^{R*} \left(\kappa_{H^k}^2 \right)_{\alpha\beta} T_0(x_{\tilde{t}_i}, x_{\chi_\alpha}, x_{\chi_\beta}) \\
& \left. - \frac{\sqrt{2x_{\chi_\alpha}}}{c_W^2} \Gamma_{\tilde{t}_i \chi_\alpha}^L \Gamma_{\tilde{t}_j \chi_\alpha}^{R*} \left(\zeta_{tH}^k \right)_{ij} T_0(x_{\chi_\alpha}, x_{\tilde{t}_i}, x_{\tilde{t}_j}) \right\}, \\
C_P^H(\mu_W) = & i \frac{s_\beta \mathcal{Z}_H^{1k}}{\mathcal{Z}_H^{2k}} C_S^H(\mu_W),
\end{aligned}$$

$$\begin{aligned}
C_S^{count}(\mu_W) &= -\frac{G_F \sqrt{x_b x_l}}{4\sqrt{2}c_\beta^2} \xi_{CKM}^{ts*} \xi_{CKM}^{tb} \chi_B \sum_{k=1}^3 \frac{1}{x_{H_k^0}} \mathcal{Z}_H^{2k} (\mathcal{Z}_H^{2k} + \Delta \mathcal{Z}_H^{3k} \\
&\quad + i[s_\beta - c_\beta \Delta] \mathcal{Z}_H^{1k}) \left[\sqrt{2} x_t (1 - x_H) P_+(x_H, x_t) \right. \\
&\quad \left. + \frac{\sqrt{x_{\chi\alpha}}}{c_\beta} \Gamma_{\tilde{t}_i \chi\alpha}^{R*} \Gamma_{\tilde{t}_i \chi\alpha}^L \varrho_{1,1}(x_{\tilde{t}_i}, x_{\chi\alpha}) \right], \\
C_P^{count}(\mu_W) &= i \frac{G_F s_\beta \sqrt{x_b x_l}}{4\sqrt{2}c_\beta^2} \xi_{CKM}^{ts*} \xi_{CKM}^{tb} \chi_B \sum_{k=1}^3 \frac{1}{x_{H_k^0}} \mathcal{Z}_H^{1k} (\mathcal{Z}_H^{2k} + \Delta \mathcal{Z}_H^{3k} \\
&\quad + i[s_\beta - c_\beta \Delta] \mathcal{Z}_H^{1k}) \left[\sqrt{2} x_t (1 - x_H) P_+(x_H, x_t) \right. \\
&\quad \left. + \frac{\sqrt{x_{\chi\alpha}}}{c_\beta} \Gamma_{\tilde{t}_i \chi\alpha}^{R*} \Gamma_{\tilde{t}_i \chi\alpha}^L \varrho_{1,1}(x_{\tilde{t}_i}, x_{\chi\alpha}) \right], \\
C_9^{box}(\mu_W) &= -\frac{\xi_{CKM}^{ts*} \xi_{CKM}^{tb}}{16s_w^2} \left\{ \left[-x_t x_l R_2(x_t) + x_t x_l \frac{\partial}{\partial x_H} \varrho_{1,1}(x_H, x_t) \right. \right. \\
&\quad \left. \left. - 2x_t x_l P_+(x_t, x_H) - 4x_t R_1(x_t) \right] \right. \\
&\quad \left. + 4\Gamma_{\tilde{t}_i \chi\beta}^L \Gamma_{\tilde{t}_i \chi\alpha}^{L*} (\mathcal{Z}_+)^{\dagger}_{\alpha 1} (\mathcal{Z}_+)^{\dagger}_{1\beta} D_1(x_{\tilde{t}_i}, x_{\tilde{\nu}_I}, x_{\chi\alpha}, x_{\chi\beta}) \right. \\
&\quad \left. - \frac{4x_l}{c_\beta^2} \Gamma_{\tilde{t}_i \chi\beta}^L \Gamma_{\tilde{t}_i \chi\alpha}^{L*} (\mathcal{Z}_-)^{\dagger}_{2\alpha} (\mathcal{Z}_-)^{\dagger}_{\beta 2} \sqrt{x_{\chi\alpha} x_{\chi\beta}} D_0(x_{\tilde{t}_i}, x_{\tilde{\nu}_I}, x_{\chi\alpha}, x_{\chi\beta}) \right\}, \\
C_{10}^{box}(\mu_W) &= -\frac{\xi_{CKM}^{ts*} \xi_{CKM}^{tb}}{16s_w^2} \left\{ \left[-x_t x_l R_2(x_t) + x_t x_l \frac{\partial}{\partial x_H} \varrho_{1,1}(x_H, x_t) \right. \right. \\
&\quad \left. \left. - 2x_t x_l P_+(x_t, x_H) - 4x_t R_1(x_t) \right] \right. \\
&\quad \left. - 4\Gamma_{\tilde{t}_i \chi\beta}^L \Gamma_{\tilde{t}_i \chi\alpha}^{L*} (\mathcal{Z}_+)^{\dagger}_{\alpha 1} (\mathcal{Z}_+)^{\dagger}_{1\beta} D_1(x_{\tilde{t}_i}, x_{\tilde{\nu}_I}, x_{\chi\alpha}, x_{\chi\beta}) \right. \\
&\quad \left. + \frac{4x_l}{c_\beta^2} \Gamma_{\tilde{t}_i \chi\beta}^L \Gamma_{\tilde{t}_i \chi\alpha}^{L*} (\mathcal{Z}_-)^{\dagger}_{2\alpha} (\mathcal{Z}_-)^{\dagger}_{\beta 2} \sqrt{x_{\chi\alpha} x_{\chi\beta}} D_0(x_{\tilde{t}_i}, x_{\tilde{\nu}_I}, x_{\chi\alpha}, x_{\chi\beta}) \right\}, \\
C_9^{box}(\mu_W) &= -\frac{\xi_{CKM}^{ts*} \xi_{CKM}^{tb}}{16s_w^2} x_l \sqrt{x_b x_s} \tan^4 \beta \left\{ \xi_H^b \left[\frac{\partial}{\partial x_H} \varrho_{1,1}(x_H, x_t) - \frac{1}{x_H} \right] \right. \\
&\quad \left. + \frac{2\chi_B}{s_\beta^4} \Gamma_{\tilde{t}_i \chi\alpha}^R \Gamma_{\tilde{t}_i \chi\beta}^{R*} (\mathcal{Z}_-)^{\dagger}_{2\alpha} (\mathcal{Z}_-)^{\dagger}_{\beta 2} D_1(x_{\tilde{t}_i}, x_{\tilde{\nu}_I}, x_{\chi\alpha}, x_{\chi\beta}) \right\}, \\
C_{10}^{box}(\mu_W) &= C_9^{box}(\mu_W), \\
C_S^{box}(\mu_W) &= -\frac{\xi_{CKM}^{ts*} \xi_{CKM}^{tb}}{4s_w^2} \sqrt{x_l x_b} \left\{ \left[\xi_G^b E(x_t) + \xi_G^b \tan^2 \beta E_+(x_H, x_t) \right] \right. \\
&\quad \left. - \frac{\chi_B}{c_\beta^2} \Gamma_{\tilde{t}_i \chi\beta}^L \Gamma_{\tilde{t}_i \chi\alpha}^{R*} (\mathcal{Z}_-)^{\dagger}_{2\alpha} (\mathcal{Z}_+)^{\dagger}_{1\beta} D_1(x_{\tilde{t}_i}, x_{\tilde{\nu}_I}, x_{\chi\alpha}, x_{\chi\beta}) \right\}, \\
C_P^{box}(\mu_W) &= C_S^{box}(\mu_W).
\end{aligned}$$

(A1)

The one-loop integrands are defined as

$$\begin{aligned}
E(x) &= \frac{x \ln x}{(1-x)^2}, \\
R_1(x) &= \frac{1}{1-x} + \frac{\ln x}{(1-x)^2}, \\
R_2(x) &= -\left(\frac{1}{1-x} + \frac{x \ln x}{(1-x)^2}\right), \\
R_3(x) &= -\left(\frac{1}{1-x} + \frac{x^2 \ln x}{(1-x)^2}\right), \\
E_+(x, y) &= \frac{y}{x-y} \left[\frac{\ln x}{1-x} - \frac{\ln y}{1-y} \right], \\
P_+(x, y) &= \frac{1}{x-y} \left[\frac{x \ln x}{1-x} - \frac{y \ln y}{1-y} \right], \\
Q_+(x, y) &= -\frac{x}{x-y} \left[\frac{\ln x}{(x-1)^2} - \frac{y \ln y}{y-1} \right], \\
\varrho_{m,n}(x, y) &= \frac{x^m \ln^n x - y^m \ln^n y}{x-y}, \\
T_0(x_1, x_2, x_3) &= \sum_{i=1}^3 \frac{x_i \ln x_i}{\prod_{j \neq i} (x_j - x_i)}, \\
T_1(x_1, x_2, x_3) &= \sum_{i=1}^3 \frac{x_i^2 \ln x_i}{\prod_{j \neq i} (x_j - x_i)}, \\
D_0(x_1, x_2, x_3, x_4) &= \sum_{i=1}^4 \frac{x_i \ln x_i}{\prod_{j \neq i} (x_j - x_i)}, \\
D_1(x_1, x_2, x_3, x_4) &= \sum_{i=1}^4 \frac{x_i^2 \ln x_i}{\prod_{j \neq i} (x_j - x_i)}. \tag{A2}
\end{aligned}$$

APPENDIX B: THE TWO-LOOP CORRECTIONS FROM THE Z , H PENGUIN-DIAGRAMS

$$\begin{aligned}
\mathcal{P}_Z^{(1)} &= -\frac{2}{3}(c_w^2 - s_w^2)(\mathcal{Z}_{\bar{s}})_{2,i}(\xi_H)_{ij} \left\{ \left[(\mathcal{Z}_{\bar{t}}^\dagger)_{j,2}(x_w x_t)^{1/2} \frac{\partial}{\partial x_H} \Psi_{1b} \right. \right. \\
&\quad \left. \left. - (\mathcal{Z}_{\bar{t}}^\dagger)_{j,1} e^{-i\theta_3}(x_w x_{\bar{g}})^{1/2} \frac{\partial}{\partial x_H} \Psi_{1a} \right] (x_{\bar{t}_j}; x_t, x_H; x_{\bar{g}}, x_{\bar{s}_i}) \right\}, \\
\mathcal{P}_Z^{(2)} &= -\frac{2}{3}(\mathcal{Z}_{\bar{s}})_{2,i}(\xi_H)_{ij} \left\{ \left[-\left(\frac{1}{4} + \frac{1}{3}s_w^2\right)(\mathcal{Z}_{\bar{t}}^\dagger)_{j,2}(x_w x_t)^{1/2} \frac{\partial}{\partial x_t} \Psi_{1b} \right. \right. \\
&\quad \left. \left. + \left(\frac{1}{4} - \frac{1}{3}s_w^2\right)(\mathcal{Z}_{\bar{t}}^\dagger)_{j,1} e^{-i\theta_3}(x_w x_{\bar{g}})^{1/2} \frac{\partial}{\partial x_t} \Psi_{1a} \right] \right\}
\end{aligned}$$

$$\begin{aligned}
& + \frac{2}{3} s_w^2 (\mathcal{Z}_t^\dagger)_{j,1} e^{i\theta_3} (x_w x_{\bar{g}})^{1/2} x_t \frac{\partial}{\partial x_t} \Psi_0 \Big] (x_{\bar{t}_j}; x_t, x_H; x_{\bar{g}}, x_{\bar{s}_i}) \Big\} , \\
\mathcal{P}_Z^{(3)} = & -\frac{2}{3} (\mathcal{Z}_{\bar{s}})_{2,i} (\xi_s)_{ik} (\xi_H)_{kj} \Big[(\mathcal{Z}_t^\dagger)_{j,2} (x_w x_t)^{1/2} - e^{-i\theta_3} (x_w x_{\bar{g}})^{1/2} (\mathcal{Z}_t^\dagger)_{j,1} \Big] \\
& \times \frac{\partial}{\partial x_{\bar{s}_i}} \Psi_{1b} (x_{\bar{t}_j}; x_t, x_H; x_{\bar{g}}, x_{\bar{s}_i}) , \\
\mathcal{P}_Z^{(4)} = & -\frac{1}{6} (\mathcal{Z}_{\bar{s}})_{2,i} (\xi_H)_{ik} (\xi_t)_{kj} \frac{1}{x_{\bar{t}_j} - x_{\bar{t}_k}} \Big\{ \Big[(\mathcal{Z}_t^\dagger)_{j,2} (x_w x_t)^{1/2} (\Psi_{1b} - \Psi_{1a}) \\
& - (\mathcal{Z}_t^\dagger)_{j,1} e^{-i\theta_3} (x_w x_{\bar{g}})^{1/2} (\Psi_{1a} - \Psi_{1b}) \Big] (x_{\bar{t}_j}; x_{\bar{g}}, x_{\bar{s}_i}; x_t, x_H) \\
& - (x_{\bar{t}_j} \rightarrow x_{\bar{t}_k}) \Big\} , \\
\mathcal{P}_Z^{(5)} = & \frac{1}{3\sqrt{2}s_\beta} (\mathcal{Z}_{\bar{s}})_{2,i} (\mathcal{Z}_{\bar{s}}^\dagger)_{i,1} (\mathcal{Z}_t^\dagger)_{j,1} (\mathcal{Z}_-^\dagger)_{\beta,2} \frac{1}{x_{\chi\alpha} - x_{\chi\beta}} \Big\{ \Big[(\mathcal{Z}_t)_{1,j} (\mathcal{Z}_-)_{1,\alpha} (\xi_\chi^1)_{\alpha\beta} (\Psi_{2b} \\
& - \Psi_{2d} - \varrho_{2,1}(x_{\chi\alpha}, x_{\bar{t}_j})) - \frac{\sqrt{2}m_{\chi\beta}x_t}{m_w s_\beta} (\mathcal{Z}_t)_{1,j} (\mathcal{Z}_+^\dagger)_{\alpha,2} (\xi_\chi^4)_{\alpha\beta} \Psi_{1b} \\
& + \frac{m_{\chi\alpha}x_t}{\sqrt{2}m_w s_\beta} (\mathcal{Z}_t)_{1,j} (\mathcal{Z}_+^\dagger)_{\alpha,2} (\xi_\chi^1)_{\alpha\beta} \Psi_{1b} - e^{-i\theta_3} (x_{\bar{g}} x_t)^{1/2} (\mathcal{Z}_t)_{2,j} (\mathcal{Z}_-)_{1,\alpha} (\xi_\chi^1)_{\alpha\beta} \Psi_{1a} \\
& + 2e^{-i\theta_3} (x_{\bar{g}} x_t x_{\chi\alpha} x_{\chi\beta})^{1/2} (\mathcal{Z}_t)_{2,j} (\mathcal{Z}_-)_{1,\alpha} (\xi_\chi^4)_{\alpha\beta} \Psi_0 \\
& + e^{-i\theta_3} \frac{\sqrt{2}m_t (x_{\bar{g}} x_{\chi\beta})^{1/2}}{m_w s_\beta} (\mathcal{Z}_t)_{2,j} (\mathcal{Z}_+^\dagger)_{\alpha,2} (\xi_\chi^4)_{\alpha\beta} (\Psi_{1a} - \Psi_{1b}) \\
& - e^{-i\theta_3} \frac{m_t (x_{\bar{g}} x_{\chi\alpha})^{1/2}}{\sqrt{2}m_w s_\beta} (\mathcal{Z}_t)_{2,j} (\mathcal{Z}_+^\dagger)_{\alpha,2} (\xi_\chi^1)_{\alpha\beta} (\Psi_{1a} - \Psi_{1b}) \Big] (x_t; x_{\chi\alpha}, x_{\bar{t}_j}; x_{\bar{g}}, x_{\bar{s}_i}) \\
& - 2(x_{\chi\alpha} x_{\chi\beta})^{1/2} (\mathcal{Z}_t)_{1,j} (\mathcal{Z}_-)_{1,\alpha} (\xi_\chi^4)_{\alpha\beta} (\Psi_{1b} - \Psi_{1a}) (x_t; x_{\bar{g}}, x_{\bar{s}_i}; x_{\chi\alpha}, x_{\bar{t}_j}) \\
& - (x_{\chi\alpha} \rightarrow x_{\chi\beta}) \Big\} , \\
\mathcal{P}_Z^{(6)} = & -\frac{1}{3\sqrt{2}s_\beta} (\mathcal{Z}_{\bar{s}})_{2,i} (\mathcal{Z}_{\bar{s}}^\dagger)_{i,1} (\xi_t)_{jk} (\mathcal{Z}_t^\dagger)_{k,1} (\mathcal{Z}_-^\dagger)_{\alpha,2} \frac{1}{x_{\bar{t}_j} - x_{\bar{t}_k}} \Big\{ \Big[(\mathcal{Z}_t)_{2,j} (\mathcal{Z}_-)_{1,\alpha} (\Psi_{2b} \\
& - \Psi_{2d} - \varrho_{2,1}(x_{\chi\alpha}, x_{\bar{t}_j})) - \frac{m_t}{\sqrt{2}m_w s_\beta} (\mathcal{Z}_t)_{2,j} (\mathcal{Z}_+^\dagger)_{\alpha,2} (x_t x_{\chi\alpha})^{1/2} \Psi_{1b} \\
& - e^{-i\theta_3} (\mathcal{Z}_t)_{2,j} (\mathcal{Z}_-)_{1,\alpha} (x_t x_{\bar{g}})^{1/2} \Psi_{1a} \\
& + e^{-i\theta_3} \frac{m_t}{\sqrt{2}m_w s_\beta} (\mathcal{Z}_t)_{2,j} (\mathcal{Z}_+^\dagger)_{\alpha,2} (x_{\bar{g}} x_{\chi\alpha})^{1/2} (\Psi_{1a} - \Psi_{1b}) \Big] (x_t; x_{\chi\alpha}, x_{\bar{t}_j}; x_{\bar{g}}, x_{\bar{s}_i}) \\
& - (x_{\bar{t}_j} \rightarrow x_{\bar{t}_k}) \Big\} , \\
\mathcal{P}_Z^{(7)} = & -\frac{1}{3\sqrt{2}s_\beta} (\mathcal{Z}_-^\dagger)_{\alpha,2} (\mathcal{Z}_{\bar{s}})_{2,i} (\xi_s)_{ik} (\mathcal{Z}_{\bar{s}}^\dagger)_{k,1} (\mathcal{Z}_t^\dagger)_{j,1} \frac{1}{x_{\bar{s}_i} - x_{\bar{s}_k}} \\
& \times \Big\{ \Big[-(\mathcal{Z}_t)_{1,j} (\mathcal{Z}_-)_{1,\alpha} (\varrho_{2,1}(x_{\bar{g}}, x_{\bar{s}_i}) + \Psi_{2d} - \Psi_{2b}) \Big]
\end{aligned}$$

$$\begin{aligned}
& -\frac{m_t}{\sqrt{2}m_w s_\beta}(\mathcal{Z}_{\bar{t}})_{1,j}(\mathcal{Z}_+^\dagger)_{\alpha,2}(x_t x_{\chi\alpha})^{1/2}\Psi_{1a} + e^{-i\theta_3}(\mathcal{Z}_{\bar{t}})_{2,j}(\mathcal{Z}_-)_{1,\alpha}(x_{\bar{g}}x_t)^{1/2}\Psi_{1b} \\
& + e^{-i\theta_3}\frac{m_t}{\sqrt{2}m_w s_\beta}(\mathcal{Z}_{\bar{t}})_{2,j}(\mathcal{Z}_+^\dagger)_{\alpha,2}(x_{\bar{g}}x_{\chi\alpha})^{1/2}(\Psi_{1b} - \Psi_{1a})\Big](x_t; x_{\bar{g}}, x_{\bar{s}_i}; x_{\bar{t}_j}, x_{\chi\alpha}) \\
& - (x_{\bar{s}_i} \rightarrow x_{\bar{s}_k})\Big\}, \\
\mathcal{P}_Z^{(8)} = & -\frac{\sqrt{2}}{3s_\beta}(\mathcal{Z}_{\bar{s}})_{2,i}(\mathcal{Z}_{\bar{s}}^\dagger)_{i,1}(\mathcal{Z}_{\bar{t}}^\dagger)_{j,1}(\mathcal{Z}_-^\dagger)_{\alpha,2}\Big\{\Big[\Big(\frac{1}{2} - \frac{2}{3}s_w^2\Big)\Big((\mathcal{Z}_{\bar{t}})_{1,j}(\mathcal{Z}_-)_{1,\alpha}x_t\frac{\partial}{\partial x_t}\Psi_{1b} \\
& - e^{-i\theta_3}(\mathcal{Z}_{\bar{t}})_{2,j}(\mathcal{Z}_-)_{1,\alpha}(x_{\bar{g}}x_t)^{1/2}\frac{\partial}{\partial x_t}(\Psi_{1a} - \Psi_{1b}) \\
& - e^{-i\theta_3}\frac{m_t}{\sqrt{2}m_w s_\beta}(\mathcal{Z}_{\bar{t}})_{2,j}(\mathcal{Z}_+^\dagger)_{\alpha,2}(x_{\chi\alpha}x_{\bar{g}})^{1/2}\frac{\partial}{\partial x_t}(\Psi_{1a} - \Psi_{1b})\Big) \\
& - \frac{4}{3}s_w^2 e^{-i\theta_3}\Big((\mathcal{Z}_{\bar{t}})_{2,j}(\mathcal{Z}_-)_{1,\alpha}(x_t x_{\bar{g}})^{1/2}\frac{\partial}{\partial x_t}(\Psi_{1a} - \Psi_{1b}) \\
& + \frac{m_t}{\sqrt{2}m_w s_\beta}(\mathcal{Z}_{\bar{t}})_{2,j}(\mathcal{Z}_+^\dagger)_{\alpha,2}x_t(x_{\chi\alpha}x_{\bar{g}})^{1/2}\frac{\partial}{\partial x_t}\Psi_0\Big)\Big](x_t; x_{\bar{t}_j}, x_{\chi\alpha}; x_{\bar{g}}, x_{\bar{s}_i}) \\
& + \Big[\Big(\frac{1}{2} - \frac{2}{3}s_w^2\Big)\frac{m_t}{\sqrt{2}m_w s_\beta}\Big((\mathcal{Z}_{\bar{t}})_{1,j}(\mathcal{Z}_+^\dagger)_{\alpha,2}(x_{\chi\alpha}x_t)^{1/2}\frac{\partial}{\partial x_t}(\Psi_{1b} - \Psi_{1a}) \\
& - e^{-i\theta_3}(\mathcal{Z}_{\bar{t}})_{2,j}(\mathcal{Z}_+^\dagger)_{\alpha,2}(x_{\chi\alpha}x_{\bar{g}})^{1/2}\frac{\partial}{\partial x_t}(\Psi_{1a} - \Psi_{1b})\Big) \\
& + \frac{4}{3}s_w^2\Big((\mathcal{Z}_{\bar{t}})_{1,j}(\mathcal{Z}_-)_{1,\alpha}\frac{\partial}{\partial x_t}[\Psi_{2c} - 2\Psi_{2b} + \Psi_{2a}] \\
& + \frac{m_t}{\sqrt{2}m_w s_\beta}(\mathcal{Z}_{\bar{t}})_{2,j}(\mathcal{Z}_+^\dagger)_{\alpha,2}(x_{\chi\alpha}x_t)^{1/2}\frac{\partial}{\partial x_t}(\Psi_{1b} - \Psi_{1a})\Big)\Big](x_t; x_{\bar{g}}, x_{\bar{s}_i}; x_{\bar{t}_j}, x_{\chi\alpha})\Big\} \quad (B1)
\end{aligned}$$

$$\begin{aligned}
\mathcal{P}_G^{(2)} = & -\frac{2}{3}(\mathcal{Z}_{\bar{s}})_{1,i}(\xi_H)_{ij}(\mathcal{Z}_{\bar{t}}^\dagger)_{j,2}e^{i\theta_3}(x_t x_{\bar{g}})^{1/2}\Psi_0(x_{\bar{t}_j}; x_t, x_H; x_{\bar{g}}, x_{\bar{s}_i}), \\
\mathcal{P}_G^{(4)} = & -\frac{1}{3}(\mathcal{Z}_{\bar{s}})_{1,i}(\xi_H)_{ik}(\eta_H)_{kj}x_{\bar{t}_j} - x_{\bar{t}_k}\Big\{\Big[(\mathcal{Z}_{\bar{t}}^\dagger)_{j,1}\Psi_{1b} \\
& - e^{i\theta_3}(x_t x_{\bar{g}})^{1/2}(\mathcal{Z}_{\bar{t}}^\dagger)_{j,2}\Psi_0\Big](x_{\bar{t}_j}; x_t, x_H; x_{\bar{g}}, x_{\bar{s}_i}) - (x_{\bar{t}_j} \rightarrow x_{\bar{t}_k})\Big\}, \\
\mathcal{P}_G^{(5)} = & \frac{2}{3s_\beta}(\mathcal{Z}_{\bar{s}})_{1,i}(\mathcal{Z}_{\bar{s}}^\dagger)_{i,1}(\mathcal{Z}_{\bar{t}}^\dagger)_{j,1}(\mathcal{Z}_-^\dagger)_{\beta,2}\frac{1}{x_{\chi\alpha} - x_{\chi\beta}} \\
& \times \Big\{\Big[-\frac{m_t}{\sqrt{2}m_w s_\beta}(\mathcal{Z}_{\bar{t}})_{2,j}(\mathcal{Z}_+^\dagger)_{\alpha,2}(\xi_\chi^2)_{\alpha\beta}(\Psi_{2b} - \Psi_{2d} - \varrho_{2,1}(x_{\chi\alpha}, x_{\bar{t}_j})) \\
& - (\mathcal{Z}_{\bar{t}})_{2,j}(\mathcal{Z}_-)_{1,\alpha}\Big((\xi_\chi^2)_{\alpha\beta}(x_t x_{\chi\alpha})^{1/2} - (\xi_\chi^3)_{\alpha\beta}(x_t x_{\chi\beta})^{1/2}\Big)\Psi_{1b} \\
& + e^{i\theta_3}(\mathcal{Z}_{\bar{t}})_{1,j}(\mathcal{Z}_-)_{1,\alpha}(\xi_\chi^2)_{\alpha\beta}\Big((x_{\bar{g}}x_{\chi\alpha})^{1/2} - (\xi_\chi^3)_{\alpha\beta}(x_{\bar{g}}x_{\chi\beta})^{1/2}\Big)(\Psi_{1a} - \Psi_{1b}) \\
& + e^{i\theta_3}\frac{m_t}{\sqrt{2}m_w s_\beta}(\mathcal{Z}_{\bar{t}})_{1,j}(\mathcal{Z}_+^\dagger)_{\alpha,2}(\xi_\chi^2)_{\alpha\beta}(x_t x_{\bar{g}})^{1/2}\Psi_{1a}
\end{aligned}$$

$$\begin{aligned}
& -e^{i\theta_3} \frac{m_t}{\sqrt{2}m_w s_\beta} (\mathcal{Z}_{\bar{t}})_{1,j} (\mathcal{Z}_+^\dagger)_{\alpha,2} (\xi_\chi^3)_{\alpha\beta} (x_t x_{\bar{g}} x_{\chi\alpha} x_{\chi\beta})^{1/2} \Psi_0 \Big] (x_t; x_{\chi\alpha}, x_{\bar{t}_j}; x_{\bar{g}}, x_{\bar{s}_i}) \\
& + \frac{m_t}{\sqrt{2}m_w s_\beta} (\mathcal{Z}_{\bar{t}})_{2,j} (\mathcal{Z}_+^\dagger)_{\alpha,2} (\xi_\chi^3)_{\alpha\beta} (x_{\chi\alpha} x_{\chi\beta})^{1/2} (\Psi_{1b} - \Psi_{1a}) (x_t; x_{\bar{g}}, x_{\bar{s}_i}; x_{\chi\alpha}, x_{\bar{t}_j}) \\
& - (x_{\chi\alpha} \rightarrow x_{\chi\beta}) \Big\} , \\
\mathcal{P}_G^{(6)} = & -\frac{\sqrt{2}}{3s_\beta} (\mathcal{Z}_{\bar{s}})_{1,i} (\mathcal{Z}_{\bar{s}}^\dagger)_{i,1} (\mathcal{Z}_{\bar{t}}^\dagger)_{k,1} (\mathcal{Z}_-^\dagger)_{\alpha,2} (\eta_H)_{jk} \frac{1}{x_{\bar{t}_j} - x_{\bar{t}_k}} \\
& \times \left\{ \left[(\mathcal{Z}_{\bar{t}})_{2,j} (\mathcal{Z}_-)_{1,\alpha} x_t^{1/2} \Psi_{1b} - e^{i\theta_3} (\mathcal{Z}_{\bar{t}})_{1,j} (\mathcal{Z}_-)_{1,\alpha} x_{\bar{g}}^{1/2} (\Psi_{1a} - \Psi_{1b}) \right. \right. \\
& - e^{i\theta_3} \frac{m_t}{\sqrt{2}m_w s_\beta} (\mathcal{Z}_{\bar{t}})_{1,j} (\mathcal{Z}_+^\dagger)_{\alpha,2} (x_{\bar{g}} x_t x_{\chi\alpha})^{1/2} \Psi_0 \Big] (x_t; x_{\chi\alpha}, x_{\bar{t}_j}; x_{\bar{g}}, x_{\bar{s}_i}) \\
& - \frac{m_t}{\sqrt{2}m_w s_\beta} (\mathcal{Z}_{\bar{t}})_{2,j} (\mathcal{Z}_+^\dagger)_{\alpha,2} x_{\chi\alpha}^{1/2} (\Psi_{1b} - \Psi_{1a}) (x_t; x_{\bar{g}}, x_{\bar{s}_i}; x_{\chi\alpha}, x_{\bar{t}_j}) \\
& \left. \left. - (x_{\bar{t}_j} \rightarrow x_{\bar{t}_k}) \right\} , \\
\mathcal{P}_G^{(8)} = & \frac{2}{3s_\beta} (\mathcal{Z}_{\bar{s}})_{1,i} (\mathcal{Z}_{\bar{s}}^\dagger)_{i,1} (\mathcal{Z}_{\bar{t}})_{1,j} (\mathcal{Z}_{\bar{t}}^\dagger)_{j,1} (\mathcal{Z}_-^\dagger)_{\alpha,2} \left\{ (\mathcal{Z}_-)_{1,\alpha} \Psi_{1b} \right. \\
& \left. + \frac{m_t}{\sqrt{2}m_w s_\beta} (\mathcal{Z}_+^\dagger)_{\alpha,2} (x_{\chi\alpha} x_{\bar{g}})^{1/2} \Psi_0 \right\} (x_t; x_{\bar{t}_j}, x_{\chi\alpha}; x_{\bar{g}}, x_{\bar{s}_i}) . \tag{B2}
\end{aligned}$$

$$\begin{aligned}
\mathcal{P}_{H^\rho}^{(1)} = & \frac{1}{3} s_\beta (\mathcal{Z}_H)_{3,\rho} (\mathcal{Z}_{\bar{s}})_{1,i} (\xi_H)_{ij} \left\{ (\mathcal{Z}_{\bar{t}}^\dagger)_{j,1} x_w \frac{\partial}{\partial x_H} \Psi_{1b} \right. \\
& \left. - e^{i\theta_3} (\mathcal{Z}_{\bar{t}}^\dagger)_{j,2} (x_t x_{\bar{g}})^{1/2} x_w \frac{\partial}{\partial x_H} \Psi_0 \right\} (x_{\bar{t}_j}; x_t, x_H; x_{\bar{s}_i}, x_{\bar{g}}) , \\
\mathcal{P}_{H^\rho}^{(2)} = & \frac{1}{3} (s_\beta (\mathcal{Z}_H)_{2,\rho} + i (\mathcal{Z}_H)_{1,\rho}) (\mathcal{Z}_{\bar{t}})_{1,j} (\mathcal{Z}_{\bar{s}})_{1,i} (\mathcal{Z}_{\bar{s}}^\dagger)_{i,1} \frac{1}{x_H - x_w} \left\{ \left[(\mathcal{Z}_{\bar{t}}^\dagger)_{j,1} (\Psi_{2b} - 2\Psi_{2c} \right. \right. \\
& \left. \left. - \varrho_{2,1}(x_H, x_t) \right) - e^{i\theta_3} (\mathcal{Z}_{\bar{t}}^\dagger)_{j,2} (x_{\bar{g}} x_t)^{1/2} (\Psi_{1a} - 2\Psi_{1b}) \right] (x_{\bar{t}_j}; x_H, x_t; x_{\bar{g}}, x_{\bar{s}_i}) \\
& \left. - (x_H \rightarrow x_w) \right\} , \\
\mathcal{P}_{H^\rho}^{(3)} = & \frac{1}{3} [s_\beta^3 (\mathcal{Z}_H)_{2,\rho} - i (\mathcal{Z}_H)_{1,\rho}] s_\beta (\mathcal{Z}_H)_{3,\rho} (\mathcal{Z}_{\bar{s}})_{1,i} (\xi_H)_{ij} \frac{x_w}{x_H - x_w} \left\{ \left[(\mathcal{Z}_{\bar{t}}^\dagger)_{j,1} \Psi_{1b} \right. \right. \\
& \left. \left. - e^{i\theta_3} (\mathcal{Z}_{\bar{t}}^\dagger)_{j,2} (x_t x_{\bar{g}})^{1/2} \Psi_0 \right] (x_{\bar{t}_j}; x_H, x_t; x_{\bar{g}}, x_{\bar{s}_i}) - (x_H \rightarrow x_w) \right\} , \\
\mathcal{P}_{H^\rho}^{(4)} = & -\frac{1}{3} (\mathcal{Z}_H)_{3,\rho} (\mathcal{Z}_{\bar{s}})_{1,i} (\xi_H)_{ij} \left\{ 2 (\mathcal{Z}_{\bar{t}}^\dagger)_{j,1} x_t \frac{\partial}{\partial x_t} \Psi_{1b} \right. \\
& \left. - e^{i\theta_3} (\mathcal{Z}_{\bar{t}}^\dagger)_{j,2} (x_{\bar{g}} x_t)^{1/2} \frac{\partial}{\partial x_t} (\Psi_{1a} + x_t \Psi_0) \right\} (x_{\bar{t}_j}; x_H, x_t; x_{\bar{g}}, x_{\bar{s}_i}) , \\
\mathcal{P}_{H^\rho}^{(5)} = & -\frac{2}{3} (\mathcal{Z}_{\bar{s}})_{1,i} (\zeta_{sH}^\rho)_{ik} (\xi_H)_{kj} \frac{x_w}{x_{\bar{s}_i} - x_{\bar{s}_k}} \left\{ \left[(\mathcal{Z}_{\bar{t}}^\dagger)_{j,1} \Psi_{1b} \right. \right. \\
& \left. \left. - e^{i\theta_3} (\mathcal{Z}_{\bar{t}}^\dagger)_{j,2} (x_{\bar{g}} x_t)^{1/2} \Psi_0 \right] (x_{\bar{t}_j}; x_H, x_t; x_{\bar{g}}, x_{\bar{s}_i}) - (x_{\bar{s}_i} \rightarrow x_{\bar{s}_k}) \right\} ,
\end{aligned}$$

$$\begin{aligned}
\mathcal{P}_{H^\rho}^{(6)} &= \frac{2}{3}(\mathcal{Z}_{\bar{s}})_{1,i}(\xi_H)_{ik}(\zeta_{tH}^\rho)_{kj} \frac{x_w}{x_{\bar{t}_j} - x_{\bar{t}_k}} \left\{ \left[(\mathcal{Z}_{\bar{t}}^\dagger)_{j,1} \Psi_{1b} \right. \right. \\
&\quad \left. \left. - e^{i\theta_3} (\mathcal{Z}_{\bar{t}}^\dagger)_{j,2} (x_t x_{\bar{g}})^{1/2} \Psi_0 \right] (x_{\bar{t}_j}; x_H, x_t; x_{\bar{g}}, x_{\bar{s}_i}) - (x_{\bar{t}_j} \rightarrow x_{\bar{t}_k}) \right\}, \\
\mathcal{P}_{H^\rho}^{(7)} &= -\frac{2}{3s_\beta} (\mathcal{Z}_{\bar{s}})_{1,i} (\mathcal{Z}_{\bar{s}}^\dagger)_{i,1} (\mathcal{Z}_{\bar{t}}^\dagger)_{j,1} (\mathcal{Z}_-^\dagger)_{\beta,2} \frac{1}{x_{\chi_\alpha} - x_{\chi_\beta}} \\
&\quad \times \left\{ \left[-\frac{m_t}{\sqrt{2}m_w s_\beta} (\mathcal{Z}_{\bar{t}})_{2,j} (\mathcal{Z}_+^\dagger)_{\alpha,2} (\kappa_{H^\rho}^1)_{\alpha\beta} (\Psi_{2b} - \Psi_{2d} - \varrho_{2,1}(x_{\chi_\alpha}, x_{\bar{t}_j})) \right. \right. \\
&\quad - (\mathcal{Z}_{\bar{t}})_{2,j} (\mathcal{Z}_-)_{1,\alpha} \left((\kappa_{H^\rho}^2)_{\alpha\beta} (x_t x_{\chi_\beta})^{1/2} + (\kappa_{H^\rho}^1)_{\alpha\beta} (x_t x_{\chi_\alpha})^{1/2} \right) \Psi_{1b} \\
&\quad + e^{i\theta_3} (\mathcal{Z}_{\bar{t}})_{1,j} (\mathcal{Z}_-)_{1,\alpha} \left((\kappa_{H^\rho}^2)_{\alpha\beta} (x_{\bar{g}} x_{\chi_\beta})^{1/2} + (\kappa_{H^\rho}^1)_{\alpha\beta} (x_{\bar{g}} x_{\chi_\alpha})^{1/2} \right) (\Psi_{1a} - \Psi_{1b}) \\
&\quad + e^{i\theta_3} \frac{m_t}{\sqrt{2}m_w s_\beta} (\mathcal{Z}_{\bar{t}})_{1,j} (\mathcal{Z}_+^\dagger)_{\alpha,2} (\kappa_{H^\rho}^1)_{\alpha\beta} (x_t x_{\bar{g}})^{1/2} \Psi_{1a} \\
&\quad + e^{i\theta_3} \frac{m_t}{\sqrt{2}m_w s_\beta} (\mathcal{Z}_{\bar{t}})_{1,j} (\mathcal{Z}_+^\dagger)_{\alpha,2} (\kappa_{H^\rho}^2)_{\alpha\beta} (x_t x_{\bar{g}} x_{\chi_\alpha} x_{\chi_\beta})^{1/2} \Psi_0 \left. \right] (x_t; x_{\chi_\alpha}, x_{\bar{t}_j}; x_{\bar{g}}, x_{\bar{s}_i}) \\
&\quad - \frac{m_t}{\sqrt{2}m_w s_\beta} (\mathcal{Z}_{\bar{t}})_{2,j} (\mathcal{Z}_+^\dagger)_{\alpha,2} (\kappa_{H^\rho}^2)_{\alpha\beta} (x_{\chi_\alpha} x_{\chi_\beta})^{1/2} (\Psi_{1b} - \Psi_{1a}) (x_t; x_{\bar{g}}, x_{\bar{s}_i}; x_{\chi_\alpha}, x_{\bar{t}_j}) \\
&\quad \left. - (x_{\chi_\alpha} \rightarrow x_{\chi_\beta}) \right\}, \\
\mathcal{P}_{H^\rho}^{(8)} &= \frac{2}{3s_\beta} (\mathcal{Z}_{\bar{s}})_{1,i} (\mathcal{Z}_{\bar{s}}^\dagger)_{i,1} (\mathcal{Z}_{\bar{t}}^\dagger)_{k,1} (\mathcal{Z}_-^\dagger)_{\alpha,2} (\zeta_{tH}^\rho)_{jk} \frac{1}{x_{\bar{t}_j} - x_{\bar{t}_k}} \\
&\quad \times \left\{ \left[(\mathcal{Z}_{\bar{t}})_{2,j} (\mathcal{Z}_-)_{1,\alpha} (x_w x_t)^{1/2} \Psi_{1b} - e^{i\theta_3} (\mathcal{Z}_{\bar{t}})_{1,j} (\mathcal{Z}_-)_{1,\alpha} (x_w x_{\bar{g}})^{1/2} (\Psi_{1a} - \Psi_{1b}) \right. \right. \\
&\quad - e^{i\theta_3} \frac{m_t}{\sqrt{2}m_w s_\beta} (\mathcal{Z}_{\bar{t}})_{1,j} (\mathcal{Z}_+^\dagger)_{\alpha,2} (x_w x_{\bar{g}} x_t x_{\chi_\alpha})^{1/2} \Psi_0 \left. \right] (x_t; x_{\chi_\alpha}, x_{\bar{t}_j}; x_{\bar{g}}, x_{\bar{s}_i}) \\
&\quad - \frac{m_t}{\sqrt{2}m_w s_\beta} (\mathcal{Z}_{\bar{t}})_{2,j} (\mathcal{Z}_+^\dagger)_{\alpha,2} (x_w x_{\chi_\alpha})^{1/2} [(\Psi_{1b} - \Psi_{1a}) (x_t; x_{\bar{g}}, x_{\bar{s}_i}; x_{\chi_\alpha}, x_{\bar{t}_j}) \\
&\quad \left. - (x_{\bar{t}_j} \rightarrow x_{\bar{t}_k}) \right\}, \\
\mathcal{P}_{H^\rho}^{(10)} &= -\frac{1}{3s_\beta} (\mathcal{Z}_{\bar{s}})_{1,i} (\mathcal{Z}_{\bar{s}}^\dagger)_{i,1} (\mathcal{Z}_H)_{3,\rho} (\mathcal{Z}_{\bar{t}}^\dagger)_{j,1} (\mathcal{Z}_-^\dagger)_{\alpha,2} \left\{ \left[-(\mathcal{Z}_{\bar{t}})_{2,j} (\mathcal{Z}_-)_{1,\alpha} \left(1 + 2x_t \frac{\partial}{\partial x_t} \right) \Psi_{1b} \right. \right. \\
&\quad + 2e^{i\theta_3} (\mathcal{Z}_{\bar{t}})_{1,j} (\mathcal{Z}_-)_{1,\alpha} (x_t x_{\bar{g}})^{1/2} \frac{\partial}{\partial x_t} (\Psi_{1a} - \Psi_{1b}) \\
&\quad + e^{i\theta_3} \frac{m_t}{\sqrt{2}m_w s_\beta} (\mathcal{Z}_{\bar{t}})_{2,j} (\mathcal{Z}_+^\dagger)_{\alpha,2} (x_{\bar{g}} x_{\chi_\alpha})^{1/2} \left(1 + 2x_t \frac{\partial}{\partial x_t} \right) \Psi_0 \left. \right] (x_t; x_{\chi_\alpha}, x_{\bar{t}_j}; x_{\bar{g}}, x_{\bar{s}_i}) \\
&\quad \left. - \frac{\sqrt{2}m_t}{m_w s_\beta} (\mathcal{Z}_{\bar{t}})_{2,j} (\mathcal{Z}_+^\dagger)_{\alpha,2} (x_t x_{\chi_\alpha})^{1/2} \frac{\partial}{\partial x_t} (\Psi_{1b} - \Psi_{1a}) (x_t; x_{\bar{g}}, x_{\bar{s}_i}; x_{\chi_\alpha}, x_{\bar{t}_j}) \right\}. \quad (\text{B3})
\end{aligned}$$

APPENDIX C: THE TWO-LOOP CORRECTIONS FROM THE BOX DIAGRAMS

$$\begin{aligned}
\mathcal{B}_V &= -\frac{m_b}{\sqrt{2}m_w s_\beta} (\mathcal{Z}_{\bar{s}})_{1,j} (\mathcal{Z}_{\bar{b}})_{i,1}^\dagger (\mathcal{Z}_+)_{\alpha 1}^\dagger (\mathcal{Z}_+)_{1\beta} \left(\Gamma_{\bar{b}_i \chi_\alpha}^R \right) \left(\Gamma_{\bar{s}_j \chi_\beta}^R \right)^* (x_t x_{\chi_\beta})^{1/2} \\
&\quad \times \sum_{\rho=\{\chi_\alpha, \chi_\beta\}} \frac{1}{\prod_{\sigma \neq \rho} (x_\rho - x_\sigma)} \sum_{\varrho=\{\bar{b}_i, \bar{s}_j\}} \frac{1}{\prod_{\varsigma \neq \varrho} (x_\varrho - x_\varsigma)} \Psi_{1b}(x_t; x_\rho, x_{\bar{\nu}_I}; x_\varrho, x_{\bar{g}}) , \\
\mathcal{B}_A &= -\mathcal{B}_V .
\end{aligned} \tag{C1}$$

$$\begin{aligned}
\mathcal{B}_V^{(1)} &= \mathcal{B}_V , \\
\mathcal{B}_A^{(1)} &= -\mathcal{B}_V^{(1)} , \\
\mathcal{B}_V^{(2)} &= -\frac{m_{lI} m_t}{m_w^2 s_\beta^2} (\mathcal{Z}_-)_{\alpha 2}^\dagger (\mathcal{Z}_+)_{1\beta} \left(\Gamma_{\bar{t}_j \chi_\beta}^L \right) \left(\Gamma_{\bar{t}_i \chi_\alpha}^R \right)^* \sum_{\rho=\{\chi_\alpha, \beta, \bar{t}_{i,j}, \bar{\nu}_k\}} \frac{1}{\prod_{\sigma \neq \rho} (x_\rho - x_\sigma)} \\
&\quad \times \left\{ \left[(\mathcal{Z}_{\bar{t}})_{1,i} (\mathcal{Z}_{\bar{t}})_{j,1}^\dagger + (\mathcal{Z}_{\bar{t}})_{2,i} (\mathcal{Z}_{\bar{t}})_{j,2}^\dagger \right] \left[-\frac{1}{4} (2x_t - x_\rho + 2x_{\bar{g}}) x_\rho^2 \ln x_\rho \right. \right. \\
&\quad \left. \left. + \Theta_2(x_t, x_\rho, x_{\bar{g}}) \right] - \left[(\mathcal{Z}_{\bar{t}})_{1,i} (\mathcal{Z}_{\bar{t}})_{j,2}^\dagger e^{i\theta_3} + (\mathcal{Z}_{\bar{t}})_{2,i} (\mathcal{Z}_{\bar{t}})_{j,2}^\dagger e^{-i\theta_3} \right] \right. \\
&\quad \left. \times (x_t x_{\bar{g}})^{1/2} \left[\frac{1}{2} x_\rho^2 \ln x_\rho + \Theta_{1a}(x_t, x_\rho, x_{\bar{g}}) \right] \right\} , \\
\mathcal{B}_A^{(2)} &= \mathcal{B}_V^{(2)} .
\end{aligned} \tag{C2}$$

$$\begin{aligned}
\mathcal{B}_S^{(1)} &= -\left(x_{\bar{g}} x_{lI} \right)^{1/2} e^{i\theta_3} (\mathcal{Z}_{\bar{b}})_{1,i} (\mathcal{Z}_{\bar{b}})_{i,1}^\dagger (\mathcal{Z}_{\bar{s}})_{1,k} \left(\mathcal{A}_{st} \right)_{kj}^\dagger (\mathcal{Z}_{\bar{t}})_{j,1}^\dagger \sum_{\rho=\{\nu, W\}} \frac{1}{\prod_{\sigma \neq \rho} (x_\rho - x_\sigma)} \\
&\quad \times \sum_{\varrho=\{\bar{b}_i, \bar{s}_k\}} \frac{1}{\prod_{\varsigma \neq \varrho} (x_\varrho - x_\varsigma)} \left\{ \left(\Psi_{1a} - 2\Psi_{1b} \right) (x_{\bar{t}_j}; x_\rho, x_H; x_{\bar{g}}, x_\varrho) \right\} , \\
\mathcal{B}_P^{(1)} &= \mathcal{B}_S^{(1)} , \\
\mathcal{B}_S^{(2)} &= -\sum_{\rho=W, H} \frac{1}{\prod_{\sigma \neq \rho} (x_\rho - x_\sigma)} \left\{ \left[\left(x_{\bar{g}} x_{lI} \right)^{1/2} e^{i\theta_3} (\mathcal{Z}_{\bar{t}})_{1,i} \left(\mathcal{A}_{bt} \right)_{ij} (\mathcal{Z}_{\bar{b}})_{j,2}^\dagger \right. \right. \\
&\quad \left. \left. - \left(x_t x_{lI} \right)^{1/2} (\mathcal{Z}_{\bar{t}})_{2,i} \left(\mathcal{A}_{bt} \right)_{ij} (\mathcal{Z}_{\bar{b}})_{j,2}^\dagger \right] \Psi_0(x_{\bar{t}_i}; x_\rho, x_t; x_{\bar{g}}, x_{\bar{b}_j}) \right\} , \\
\mathcal{B}_P^{(2)} &= -\mathcal{B}_S^{(2)} ,
\end{aligned}$$

$$\begin{aligned}
\mathcal{B}_S^{(3)} = & -\frac{m_b m_e t_\beta}{m_w^2} \left\{ (\mathcal{Z}_{\bar{t}})_{1,i} (\mathcal{Z}_{\bar{t}})_{i,1}^\dagger (\mathcal{Z}_{\bar{s}})_{j,1}^\dagger (\mathcal{Z}_{\bar{s}})_{1,j} \left[-\varrho_{1,1}(1, x_t) - \varrho_{1,1}(x_H, x_t) \right. \right. \\
& + \sum_{\rho=\nu, W, H} \frac{1}{\prod_{\sigma \neq \rho} (x_\rho - x_\sigma)} \left(-3\varrho_{2,1}(x_\rho, x_t) + [\Psi_{2b} - 2\Psi_{2c}](x_{\bar{t}_i}; x_\rho, x_t; x_{\bar{g}}, x_{\bar{s}_j}) \right) \Big] \\
& - (x_{\bar{g}} x_t)^{1/2} e^{i\theta_3} (\mathcal{Z}_{\bar{t}})_{1,i} (\mathcal{Z}_{\bar{t}})_{i,2}^\dagger (\mathcal{Z}_{\bar{s}})_{j,1}^\dagger (\mathcal{Z}_{\bar{s}})_{2,j} \sum_{\rho=\nu, W, H} \frac{1}{\prod_{\sigma \neq \rho} (x_\rho - x_\sigma)} \left[\Psi_{1a} \right. \\
& \left. \left. - 2\Psi_{1b} \right] (x_{\bar{t}_i}; x_\rho, x_t; x_{\bar{g}}, x_{\bar{s}_j}) \right\},
\end{aligned}$$

$$\mathcal{B}_P^{(3)} = -\mathcal{B}_S^{(3)},$$

$$\begin{aligned}
\mathcal{B}_S^{(4)} = & - (x_{\bar{g}} x_{lI})^{1/2} e^{i\theta_3} (\mathcal{Z}_{\bar{s}})_{1,k} (\mathcal{Z}_{\bar{s}})_{k,1}^\dagger (\mathcal{Z}_{\bar{t}})_{1,j} (\mathcal{A}_{bt})_{j\bar{t}} (\mathcal{Z}_{\bar{b}})_{i,2}^\dagger \sum_{\rho=\nu, W} \frac{1}{\prod_{\sigma \neq \rho} (x_\rho - x_\sigma)} \\
& \times \sum_{\varrho=\bar{b}_i, \bar{s}_k} \frac{1}{\prod_{\varsigma \neq \varrho} (x_\varrho - x_\varsigma)} \left\{ (\Psi_{1a} - 2\Psi_{1b})(x_{\bar{t}_j}; x_\rho, x_H; x_{\bar{g}}, x_{\bar{e}}) \right\},
\end{aligned}$$

$$\mathcal{B}_P^{(4)} = -\mathcal{B}_S^{(4)},$$

$$\begin{aligned}
\mathcal{B}_S^{(5)} = & -\frac{m_b m_{lI} t_\beta}{m_w^2} \left\{ (\mathcal{Z}_{\bar{t}})_{1,i} (\mathcal{Z}_{\bar{t}})_{i,1}^\dagger \frac{\partial}{\partial x_t} \left[\sum_{\rho=t, W, H} \frac{1}{\prod_{\sigma \neq \rho} (x_\rho - x_\sigma)} \left(\frac{1}{4} x_\rho^2 \ln x_\rho \right. \right. \right. \\
& \left. \left. \left. + \Theta_{1b}(x_{\bar{t}_i}, x_\rho, x_{\bar{g}}) \right) \right] - (x_t x_{\bar{g}})^{1/2} e^{-i\theta_3} (\mathcal{Z}_{\bar{t}})_{2,i} (\mathcal{Z}_{\bar{t}})_{i,1}^\dagger \right. \\
& \times \frac{\partial}{\partial x_t} \left[\sum_{\rho=t, W, H} \frac{1}{\prod_{\sigma \neq \rho} (x_\rho - x_\sigma)} \left(\frac{1}{2} x_\rho \ln x_\rho + \Theta_0(x_{\bar{t}_i}, x_\rho, x_{\bar{g}}) \right) \right] \\
& - (x_t x_{\bar{g}})^{1/2} e^{i\theta_3} (\mathcal{Z}_{\bar{t}})_{1,i} (\mathcal{Z}_{\bar{t}})_{i,2}^\dagger \frac{\partial}{\partial x_t} \left[\sum_{\rho=t, W, H} \frac{1}{\prod_{\sigma \neq \rho} (x_\rho - x_\sigma)} \left(\frac{1}{2} x_\rho \ln x_\rho \right. \right. \\
& \left. \left. + \Theta_0(x_{\bar{t}_i}, x_\rho, x_{\bar{g}}) \right) \right] + x_t (\mathcal{Z}_{\bar{t}})_{2,i} (\mathcal{Z}_{\bar{t}})_{i,2}^\dagger \frac{\partial}{\partial x_t} \left[\sum_{\rho=\nu, t, W, H} \frac{1}{\prod_{\sigma \neq \rho} (x_\rho - x_\sigma)} \left(\frac{1}{4} x_\rho^2 \ln x_\rho \right. \right. \\
& \left. \left. + \Theta_{1b}(x_{\bar{t}_i}, x_\rho, x_{\bar{g}}) \right) \right] \Big\},
\end{aligned}$$

$$\mathcal{B}_P^{(5)} = -\mathcal{B}_S^{(5)},$$

$$\begin{aligned}
\mathcal{B}_S^{(6)} = & (\mathcal{Z}_-)^{\dagger}_{\alpha 2} (\mathcal{Z}_+)_{1\beta} (\Gamma_{\bar{t}_i \chi \beta}^L) \sum_{\rho=\{\chi_\alpha, \chi_\beta, \bar{t}_i\}} \frac{1}{\prod_{\sigma \neq \rho} (x_\rho - x_\sigma)} \left\{ -\frac{\sqrt{2} m_{lI}}{m_w s_\beta} (\Gamma_{\bar{b}_j \chi \alpha}^L) \right. \\
& \times (\mathcal{Z}_{\bar{t}})_{i,1}^\dagger (\mathcal{Z}_{\bar{b}})_{j,2}^\dagger \left[\frac{1}{2} \varrho_{2,1}(x_\rho, x_{\bar{\nu}_I}) + (\Psi_{2b} - \Psi_{2d})(x_t; x_\rho, x_{\bar{\nu}_I}; x_{\bar{g}}, x_{\bar{b}_j}) \right] \\
& \left. + \frac{\sqrt{2} m_{lI}}{m_w s_\beta} (\Gamma_{\bar{b}_j \chi \alpha}^L) (\mathcal{Z}_{\bar{t}})_{i,2}^\dagger (\mathcal{Z}_{\bar{b}})_{j,2}^\dagger (x_t x_{\bar{g}})^{1/2} e^{i\theta_3} \Psi_{1a}(x_t; x_\rho, x_{\bar{\nu}_I}; x_{\bar{g}}, x_{\bar{b}_j}) \right\}
\end{aligned}$$

$$\begin{aligned}
& + \frac{m_{l^I} m_t}{m_w^2 s_\beta^2} (\Gamma_{\tilde{b}_j \chi_\alpha}^R) (\mathcal{Z}_{\tilde{t}}^\dagger)_{i,1} (\mathcal{Z}_{\tilde{b}}^\dagger)_{j,2} (x_t x_{\chi_\alpha})^{1/2} \Psi_{1b} (x_t; x_\rho, x_{\tilde{\nu}_I}; x_{\tilde{g}}, x_{\tilde{b}_j}) \\
& - \frac{m_{l^I} m_t}{m_w^2 s_\beta^2} (\Gamma_{\tilde{b}_j \chi_\alpha}^R) (\mathcal{Z}_{\tilde{t}}^\dagger)_{i,2} (\mathcal{Z}_{\tilde{b}}^\dagger)_{j,2} (x_t x_{\tilde{g}})^{1/2} e^{i\theta_3} \left(\Psi_{1a} - \Psi_{1b} \right) (x_t; x_\rho, x_{\tilde{\nu}_I}; x_{\tilde{g}}, x_{\tilde{b}_j}) \Big\} , \\
\mathcal{B}_P^{(6)} &= -\mathcal{B}_S^{(6)} , \\
\mathcal{B}_S^{(7)} &= \frac{m_{l^I} m_t}{m_w^2 s_\beta^2} (\mathcal{Z}_-)_{\alpha 2}^\dagger (\mathcal{Z}_+)_{1\beta} (\Gamma_{\tilde{s}_j \chi_\beta}^L)^* (\Gamma_{\tilde{t}_i \chi_\alpha}^R)^* \sum_{\rho=\{\chi_\alpha, \chi_\beta, \tilde{t}_i\}} \frac{1}{\prod_{\sigma \neq \rho} (x_\rho - x_\sigma)} \\
& \times \left\{ \left[(\mathcal{Z}_{\tilde{s}})_{1,j} (\mathcal{Z}_{\tilde{t}})_{2,i} (x_t x_{\chi_\beta})^{1/2} \Psi_{1b} (x_t; x_\rho, x_{\tilde{\nu}_I}; x_{\tilde{g}}, x_{\tilde{b}_j}) \right. \right. \\
& \left. \left. - (\mathcal{Z}_{\tilde{s}})_{1,j} (\mathcal{Z}_{\tilde{t}})_{1,i} (x_{\chi_\beta} x_{\tilde{g}})^{1/2} e^{i\theta_3} \left(\Psi_{1a} - \Psi_{1b} \right) (x_t; x_\rho, x_{\tilde{\nu}_I}; x_{\tilde{g}}, x_{\tilde{b}_j}) \right] \right\} , \\
\mathcal{B}_P^{(7)} &= -\mathcal{B}_S^{(7)} , \\
\mathcal{B}_S^{(8)} &= \frac{2\sqrt{2} m_{l^I}}{m_w s_\beta} (\mathcal{Z}_-)_{\alpha 2}^\dagger (\mathcal{Z}_+)_{1\beta} (\Gamma_{\tilde{b}_i \chi_\alpha}^L) (\Gamma_{\tilde{s}_j \chi_\beta}^L)^* (\mathcal{Z}_{\tilde{s}})_{2,j} (\mathcal{Z}_{\tilde{b}}^\dagger)_{i,1} (x_{\chi_\beta} x_{\tilde{g}})^{1/2} e^{-i\theta_3} \\
& \times \sum_{\rho=\{\chi_\alpha, \chi_\beta\}} \frac{1}{\prod_{\sigma \neq \rho} (x_\rho - x_\sigma)} \sum_{\varrho=\{\tilde{b}_i, \tilde{s}_j\}} \frac{1}{\prod_{\varsigma \neq \varrho} (x_\varrho - x_\varsigma)} \left\{ \left(\Psi_{1a} - \Psi_{1b} \right) (x_t; x_\rho, x_{\tilde{\nu}_I}; x_\varrho, x_{\tilde{g}}) \right\} , \\
\mathcal{B}_P^{(8)} &= -\mathcal{B}_S^{(8)} , \\
\mathcal{B}_S^{(9)} &= (\Gamma_{3\tilde{s}_j \chi_\beta}^L) (\mathcal{Z}_{\tilde{s}})_{2,j} (\mathcal{Z}_{\tilde{b}}^\dagger)_{i,1} (x_{\chi_\beta} x_{\tilde{g}})^{1/2} e^{-i\theta_3} \sum_{\rho=\{\chi_\alpha, \chi_\beta\}} \frac{1}{\prod_{\sigma \neq \rho} (x_\rho - x_\sigma)} \\
& \times \sum_{\varrho=\{\tilde{b}_i, \tilde{s}_j\}} \frac{1}{\prod_{\varsigma \neq \varrho} (x_\varrho - x_\varsigma)} \left\{ \left[\frac{2\sqrt{2} m_{l^I}}{m_w s_\beta} (\mathcal{Z}_+)_{\alpha 1}^\dagger (\mathcal{Z}_-)_{2\beta} (\Gamma_{\tilde{b}_i \chi_\alpha}^L) (\Psi_{1a} - \Psi_{1b}) \right. \right. \\
& - \frac{2m_{l^I} m_b}{m_w^2 s_\beta c_\beta} (\mathcal{Z}_+)_{\alpha 1}^\dagger (\mathcal{Z}_-)_{2\beta} (\Gamma_{\tilde{b}_i \chi_\alpha}^R) \Psi_{1a} \\
& \left. \left. - \frac{2m_{l^I} m_b}{m_w^2 s_\beta c_\beta} (\mathcal{Z}_-)_{\alpha 2}^\dagger (\mathcal{Z}_+)_{1\beta} (\Gamma_{\tilde{b}_i \chi_\alpha}^R) (x_t x_{\chi_\alpha})^{1/2} \Psi_0 \right] (x_t; x_\rho, x_{\tilde{\nu}_I}; x_\varrho, x_{\tilde{g}}) \right\} , \\
\mathcal{B}_P^{(9)} &= \mathcal{B}_S^{(9)} . \tag{C3}
\end{aligned}$$

$$\begin{aligned}
\mathcal{B}_S^{\prime(1)} &= - \sum_{\rho=\nu, W, H} \frac{1}{\prod_{\sigma \neq \rho} (x_\rho - x_\sigma)} \left\{ \left[(x_t x_{l^I})^{1/2} (\mathcal{Z}_{\tilde{s}})_{2,j} (\mathcal{A}_{st})_{ji}^\dagger (\mathcal{Z}_{\tilde{t}}^\dagger)_{i,2} \Psi_{1b} \right. \right. \\
& \left. \left. + (x_{\tilde{g}} x_{l^I})^{1/2} e^{-i\theta_3} (\mathcal{Z}_{\tilde{s}})_{2,j} (\mathcal{A}_{st})_{ji}^\dagger (\mathcal{Z}_{\tilde{t}}^\dagger)_{i,1} \Psi_{1a} \right] (x_{\tilde{t}_i}; x_\rho, x_t; x_{\tilde{g}}, x_{\tilde{s}_j}) \right\} , \\
\mathcal{B}_P^{\prime(1)} &= -\mathcal{B}_S^{\prime(1)} , \\
\mathcal{B}_S^{\prime(2)} &= - (x_{\tilde{g}} x_{l^I})^{1/2} e^{-i\theta_3} (\mathcal{Z}_{\tilde{b}})_{1,i} (\mathcal{Z}_{\tilde{b}}^\dagger)_{i,1} (\mathcal{Z}_{\tilde{s}})_{2,k} (\mathcal{A}_{st})_{kj}^\dagger (\mathcal{Z}_{\tilde{t}}^\dagger)_{j,1} \sum_{\rho=\{\nu, W\}} \frac{1}{\prod_{\sigma \neq \rho} (x_\rho - x_\sigma)}
\end{aligned}$$

$$\begin{aligned}
& \times \sum_{\varrho=\{\tilde{b}_i, \tilde{s}_k\}} \frac{1}{\prod_{\varsigma \neq \varrho} (x_\varrho - x_\varsigma)} \left\{ (\Psi_{1a} - 2\Psi_{1b})(x_{\tilde{t}_j}; x_\rho, x_H; x_{\tilde{g}}, x_\varrho) \right\}, \\
\mathcal{B}_P'^{(2)} &= \mathcal{B}_S'^{(2)}, \\
\mathcal{B}_S'^{(3)} &= - (x_{\tilde{g}} x_{l_I})^{1/2} e^{-i\theta_3} (\mathcal{Z}_{\tilde{s}})_{2,k} (\mathcal{Z}_{\tilde{s}})_{k,1}^\dagger (\mathcal{Z}_{\tilde{t}})_{1,j} (\mathcal{A}_{bt})_{ji} (\mathcal{Z}_{\tilde{b}})_{i,1}^\dagger \sum_{\rho=\{\nu, W\}} \frac{1}{\prod_{\sigma \neq \rho} (x_\rho - x_\sigma)} \\
& \times \sum_{\varrho=\{\tilde{b}_i, \tilde{s}_k\}} \frac{1}{\prod_{\varsigma \neq \varrho} (x_\varrho - x_\varsigma)} \left\{ (\Psi_{1a} - 2\Psi_{1b})(x_{\tilde{t}_j}; x_\rho, x_H; x_{\tilde{g}}, x_\varrho) \right\}, \\
\mathcal{B}_P'^{(3)} &= -\mathcal{B}_S'^{(3)}, \\
\mathcal{B}_S'^{(4)} &= \sum_{\rho=\{\chi_\alpha, \chi_\beta, \tilde{t}_i\}} \frac{1}{\prod_{\sigma \neq \rho} (x_\rho - x_\sigma)} \left\{ -\frac{\sqrt{2}m_{l_I}}{m_w s_\beta} (\mathcal{Z}_+)_{\alpha 1}^\dagger (\mathcal{Z}_-)_{2\beta} (\Gamma_{\tilde{s}_j \chi_\beta}^L)^* (\Gamma_{\tilde{t}_i \chi_\alpha}^L)^* \right. \\
& \times \left[(\mathcal{Z}_{\tilde{s}})_{2,j} (\mathcal{Z}_{\tilde{t}})_{1,i} \left(\frac{1}{2} \varrho_{2,1}(x_\rho, x_{\tilde{\nu}_k}) + [\Psi_{2b} - \Psi_{2d}](x_t; x_\rho, x_{\tilde{\nu}_k}; x_{\tilde{g}}, x_{\tilde{b}_j}) \right) \right. \\
& \left. \left. - (\mathcal{Z}_{\tilde{s}})_{2,j} (\mathcal{Z}_{\tilde{t}})_{2,i} (x_t x_{\tilde{g}})^{1/2} e^{-i\theta_3} \Psi_{1a}(x_t; x_\rho, x_{\tilde{\nu}_k}; x_{\tilde{g}}, x_{\tilde{b}_j}) \right] \right\}, \\
\mathcal{B}_P'^{(4)} &= \mathcal{B}_S'^{(4)}, \\
\mathcal{B}_S'^{(5)} &= \frac{2\sqrt{2}m_{l_I}}{m_w s_\beta} (\mathcal{Z}_-)_{\alpha 2}^\dagger (\mathcal{Z}_+)_{1\beta} (\Gamma_{\tilde{b}_i \chi_\alpha}^L) (\Gamma_{\tilde{s}_j \chi_\beta}^L)^* (\mathcal{Z}_{\tilde{s}})_{2,j} (\mathcal{Z}_{\tilde{b}})_{i,1}^\dagger (x_{\chi_\beta} x_{\tilde{g}})^{1/2} e^{-i\theta_3} \\
& \times \sum_{\rho=\{\chi_\alpha, \chi_\beta\}} \frac{1}{\prod_{\sigma \neq \rho} (x_\rho - x_\sigma)} \sum_{\varrho=\{\tilde{b}_i, \tilde{s}_j\}} \frac{1}{\prod_{\varsigma \neq \varrho} (x_\varrho - x_\varsigma)} \left\{ (\Psi_{1a} - \Psi_{1b})(x_t; x_\rho, x_{\tilde{\nu}_k}; x_\varrho, x_{\tilde{g}}) \right\}, \\
\mathcal{B}_P'^{(5)} &= -\mathcal{B}_S'^{(5)}, \\
\mathcal{B}_S'^{(6)} &= (\Gamma_{\tilde{s}_j \chi_\beta}^L)^* (\mathcal{Z}_{\tilde{s}})_{2,j} (\mathcal{Z}_{\tilde{b}})_{i,1}^\dagger (x_{\chi_\beta} x_{\tilde{g}})^{1/2} e^{-i\theta_3} \sum_{\rho=\{\chi_\alpha, \chi_\beta\}} \frac{1}{\prod_{\sigma \neq \rho} (x_\rho - x_\sigma)} \\
& \times \sum_{\varrho=\{\tilde{b}_i, \tilde{s}_j\}} \frac{1}{\prod_{\varsigma \neq \varrho} (x_\varrho - x_\varsigma)} \left\{ \left[\frac{2\sqrt{2}m_{l_I}}{m_w s_\beta} (\mathcal{Z}_+)_{\alpha 1}^\dagger (\mathcal{Z}_-)_{2\beta} (\Gamma_{\tilde{b}_i \chi_\alpha}^L) (\Psi_{1a} - \Psi_{1b}) \right. \right. \\
& - \frac{2m_{l_I} m_b}{m_w^2 s_\beta c_\beta} (\mathcal{Z}_+)_{\alpha 1}^\dagger (\mathcal{Z}_-)_{2\beta} (\Gamma_{\tilde{b}_i \chi_\alpha}^R) \Psi_{1a} \\
& \left. \left. - \frac{2m_{l_I} m_b}{m_w^2 s_\beta c_\beta} (\mathcal{Z}_-)_{\alpha 2}^\dagger (\mathcal{Z}_+)_{1\beta} (\Gamma_{\tilde{b}_i \chi_\alpha}^R) (x_t x_{\chi_\alpha})^{1/2} \Psi_0 \right] (x_t; x_\rho, x_{\tilde{\nu}_k}; x_\varrho, x_{\tilde{g}}) \right\}, \\
\mathcal{B}_P'^{(6)} &= \mathcal{B}_S'^{(6)}. \tag{C4}
\end{aligned}$$

Here, some two-loop functions are defined as

$$\begin{aligned}
\Theta_0(x_0, x_1, x_2) &= \frac{1}{2} \left[2x_1 \ln x_1 - x_1 \ln^2 x_1 - \Phi(x_0, x_1, x_2) \right], \\
\Theta_{1a}(x_0, x_1, x_2) &= -\frac{1}{2} \left[x_1^2 \ln^2 x_1 + x_1 \Phi(x_0, x_1, x_2) \right],
\end{aligned}$$

$$\begin{aligned}
\Theta_{1b}(x_0, x_1, x_2) &= \frac{1}{4} \left[-4(x_0 - x_2)x_1 \ln x_1 + x_1^2 \ln^2 x_1 + (x_0 + x_1 + x_2)\Phi(x_0, x_1, x_2) \right], \\
\Theta_2(x_0, x_1, x_2) &= \frac{1}{4} \left[2x_1^3 \ln x_1 + (2x_0 - x_1 + 2x_2)x_1^2 \ln^2 x_1 + x_1(x_0 - x_1 + x_2)\Phi(x_0, x_1, x_2) \right].
\end{aligned} \tag{C5}$$

For the functions $\Psi_{2b,2c,2d,1a,1b}$ as well as $\Phi(x_0, x_1, x_2)$ can be found in our forthcoming work [44]

In those expressions, we have defined the short notations

$$\begin{aligned}
\Gamma_{\tilde{t}_i \chi_\alpha}^L &= (\mathcal{Z}_{\tilde{t}})_{1i} (\mathcal{Z}_+)_{\alpha 1}^\dagger - \frac{m_t}{\sqrt{2}m_w s_\beta} (\mathcal{Z}_{\tilde{t}})_{2i} (\mathcal{Z}_+)_{\alpha 2}^\dagger, \\
\Gamma_{\tilde{t}_i \chi_\alpha}^R &= (\mathcal{Z}_{\tilde{t}})_{1i} (\mathcal{Z}_-)_{2\alpha}, \\
\Gamma_{\tilde{D}_{\tilde{t}}^I \chi_\alpha}^L &= (\mathcal{Z}_{\tilde{D}^I})_{1i} (\mathcal{Z}_-)_{\alpha 1}^\dagger - \frac{m_{d^I}}{\sqrt{2}m_w s_\beta} (\mathcal{Z}_{\tilde{D}^I})_{2i} (\mathcal{Z}_-)_{\alpha 2}^\dagger, \\
\Gamma_{\tilde{D}_{\tilde{t}}^I \chi_\alpha}^R &= (\mathcal{Z}_{\tilde{D}^I})_{1i} (\mathcal{Z}_+)_{2\alpha}, \\
(\xi_H)_{ij} &= \left[\frac{m_t |\mu|}{m_w^2} e^{-i\theta_\mu} (\mathcal{Z}_{\tilde{t}})_{2,j} (\mathcal{Z}_{\tilde{s}}^\dagger)_{i,1} + s_\beta \frac{\sqrt{2}s_w A_s}{em_w} (\mathcal{Z}_{\tilde{t}})_{1,j} (\mathcal{Z}_{\tilde{s}}^\dagger)_{i,1} \right], \\
(\xi_q)_{ij} &= \begin{cases} (\mathcal{Z}_{\tilde{s}}^\dagger)_{i,1} (\mathcal{Z}_{\tilde{s}})_{1,j} - \frac{2}{3}s_w^2 \delta_{ij}, & q = s \\ (\mathcal{Z}_{\tilde{t}}^\dagger)_{i,1} (\mathcal{Z}_{\tilde{t}})_{1,j} - \frac{4}{3}s_w^2 \delta_{ij}, & q = t \end{cases}, \\
(\eta_H)_{ij} &= \left[\frac{m_t |\mu|}{m_w^2 t_\beta} (e^{i\theta_\mu} (\mathcal{Z}_{\tilde{t}}^\dagger)_{i,1} (\mathcal{Z}_{\tilde{t}})_{2,j} - e^{-i\theta_\mu} (\mathcal{Z}_{\tilde{t}}^\dagger)_{i,2} (\mathcal{Z}_{\tilde{t}})_{1,j}) \right. \\
&\quad \left. + s_\beta \frac{\sqrt{2}s_w}{em_w} (A_t (\mathcal{Z}_{\tilde{t}}^\dagger)_{i,2} (\mathcal{Z}_{\tilde{t}})_{1,j} - A_t^* (\mathcal{Z}_{\tilde{t}}^\dagger)_{i,1} (\mathcal{Z}_{\tilde{t}})_{2,j}) \right], \\
(\xi_\chi^i)_{\alpha\beta} &= \begin{cases} 2\delta_{\alpha\beta} (c_w^2 - s_w^2) + (\mathcal{Z}_+)_{1,\alpha} (\mathcal{Z}_+)_{\beta,1}^\dagger, & i = 1 \\ c_\beta (\mathcal{Z}_+)_{1,\alpha} (\mathcal{Z}_-)_{2,\beta} - s_\beta (\mathcal{Z}_+)_{2,\alpha} (\mathcal{Z}_-)_{1,\beta}, & i = 2 \\ c_\beta (\mathcal{Z}_-)_{\alpha,2} (\mathcal{Z}_+)_{\beta,1}^\dagger - s_\beta (\mathcal{Z}_-)_{\alpha,1} (\mathcal{Z}_+)_{\beta,2}^\dagger, & i = 3 \\ 2\delta_{\alpha\beta} (c_w^2 - s_w^2) + (\mathcal{Z}_-)_{\alpha,1} (\mathcal{Z}_-)_{1,\beta}, & i = 4 \end{cases}, \\
(\zeta_{sH}^\rho)_{ij} &= \frac{s_\beta}{6c_w^2} \left[(1 + 2c_w^2) (\mathcal{Z}_{\tilde{s}}^\dagger)_{i,1} (\mathcal{Z}_{\tilde{s}})_{1,j} + 2s_w^2 (\mathcal{Z}_{\tilde{s}}^\dagger)_{i,1} (\mathcal{Z}_{\tilde{s}})_{1,j} \right] (\mathcal{Z}_H)_{3,\rho} \\
&\quad + \frac{s_w}{\sqrt{2}em_w} \left[A_{\tilde{s}}^* (\mathcal{Z}_{\tilde{s}}^\dagger)_{i,1} (\mathcal{Z}_{\tilde{s}})_{2,j} + A_{\tilde{s}} (\mathcal{Z}_{\tilde{s}}^\dagger)_{i,2} (\mathcal{Z}_{\tilde{s}})_{1,j} \right] (\mathcal{Z}_H)_{2,\rho}
\end{aligned}$$

$$\begin{aligned}
& -i \frac{s_\beta s_w}{\sqrt{2}em_w} \left[A_s^*(\mathcal{Z}_s^\dagger)_{i,1}(\mathcal{Z}_s)_{2,j} - A_s(\mathcal{Z}_s^\dagger)_{i,2}(\mathcal{Z}_s)_{1,j} \right] (\mathcal{Z}_H)_{1,\rho} , \\
(\zeta_{tH}^\rho)_{ij} &= \frac{m_t |\mu|}{2m_w^2 s_\beta} \left[e^{i\theta_\mu} (\mathcal{Z}_t)_{2,j} (\mathcal{Z}_t^\dagger)_{i,1} - e^{-i\theta_\mu} (\mathcal{Z}_t)_{1,j} (\mathcal{Z}_t^\dagger)_{i,2} \right] (\mathcal{Z}_H)_{2,\rho} \\
& + \left[\left(\frac{(4c_w^2 - 1)s_\beta}{6c_w^2} - \frac{m_t^2}{m_w^2 s_\beta} \right) (\mathcal{Z}_t)_{1,j} (\mathcal{Z}_t^\dagger)_{i,1} + \left(\frac{2s_w^2 s_\beta}{3c_w^2} - \frac{m_t^2}{m_w^2 s_\beta} \right) (\mathcal{Z}_t)_{2,j} (\mathcal{Z}_t^\dagger)_{i,2} \right. \\
& - \frac{s_w}{\sqrt{2}em_w} \left(A_t^*(\mathcal{Z}_t)_{2,j} (\mathcal{Z}_t^\dagger)_{i,1} + A_t(\mathcal{Z}_t)_{1,j} (\mathcal{Z}_t^\dagger)_{i,2} \right) \left. \right] (\mathcal{Z}_H)_{3,\rho} \\
& + i \frac{m_t |\mu|}{2m_w^2} \left[e^{i\theta_\mu} (\mathcal{Z}_t)_{2,j} (\mathcal{Z}_t^\dagger)_{i,1} - e^{-i\theta_\mu} (\mathcal{Z}_t)_{1,j} (\mathcal{Z}_t^\dagger)_{i,2} \right] (\mathcal{Z}_H)_{1,\rho} , \\
(\kappa_{H^\rho}^i)_{\alpha\beta} &= \begin{cases} (\mathcal{Z}_+)_{1,\alpha} (\mathcal{Z}_-)_{2,\beta} (\mathcal{Z}_H)_{2,\rho} + (\mathcal{Z}_+)_{2,\alpha} (\mathcal{Z}_-)_{1,\beta} (\mathcal{Z}_H)_{3,\rho} \\ + i s_\beta (\mathcal{Z}_+)_{1,\alpha} (\mathcal{Z}_-)_{2,\beta} (\mathcal{Z}_H)_{1,\rho} , & i = 1 \\ (\mathcal{Z}_-^\dagger)_{\alpha,2} (\mathcal{Z}_+^\dagger)_{\beta,1} (\mathcal{Z}_H)_{2,\rho} + (\mathcal{Z}_-^\dagger)_{\alpha,1} (\mathcal{Z}_+^\dagger)_{\beta,2} (\mathcal{Z}_H)_{3,\rho} \\ - i s_\beta (\mathcal{Z}_-^\dagger)_{\alpha,2} (\mathcal{Z}_+^\dagger)_{\beta,1} (\mathcal{Z}_H)_{1,\rho} , & i = 2 \end{cases} . \tag{C6}
\end{aligned}$$

-
- [1] J. F. Gunion, H. E. Haber, G. Kane, and S. Dawson, *The Higgs Hunter's Guide*, Addison-Wesley, Reading, MA, 1990; hep-ph/9302272.
- [2] M. Brhlik, G. J. Good, G. L. Kane, Phys. Rev. **D59**, 115004(1999).
- [3] E. Commins *et.al.*, Phys. Rev. **A50**, 2960(1994).
- [4] P. G. Harris *et.al.*, Phys. Rev. Lett. **82**, 904(1999).
- [5] S. K. Lamoreaux *et. al.*, Phys. Rev. Lett. **57**, 3125(1986).
- [6] J. Ellis, S. Ferrara, and D. V. Nanopoulos, Phys. Lett. B. **114**, 231(1982); W. Buchmuller and D. Wyler, *ibid.* **121**, 321(1983); J. Polchinski and M. B. Wise, *ibid.* **125**, 393(1983).
- [7] P. Nath, Phys. Rev. Lett. **66**, 2565(1991); Y. Kizukuri and N. Oshimo, Phys. Rev. D. **46**, 3025(1992); **45**, 1806(1992); D. Chang, W. Y. Keung, A. Pilaftsis, Phys. Rev. Lett. **82**, 900(1999); **83**, 3972(1999)(E); A. Pilaftsis, Phys. Lett. B. **471**, 174(1999); Nucl. Phys. B. **644**, 263(2002); D. Chang, W. F. Chang, and W. F. Keung, Phys. Lett. B. **478**, 239(2000); T. F. Feng, T. Huang, X. Q. Li, S. M. Zhao, and X. M. Zhang, Phys. Rev. D. **68**, 016004(2003).
- [8] T. Ibrahim, P. Nath, Phys. Rev. D. **58**, 111301(1998); M. Brhlik, G. J. Good, G. L. Kane, *ibid.* **59**, 115004(1999); T. Ibrahim, P. Nath, Phys. Lett. B. **418**, 98(1998); J. Dai, H. Dykstra,

- R. G. Leigh, S. Paban, D. A. Dicus, Phys. Lett. B. **237**, 216(1990); J. Diaz-Cruz, J. Ferrandis, Phys. Rev. D **72**, 035003(2005).
- [9] A. Pilaftsis, Phys. Rev. **D58**, 096010(1998); Phys. Lett. **B435**, 88(1998).
- [10] A. Pilaftsis, C. E. M. Wagner, Nucl. Phys. **B533**, 3(1999).
- [11] M. Carena, J. Ellis, A. Pilaftsis, C. E. M. Wagner, Nucl. Phys. **B586**, 92(2000).
- [12] M. Carena, J. Ellis, A. Pilaftsis, C. E. M. Wagner, Nucl. Phys. **B625**, 345(2002).
- [13] G. Buchalla, A. Buras, Nucl. Phys. **B400**, 225(1993); **B548**, 309(1999).
- [14] X. G. He, T. D. Nguyen, and R. R. Volkas, Phys. Rev. **D38**, 814(1988); J. L. Hewett, S. Nandi, and T. G. Rizzo, *ibid.* **39**, 250(1989); M. J. Savage, Phys. Lett. **B266**, 135(1991); Y. Grossman, Nucl. Phys. **B426**, 355(1994).
- [15] W. Skiba, J. Kalinowski, Nucl. Phys. **B404**, 3(1993), and references therein.
- [16] Y. Grossmann, Z. Ligeti, E. Nardi, Phys. Rev. **D55**, 2768(1997).
- [17] D. Guetta, E. Nardi, Phys. Rev. **D58**, 012001(1998).
- [18] H. E. Logan, U. Nierste, Nucl. Phys. **B586**, 39(2000).
- [19] T. Ibrahim, P. Nath, Phys. Rev. **D67**, 016005(2003).
- [20] K. S. Babu, C. Kolda, Phys. Rev. Lett. **84**, 228(2000).
- [21] A. Dedes, A. Pilaftsis, Phys. Rev. **D67**, 015012(2003).
- [22] M. Carena, D. Garcia, U. Nierste, C. E. M. Wagner, Nucl. Phys. **B577**, 120(2000).
- [23] D. M. Pierce, J. A. Bagger, K. Matchev, R. Zhang, Nucl. Phys. **B491**, 3(1997).
- [24] F. Borzumati, C. Greub, and Y. Yamada, Phys. Rev. **D69**, 055005(2004).
- [25] T.-F. Feng, Phys. Rev. **D70**, 096012(2004).
- [26] C. Bobeth, A. J. Buras, F. Kruger and J. Urban, Nucl. Phys. **B630**, 87(2002); Z. Xiong, J. M. Yang, Nucl. Phys. **B628**, 193(2002).
- [27] Tai-Fu Feng, Xue-Qian Li, Guo-Li Wang, Phys. Rev. **D65**, 055007(2002).
- [28] C. Bobeth, T. Ewerth, F. Krüger, J. Urban, Phys. Rev. **D64**, 074014(2001).
- [29] Tai-Fu Feng, Xue-Qian Li, Jukka Maalampi, Xinmin Zhang, Phys. Rev. D. **71**, 056005(2005).
- [30] A. Buras, hep-ph/0101336.
- [31] B. Grinstein, M. Savage, M. Wise, Nucl. Phys. **B319**, 271(1989).
- [32] C. Bobeth *et.al.* in Ref.[26].
- [33] R. Grigjanis, P. J. O'Donnell, M. Sutherland, H. Navelet, Phys. Rep. **228**, 93(1993).
- [34] S. Chen *et. al.* (CLEO Collaboration), Phys. Rev. Lett. **87**, 251807(2001).

- [35] A. L. Kagan, M. Neubert, Eur. Phys. J. **C7**, 5(1999).
- [36] N. Cabibbo, L. Maiani, Phys. Lett. **B79**, 109(1978); J. L. Cortes, X. Y. Pham, A. Tounsi, Phys. Rev. **D25**, 188(1982); G. L. Fogli, *ibid.* **28**, 1153(1983).
- [37] CLEO Collaboration, T. E. Coan *et al.*, Phys. Rev. Lett. **86**, 5661(2001).
- [38] A. L. Kagan, M. Neubert, Phys. Rev. **D58**, 094012(2000).
- [39] C. S. Huang, hep-ph/0210314.
- [40] M. Wirbel, B. Stech, M. Bauer, Z. Phys. **C29**, 637(1985); A. Ali, P. Ball, L. T. Handoko, G. Hiller, Phys. Rev. **D61**, 074024(2000); D. Melikhov, B. Stech, Phys. Rev. **D62**, 014006(2000).
- [41] Particle data group, Phys. Lett. **B592**, 1(2004).
- [42] Peter Ratoff, Search for Sbottom and Stop in D-zero at the Tevatron (Run II), SUSY'05, Durham.
- [43] The CDF Collaboration, hep-ex/0508036; C.-S. Huang, P. Ko, X.-H. Wu, and Y.-D. Yang, hep-ph/0511129.
- [44] Tai-Fu Feng *et.al.*, The two-loop supersymmetric corrections to lepton anomalous dipole moments (in preparation, will be released for publication soon).